

Kinetic and metabolic behaviors of aerobic granules developed in sequencing batch reactors

Li, Yong

2009

Li, Y. (2009). Kinetic and metabolic behaviors of aerobic granules developed in sequencing batch reactors. Doctoral thesis, Nanyang Technological University, Singapore.

<https://hdl.handle.net/10356/15151>

<https://doi.org/10.32657/10356/15151>



**NANYANG
TECHNOLOGICAL
UNIVERSITY**

**KINETIC AND METABOLIC BEHAVIORS OF
AEROBIC GRANULES DEVELOPED IN
SEQUENCING BATCH REACTORS**

KINETIC AND METABOLIC BEHAVIORS OF AEROBIC GRANULES
DEVELOPED IN SEQUENCING BATCH REACTORS

LI YONG

LI YONG

SCHOOL OF CIVIL & ENVIRONMENTAL ENGINEERING

2009

2009

Kinetic and Metabolic Behaviors of Aerobic Granules Developed in Sequencing Batch Reactors

Li Yong

School of Civil & Environmental Engineering

A thesis submitted to the Nanyang Technological University
in fulfillment of the requirement for the degree of
Doctor of Philosophy

2009

ACKNOWLEDGEMENTS

I would like to express gratitude to my supervisor, Associate Professor Liu Yu, for his patient guidance and continuous encouragement. His strong academic background and deep insights into the research problems really helped me to save a lot of strength during my research. His meticulous attitude to research also impressed me very much. I learned a lot from him during my PhD study.

I thank all my friends in the lab: Liu Qishan, Yang Shufang, Qin Lei, Xu Hui, Wang Zhiwu, Shen Liang, Xiong Yanghui, Jiang Bo, Liu Yajuan, Feng Jing, Jiang Xia, Liu Xueyan, Zeng Ping, Zhu Baowei, Goh Kok Hui, Ding Hongbo, Luo Yiqun, Lee Pei Fung, Kuang Shengli, Qi Wei, Zhang Zhenpeng, Du Jianhong, Khor Swee Loong, Zhang Yi, Yi Shan, Zhuang Weiqin, Guo Chenghong, Wang Yining, Zheng Sha, Mao Taohong, Moy Yan Pui Benjamin, Jiang Helong, Wu Weiwei, Zhang Xing, Liu Yongqiang, Pan Zhehao, Xu Shiping, Li Ying, Chen Feng, Zhao Li, Xu Shasha, Li Ning, Liao Kai. Their help and encouragement made my PhD life easier and happier.

I thank Dr. Xu Hailou and his students from Singapore Polytechnic for their help in biological analysis.

I would like to thank the technical staff in the environment laboratory for their technical support. Without their kind help, my research would be impossible.

Finally, I thank Nanyang Technological University for offering me the opportunity of PhD study and for providing me the research scholarship.

TABLE OF CONTENTS

| | |
|------------------------------------------------------------|-------------|
| ACKNOWLEDGEMENTS | I |
| TABLE OF CONTENTS | II |
| ABSTRACT | VI |
| PUBLICATIONS | VIII |
| NOMENCLATURE..... | IX |
| LIST OF FIGURES | XI |
| LIST OF TABLES | XV |
| | |
| CHAPTER 1 INTRODUCTION | 1 |
| 1.1 BACKGROUND | 1 |
| 1.2 OBJECTIVES AND SCOPE..... | 2 |
| 1.3 ORGANIZATION OF THE THESIS..... | 2 |
| | |
| CHAPTER 2 LITERATURE REVIEW | 3 |
| 2.1 INTRODUCTION | 3 |
| 2.2.1 Essential conditions for anaerobic granulation | 4 |
| 2.2.2 Other factors affecting anaerobic granulation | 6 |
| 2.3 AEROBIC GRANULATION..... | 10 |
| 2.3.3 Drawbacks of aerobic granules | 20 |
| 2.3.4 Microbial structure and diversity | 20 |
| 2.4 MASS TRANSFER INSIDE MICROBIAL AGGREGATES..... | 26 |
| 2.4.1 Mass transfer inside activated sludge | 26 |
| 2.5 GROWTH KINETICS AND METABOLISM OF AEROBIC GRANULES.... | 31 |
| 2.6 THE ROLE OF CALCIUM IN AGGREGATES | 32 |
| 2.6.1 The role of calcium in anaerobic granules | 32 |
| 2.6.3 The effect of calcium on aerobic granulation | 34 |
| 2.7 SLUDGE RETENTION TIME | 35 |
| 2.7.1 The effect of SRT on carbon removal..... | 35 |
| 2.7.2 The effect of SRT on nitrification..... | 36 |
| 2.7.3 The effect of SRT on phosphate removal | 36 |
| 2.7.4 The effect of SRT on bioflocculation | 37 |

2.7.5 The effect of SRT on sludge structure38

CHAPTER 3 DIFFUSION OF SUBSTRATE AND OXYGEN IN AEROBIC GRANULE.....39

| | |
|--------------------------------------------|----|
| 3.1 INTRODUCTION | 39 |
| 3.2 MATERIALS AND METHODS..... | 40 |
| 3.2.1 Cultivation of aerobic granules..... | 40 |
| 3.2.2 Batch experiments..... | 41 |
| 3.3 RESULTS | 41 |
| 3.3.1 Development of model system | 41 |
| 3.4 DISCUSSION | 56 |
| 3.4.1 Diffusion of DO and substrate | 56 |
| 3.4.2 Microbiological implications..... | 58 |
| 3.5 CONCLUSIONS | 61 |

**CHAPTER 4 MECHANISM OF CALCIUM ACCUMULATION IN
ACETATE-FED AEROBIC GRANULE63**

| | |
|--------------------------------------------------------------------------------------------------|----|
| 4.1 INTRODUCTION | 63 |
| 4.2 MATERIALS AND METHODS..... | 64 |
| 4.2.1 Cultivation of aerobic granules..... | 64 |
| 4.2.2 Elemental analysis | 64 |
| 4.2.3 Calcium mapping by EDX..... | 65 |
| 4.3. Model development | 66 |
| 4.3.1 Ionic equilibrium of carbonate ion..... | 66 |
| 4.3.2 Diffusion kinetics of substances in aerobic granule | 67 |
| 4.4 RESULTS | 71 |
| 4.4.1 Chemical form of calcium accumulated in acetate-fed aerobic granule | 71 |
| 4.4.2 Calcium distribution in acetate-fed aerobic granules | 72 |
| 4.4.3 Granule size-dependent CaCO ₃ formation in acetate-fed aerobic granule | 74 |
| 4.5 DISCUSSION..... | 78 |

| | |
|-----------------------|----|
| 4.6 CONCLUSIONS | 79 |
|-----------------------|----|

CHAPTER 5 STOICHIOMETRIC ANALYSIS OF DOC FLUX INTO

STORAGE AND GROWTH IN AEROBIC GRANULES81

| | |
|-----------------------------------------------------------------------------|-----|
| 5.1 INTRODUCTION | 81 |
| 5.2 MATERIALS AND METHODS..... | 82 |
| 5.3 RESULTS AND DISCUSSION | 83 |
| 5.3.1 Respirometric profiles of aerobic granules with different sizes | 83 |
| 5.3.2 Carbon flux in aerobic granules with different sizes | 86 |
| 5.3.3 Stoichiometric analysis of metabolisms of aerobic granules | 89 |
| 5.3.4 Conversion of DOC to storage material..... | 95 |
| 5.3.5 Conversion of storage material to new biomass | 96 |
| 5.3.6 Specific consumption rate of storage material..... | 97 |
| 5.3.7 Overall growth yield of aerobic granules | 99 |
| 5.3.8 Overall growth rate of aerobic granules | 100 |
| 5.3.9 Endogenous respiration of aerobic granules | 103 |
| 5.4 CONCLUSION..... | 104 |

CHAPTER 6 THE EFFECT OF SLUDGE RETENTION TIME ON

AEROBIC GRANULATION106

| | |
|-------------------------------------------------------|-----|
| 6.1 INTRODUCTION | 106 |
| 6.2 MATERIALS AND METHODS..... | 107 |
| 6.2.1 Experimental set-up and operation | 107 |
| 6.2.2 Control of SRT..... | 108 |
| 6.2.3 Analytical methods | 108 |
| 6.2.4 Bacterial tests | 109 |
| 6.3. RESULTS | 110 |
| 6.3.1 General observation by image analysis | 110 |
| 6.3.2 Evolution and distribution of sludge size | 117 |
| 6.3.3 Settleability of sludge | 119 |
| 6.3.4 Biomass concentration..... | 119 |
| 6.3.5 Substrate removal kinetics | 120 |
| 6.3.6 Cell surface hydrophobicity..... | 122 |

| | |
|------------------------------------------------------------|------------|
| 6.3.7 Shift in microbial population | 122 |
| 6.4 DISCUSSION | 125 |
| 6.5 CONCLUSIONS | 132 |
| CHAPTER 7 CONCLUSIONS AND RECOMMENDATIONS | 133 |
| 7.1 CONCLUSIONS | 134 |
| 7.2 RECOMMENDATIONS | 136 |
| REFERENCES | 136 |

ABSTRACT

The previous research on aerobic granulation was mainly focused on the factors affecting aerobic granulation. However, little has been known about the metabolic behaviors and modeling of aerobic granular sludge process. In this study, a one-dimensional model was developed and successfully applied to aerobic granular sludge SBR. The diffusion profiles of organic substrate and dissolved oxygen in aerobic granules were simulated using the proposed model system under various conditions. It was found that diffusions of organic substrate and oxygen in aerobic granule would be a dynamic process, and were closely interrelated. Simulation of the overall performance of aerobic granular sludge SBR showed that dissolved oxygen would be a main limiting factor of the metabolic activity of aerobic granules. Smaller aerobic granules exhibited higher metabolic activity in terms of the substrate removal rate. For a SBR dominated by aerobic granules larger than 0.5 mm, dissolved oxygen would be the bottleneck which limits the substrate utilization rate. It is expected that the model system developed in this study can provide an effective and useful tool for predicting and optimizing the performance of aerobic granular sludge reactor.

The model system developed was further extended to study of the calcium accumulation mechanism in acetate-fed aerobic granules. It was demonstrated from both experimental and stoichiometric approaches that the accumulation of calcium ions was closely related to the size-dependent diffusion limitation of oxygen inside aerobic granules. This means that the calcium accumulation was governed by the size of acetate-fed aerobic granules, e.g., substantial accumulation of calcium ions was only found in aerobic granules with the size of larger than 0.5 mm. Almost all the calcium ions accumulated in acetate-fed aerobic granules was in the form of CaCO_3 , and was mainly located in the deeper part of the acetate-fed aerobic granule. This piece of study clearly revealed that the accumulation of calcium ions in aerobic granules would not be the prerequisite of granulation.

To further look into metabolic and kinetic behaviors of aerobic granules, a series of respirometric experiments were conducted using aerobic granules with the mean sizes of 0.75, 1.5, 2.4 and 3.4 mm respectively. The dissolved organic carbon (DOC) fluxes into storage, new biomass and carbon dioxide were tracked in the course of the experiments. It was found that the metabolisms of aerobic granule followed a three-phase pattern: (i) conversion of external DOC to PHB-like storage materials; (ii) growth of aerobic granules on the storage material; and (iii) endogenous respiration. Stoichiometric analyses further revealed that aerobic granules with different sizes exhibited the similar response pattern in each metabolic phase, i.e. the metabolism of aerobic granules would be unlikely dependent on their sizes. For instance, the conversion yields of external DOC to storage material by different-size aerobic granules were found to be comparable. However, in the sense of reaction rate, smaller aerobic granules would be more active than bigger granules.

Although a number of operating parameters involved in aerobic granulation have been studied, sludge retention time (SRT) as one of the most important design and operation parameter of biological process has been hardly investigated. In order to identify the role of SRT in aerobic granulation, five SBRs were operated at different SRTs in the range of 3 to 40 days, while hydraulic selection pressures in the SBRs were controlled at extremely low level to avoid its interferences. The results showed that no successful aerobic granulation was observed at all studied SRTs, i.e., bioflocs were the dominant form of biomass at the SRT studied. A comparison analysis further revealed that hydraulic selection pressure in terms of $(V_s)_{\min}$ would be much more effective than SRT for enhancing aerobic granulation in SBR. In conclusion, SRT would not be essential for successful aerobic granulation. This offers in-depth insights into aerobic granulation in SBR.

PUBLICATIONS

SCI journal papers from this thesis:

1. **Li Y**, Liu Y (2005) Diffusion of substrate and oxygen in aerobic granule. *Biochemical Engineering Journal*, 27, 45–52.
2. Wang ZW, **Li Y**, Liu Y (2007) Mechanism of calcium accumulation in acetate-fed aerobic granule. *Applied Microbiology and Biotechnology*, 74, 467-473.
3. **Li Y**, Liu Y, Xu HL (2008) Is sludge retention time a decisive factor for aerobic granulation in SBR? *Bioresource Technology*, 99, 7672-7677.
4. **Li Y**, Liu Y, Shen L, Chen F (2008) DO diffusion profile in aerobic granule and its microbiological implications. *Enzyme and Microbial Technology*, 43, 349-354.
5. **Li Y**, Liu Y (2008) Stoichiometric analysis of DOC flux into storage and growth in aerobic granules. *Biotechnology Journal*, 4, 238-246.

International conference papers from this thesis:

6. Liu Y, **Li Y**, Shen L, Chen F (2008) Direct measurement of DO diffusion in aerobic granule by a microoxygen electrode. Oral presentation in IWA Biofilm Technologies Conference, 111-115, 8-11 Jan, 2008, Singapore.
7. Wang ZW, **Li Y**, Shen L, and Liu Y (2008) Kinetics and energetics of aerobic granules. In Proceeding of IWA Biofilm Technologies Conference, 67-71, 8-11 Jan, 2008, Singapore.

Book chapter:

8. **Li Y**, Wang ZW, Y Liu. (2007) Diffusion of substrate and oxygen in aerobic granules. In: *Wastewater Purification: Aerobic Granulation in Sequencing Batch Reactors*, Chapter 8, pp 131-148. CRC Press.

Co-authored SCI journal papers:

9. Wang ZW, **Li Y**, Liu Y, Zhou JQ (2006) The influence of short-term starvation on aerobic granules. *Process Biochemistry*, 41, 2373-2378.
10. Liu Y, Yang SF, Tay J H, Liu QS, Qin L, **Li Y** (2004) Cell hydrophobicity is a triggering force of biogranulation. *Enzyme and Microbial Technology*, 34, 371–379.

NOMENCLATURE

| | |
|-----------------|--------------------------------------------------|
| ASM | Activated sludge model |
| C_{O_2} | Dissolved oxygen concentration |
| C_{H^+} | H^+ concentration |
| $C_{HCO_3^-}$ | HCO_3^- concentration |
| $C_{CO_3^{2-}}$ | CO_3^{2-} concentration |
| CPR | Carbon dioxide production rate |
| D_s | Acetate diffusion coefficient |
| D_{fo} | Oxygen diffusion coefficient |
| D_{O_2} | Diffusion coefficient of O_2 |
| D_{H^+} | Diffusion coefficient of H^+ |
| $D_{HCO_3^-}$ | Diffusion coefficient of HCO_3^- |
| $D_{CO_3^{2-}}$ | Diffusion coefficient of CO_3^{2-} |
| DOC | Dissolved organic carbon |
| k_d | Decay constant |
| K_s | Half rate constant |
| K_{CaCO_3} | Solubility product constant |
| K_{h,CO_2} | Henry's law constant of CO_2 |
| K_{a1} | 1st step dissociation constant of carbonate acid |
| K_{a2} | 2nd step dissociation constant of carbonate acid |
| m | Number of aerobic granules in a reactor |
| P_{CO_2} | Partial CO_2 pressure in air |
| ρ_x | Biomass density |
| q_{sto} | specific cellular storage consumption rate |
| R | The radius of a granule |
| Δr | The thickness of one layer |

| | |
|--------------------------|--------------------------------------------------|
| R_{CaCO_3} | CaCO ₃ formation zone |
| \bar{R} | Average radius of all granules |
| r | Distance to granule center |
| R_s | Substance utilization rate |
| R_{O_2} | O ₂ utilization rate |
| R_{H^+} | H ⁺ consumption rate |
| $R_{\text{HCO}_3^-}$ | HCO ₃ ⁻ production rate |
| $R_{\text{CO}_3^{2-}}$ | CO ₃ ²⁻ production rate |
| S_{bulk} | Bulk substrate concentration |
| s_i | Substrate concentration at no. i layer |
| s | Substrate concentration at a point of a granule |
| ΔS_{bulk} | The change of bulk substrate concentration |
| S_{bulk0} | Initial bulk substrate concentration |
| SRT | Sludge retention time |
| $\mu(s)$ | Growth rate at substrate concentrations |
| μ_{max} | Maximum growth rate |
| μ_{obs} | Observed growth rate |
| v | Substrate conversion rate |
| v_1 | Substrate conversion rate of a granule |
| V | Volume of the reactor |
| V_{all} | Substrate conversion rate of all granules |
| V_e | volume of discharged supernatant |
| V_s | volume of discharged mixed-liquor in each cycle |
| $(V_s)_{\text{min}}$ | Minimum settling velocity |
| X | Biomass concentration |
| X_e | suspended solid concentration in the supernatant |
| $Y_{x/o}$ | Growth yield of biomass over oxygen |
| $Y_{x/s}$ | Growth yield of biomass over substrate |
| $Y_{\text{sto/s}}$ | storage yield over substrate |

LIST OF FIGURES

| | |
|----------------------------------------------------------------------------------------------------------------------------------------------------------------------------------------------------------|----|
| Figure 3. 1 Simulated concentration profiles of substrate (dash line) and oxygen (solid line) in aerobic granule with a radius of 0.1 mm. | 46 |
| Figure 3. 2 Simulated concentration profiles of substrate (dash line) and oxygen (solid line) in aerobic granule with a radius of 0.4 mm. | 47 |
| Figure 3. 3 Simulated concentration profiles of substrate (dash line) and oxygen (solid line) in aerobic granule with a radius of 0.5 mm. | 48 |
| Figure 3. 4 Simulated concentration profiles of substrate (dash line) and oxygen (solid line) in aerobic granule with a radius of 0.75 mm. | 48 |
| Figure 3. 5 Simulated concentration profiles of substrate (dash line) and oxygen (solid line) in aerobic granule with a radius of 1.0 mm. | 49 |
| Figure 3. 6 Simulated concentration profiles of substrate (dash line) and oxygen (solid line) in aerobic granules with a radius of 0.5 mm at substrate concentration = 300 mg COD L ⁻¹ | 50 |
| Figure 3. 7 Simulated concentration profiles of substrate (dash line) and oxygen (solid line) in aerobic granules with a radius of at substrate concentration = 200 mg COD L ⁻¹ | 50 |
| Figure 3. 8 Diffusion profiles of substrate (dash line) and oxygen (solid line) in aerobic granules at substrate concentration = 100 mg COD L ⁻¹ | 51 |
| Figure 3. 9 Diagram of algorithm used to simulate substrate-time profiles in reactor. | 52 |
| Figure 3. 10 Substrate-time profile in aerobic granular sludge SBR dominated by granules with a size of 0.1 mm. -: simulation; Δ: experimental data. | 54 |
| Figure 3. 11 Substrate-time profile in aerobic granular sludge SBR dominated by granules with a size of 0.5 mm. -: simulation; Δ: experimental data. | 54 |
| Figure 3. 12 Substrate-time profile in aerobic granular sludge SBR dominated by granules with a size of 0.75mm. -: simulation; Δ: experimental data. | 55 |

| | |
|---------------------------------------------------------------------------------------------------------------------------------------------------------------------------------------------------------------------------------------------------------------------------------------------------------------------------------|----|
| Figure 3. 13 Substrate-time profile in aerobic granular sludge SBR dominated by granules with a size of 1.0 mm. - : simulation; Δ : experimental data..... | 55 |
| Figure 3. 14 Effectiveness factor-granule radius diagram. \bullet : theoretical data; \circ : experimental data from Liu et al. (2005a) | 57 |
| Figure 4. 1 Respirometer system for analysis of carbonate in the acetate-fed aerobic granule: 1. computer for data collection; 2. respirometer; 3. fridge; 4. shaker; 5. acid containing vial; 6. reaction bottle. | 65 |
| Figure 4. 2 Ionic compositions of the acetate-fed aerobic granules. | 71 |
| Figure 4. 3 a: Cross-section view of the acetate-fed aerobic granule by SEM; b: the EDX mapping for calcium indicated by <i>blue color</i> , bar: 100 μm ; c: IA cross-section view of the acetate-fed aerobic granule; d: generation of gas bubbles during the acid-granule reaction, bar: 200 μm | 73 |
| Figure 4. 4 Simulation profiles of pH (—) and CO_3^{2-} (---) in the acetate-fed aerobic granule. | 75 |
| Figure 4. 5 Size-dependent calcium and ash contents in the acetate-fed aerobic granules. a: calcium contents in aerobic granules with different radius ranges; b: ash content (<i>line</i>) and corresponding sludge mean radius (<i>bar</i>) in the course of aerobic granulation..... | 76 |
| Figure 4. 6 Comparison of the simulated and experimentally measured CaCO_3 as well as ash contents in the acetate-fed aerobic granule. — : $(R_{\text{CaCO}_3} / R)^3$ simulation; \bullet : calcium content; \circ : ash content. | 77 |
| Figure 4. 7 Comparison of calcium (<i>left</i>) and ash (<i>right</i>) contents in the ethanol- (Liu et al. 2003) and acetate-fed aerobic granules..... | 77 |
| Figure 5. 1 Respirometer system | 83 |
| Figure 5. 2 Changes in OUR, CPR and DOC concentration during respirometric test of aerobic granules with a mean size of 0.75 mm. | 84 |
| Figure 5. 3 Changes in OUR, CPR and DOC concentration during respirometric test of aerobic granules with a mean size of 1.5 mm. | 84 |
| Figure 5. 4 Changes in OUR, CPR and DOC concentration during respirometric test of aerobic granules with a mean size of 2.4 mm. | 85 |

| | |
|-----------------------------------------------------------------------------------------------------------------------------------------|-----|
| Figure 5. 5 Changes in OUR, CPR and DOC concentration during respirometric test of aerobic granules with a mean size of 3.0 mm. | 85 |
| Figure 5. 6 Carbon fluxes in the culture of aerobic granules with the mean size of 0.75mm. | 87 |
| Figure 5. 7 Carbon fluxes in the culture of aerobic granules with the mean size of 1.5mm | 87 |
| Figure 5. 8 Carbon fluxes in the culture of aerobic granules with the mean size of 2.4mm | 88 |
| Figure 5. 9 Carbon fluxes in the culture of aerobic granules with the mean size of 3.0mm | 88 |
| Figure 5.10 Conversion yield of DOC to storage material in aerobic granules with different sizes. | 95 |
| Figure 5.11 Growth yields of biomass on storage material for aerobic granules with different sizes. | 97 |
| Figure 5.12 Specific storage consumption rates in phase II for aerobic granules with different sizes. | 99 |
| Figure 5.13 The observed growth yields of aerobic granules with different sizes.. | 100 |
| Figure 5.14 Overall growth rates of aerobic granules with different sizes..... | 102 |
| Figure 5. 15 Specific biomass decay rate (k_d) of aerobic granules with different size.... | 104 |
| Figure 6. 1 Diagram of cyclic operation stages in R1 to R5..... | 107 |
| Figure 6. 2 Morphology of seed sludge. | 111 |
| Figure 6. 3Morphology of sludge cultivated in R1 on day 3..... | 111 |
| Figure 6. 4 Morphology of sludge cultivated in R1 on day 30..... | 112 |
| Figure 6. 5 Morphology of sludge cultivated in R2 on day 4..... | 112 |
| Figure 6. 6 Morphology of sludge cultivated in R2 on day 30..... | 113 |
| Figure 6. 7Morphology of sludge cultivated in R3 on day 4..... | 113 |
| Figure 6. 8 Morphology of sludge cultivated in R3 on day 30..... | 114 |
| Figure 6. 9 Morphology of sludge cultivated in R4 on day 4..... | 114 |
| Figure 6. 10 Morphology of sludge cultivated in R4 on day 30..... | 115 |
| Figure 6. 11Morphology of sludge cultivated in R5 on day 5. | 115 |
| Figure 6. 12 Morphology of sludge cultivated in R5 on day 30..... | 116 |
| Figure 6. 13 Changes in aggregate size in the course of operation of SBRs. | 117 |

| | |
|---------------------------------------------------------------------------------------------------------------------------------------|-----|
| Figure 6. 14 Size distribution of aggregates cultivated at different SRTs. | 118 |
| Figure 6. 15 Fraction of aerobic granules in the SBRs run at different SRTs. | 118 |
| Figure 6. 16 Changes in SVI in course of SBR operation at different SRTs. | 119 |
| Figure 6. 17 Biomass concentration versus operation time. | 119 |
| Figure 6. 18 (a) TOC profile on day 30 in a cycle; (b) TOC removal kinetics versus SRT. | 121 |
| Figure 6. 19 Cell surface hydrophobicity of sludges cultivated at different SRTs, and dashed line represents the seed sludge. | 122 |
| Figure 6. 20 Y_{obs} versus SRT observed in R1 to R5. | 126 |
| Figure 6. 21 $1/SRT$ versus q_s | 127 |
| Figure 6. 22 Illustration of the $(V_s)_{min}$ concept in SBR (Liu et al. 2005). | 128 |
| Figure 6. 23 Fraction of aerobic granules versus $(V_s)_{min}$ | 130 |
| Figure 6. 24 Effects of $(V_s)_{min}$ and SRT on aerobic granulation in SBR. | 131 |
| Figure 6. 25 Aggregate size against $(V_s)_{min}$ and SRT. | 132 |

LIST OF TABLES

| | |
|----------------------------------------------------------------------------------------------------------------------------------|-----|
| Table 3.1 Symbols and values of constants used | 45 |
| Table 4.1 Symbols and values of constants used | 70 |
| Table 5.1 Reaction stoichiometry of aerobic granules with different sizes. | 92 |
| Table 5.2 Composition of storage materials in aerobic granules with different sizes. | 93 |
| Table 5.3 Yield coefficients obtained in this study and reported in literatures. All units in C-mol C-mol ⁻¹ | 94 |
| Table 6. 1 Distribution of microbial isolates identified in the course of operation of R2 and R3. | 124 |

CHAPTER 1

INTRODUCTION

1.1 CHALLENGES IN AEROBIC GRANULATION RESEARCH

The research on aerobic granules has been intense in recent years. Many factors affecting aerobic granulation are identified and have been studied thoroughly. However, the kinetic and metabolic behaviours of aerobic granules are not well understood yet. Several questions pertaining to metabolic behaviours of aerobic granules remain unanswered.

The kinetics of aerobic granules is dependent on the availability of substances inside aerobic granules, which will be largely determined by diffusion of substances in aerobic granules. It should be realized that the diffusion of substances in aerobic granules has seldom been studied so far. The diffusion limitation inside aerobic granules may suppress the organic degradation by aerobic granules in cases where substrate or oxygen could not penetrate into the deeper parts of aerobic granule. In this regard, two questions still remain unanswered: whether substrate or oxygen is the limiting factor and what are the effects of the diffusion limitation on aerobic granules. To address these questions, obviously a model-based theoretical approach will be helpful for studying the diffusion in aerobic granules and its effects on kinetics of aerobic granules.

The diffusion in aerobic granules is likely to affect the ion distribution in aerobic granules. For instance, high calcium content has been found in acetate-fed aerobic granules. The mechanism of calcium accumulation inside acetate-fed aerobic granules and the form of the accumulated calcium have not yet been reported. It appears from the above that the calcium accumulation needs to be analyzed together with diffusion phenomenon observed in aerobic granules.

The kinetics of aerobic granules with various sizes would depend on the size-associated diffusion resistance. However, it remains unknown that if the metabolism

of aerobic granules would also be size-dependent, and another challenge is whether the carbon metabolism of aerobic granules would be different from that of activated sludge or biofilms.

Sludge retention time (SRT) is an important design and operation parameter of biological processes. So far, the effect of SRT on the formation of aerobic granules is still unclear. In the previous studies, there was no a mean to isolate the effect of SRT on aerobic granulation from hydraulic selection. Study of SRT in aerobic granular sludge system will offer deep insights into the mechanism of aerobic granulation as well as the kinetics and metabolism of aerobic granules as specified above.

1.2 OBJECTIVES AND SCOPES

- To investigate the diffusion of substrate and oxygen inside aerobic granules and determine how diffusion affects the degradation process in one operation cycle;
- To study mechanism of calcium inside aerobic granules and what form of calcium inside acetate-fed aerobic granules;
- To explore how the sizes of aerobic granules affect the carbon metabolism process;
- To look into the effect of SRT on aerobic granulation.

1.3 ORGANIZATION OF THE THESIS

This thesis contains seven chapters. Chapter 1 is an introduction to the research, and Chapter 2 reviews relevant literature. Chapter 3 investigates the diffusion of substrate and oxygen inside aerobic granules. In Chapter 4, calcium distribution in aerobic granules is studied. Chapter 5 focuses on the kinetic and metabolic behaviors of aerobic granules, while Chapter 6 discovers the effect of SRT on aerobic granulation. Finally, conclusions and recommendations are summarized in Chapter 7.

CHAPTER 2

LITERATURE REVIEW

2.1 INTRODUCTION

Biogranulation is categorized into anaerobic granulation and aerobic granulation. Biogranules contain different bacterial species and form through self-immobilization of microorganisms. Compared to the conventional activated sludge, biogranules have a more regular, denser and stronger structure and better settling properties. In this chapter, the progress in granulation research is reviewed in the first two parts.

Diffusion is the driving force of mass transfer into microbial aggregates. With the increase of the size or thickness of the aggregates, the diffusion resistance is increased. It is useful to review the studies on mass transfer in aggregates, such as biofilms, for better understanding of mass transfer problem in aerobic granules.

Calcium is also found to be important in the formation of anaerobic granules and biofilms. Reviews on the role of calcium in other aggregates may help to disclose the role of calcium in aerobic granulation.

Sludge retention time (SRT) plays an important role in selection of species in reactors. SRT has effect the characteristics of sludge in the reactors. SRT also has effect on the bioflocculation, which is essential for aerobic granulation. Therefore, the review of previous research on SRT of other aggregates may give hints on the effect of SRT on aerobic granulation.

2.2 ANAEROBIC GRANULATION

2.2.1 Essential conditions for anaerobic granulation

2.2.1.1 Organic loading rate

Most research applied gradually increasing organic loading rate to cultivate anaerobic granules. Zhou et al. (2007) evaluated the effect of organic loading rate on granulation process using upflow anaerobic sludge blanket (UASB) reactors run under different conditions, and in their study, organic loading rate was manipulated by either changing feed concentration or flow rate. The results showed that increase of organic loading rate led to extracellular polymer (ECP) content increase, which greatly enhanced the granulation process. Show et al. (2004) also found that under two different stressed loading conditions the startup and granule development were accelerated by 45% and 33% respectively compared with the control reactor respectively, along with the formation of granules of superior characteristics without deteriorating loading capacity. The organic loading rate was increased by shortening the hydraulic retention time (HRT) and maintaining the influent COD concentrations at the same level. However, too high loading rate is not favorable for anaerobic granulation, because too high organic loading will cause instability of anaerobic granules (Kumar et al. 2008; Zhou et al. 2007). Zhou et al. (2007) concluded that the instability was because of the unrecoverable decay of methanogenic activity and the serious unbalance between the feedstuff and biological requirement.

Too low organic loadings also cause instability of anaerobic granules or even the complete failure of anaerobic granulation process. Kumar et al. (2008) cultivated anaerobic granules at a low organic loading rate of $2.08 \text{ kg COD m}^{-3} \text{ d}^{-1}$ at a hydraulic retention time (HRT) of 6.0 h in an anaerobic hybrid reactor. Kumar et al. (2008) found that organic loading rate lower than $2.08 \text{ COD m}^{-3} \text{ d}^{-1}$ will cause instability of anaerobic granules when HRT was increased, while the influent COD concentration was controlled at the same level.

2.2.1.2 Upflow liquid velocity

The upflow velocity is important for anaerobic granulation process. Arcand et al. (1994) found that reactors which were operated at 0.9 m h^{-1} behaved as fixed beds while those run at 2.2, 4.4 and 6.6 m h^{-1} were fluidized, because an immediate spatial gradient of the sludge particle sizes was induced. The upflow velocity had a significant positive effect on mean granule size. Henceforth the resulting final size of granules is essentially a function of the hydrodynamic regime. Major impact on granule net steady size is attributed to several mechanisms related to fluidization: improved penetration of substrates into biofilm, insignificance of liquid shear relative to the shear of gas, and reduction of particle friction and attrition with the bed voidage. However, Francese et al. (2004) found anaerobic granules formed at a smaller upflow liquid velocity of 0.5 to 2.0 m h^{-1} with an organic loading rate of $8 \text{ g COD L}^{-1} \text{ d}^{-1}$.

2.2.1.3 pH

Based on the sequence of anaerobic reaction, microbial species involved are divided into following three categories: (a) bacteria responsible for hydrolysis; (b) bacteria producing acid; and (c) bacteria producing methane. The acid-producing bacteria tolerate a low pH and have an optimal pH of 5.0 to 6.0, while most methane-producing bacteria can function optimally in a very narrow pH range of 6.7 to 7.4 (Bitton 1999). Once pH in the reactor falls outside 6.0 to 8.0, the activity of methane-producing bacteria is restricted and the decline in activity in turn poses serious operational problem that can lead to the failure of the reactor. Under normal operation conditions the pH reduction caused by acid-producing bacteria can be buffered by bicarbonate produced by the methane-producing bacteria. Therefore, aerobic granulation can form only within a narrow pH range.

2.2.1.4 Temperature

Temperature has huge effects on the activities of anaerobic granules. Bitton (1999) reported that methanogenic bacteria's generation times range from 3 days at 35 °C to as high as 50 days at 10 °C. When the reactor temperature is below 30°C, the methanogens' activity is seriously reduced. This is why mesophilic UASB reactors must be operated at a temperature of 30 to 35 °C for successful functioning. However, sludge washout and deterioration of COD removal efficiency have been observed in UASB reactors when temperature is increased from 37 to 55 °C (Fang and Lau 1996). Effluent quality from a UASB reactor operated at 70 °C was lower than that from reactors operated at 35 °C and 55 °C (Lepisto and Rintala 1999). High temperatures are known to encourage the growth of suspended biosolids and extremely high temperatures inhibit bacterial growth.

McHugh (2006) applied two laboratory-scale anaerobic hybrid reactors to treat low and high-strength whey-based wastewaters. The reactors for treating low and high-strength wastewater were run between 20 °C and 12 °C and between 20°C and 14 °C respectively. Lowering the operating temperature of reactor treating high strength wastewater to 12 °C resulted in a decrease a disintegration of granular sludge, but the granule disintegration was reversed by decreasing the organic loading rate. The reactors were operated 500 days, which is a manifest that anaerobic granulation can endure psychrophilic conditions if the organic loading can be controlled well.

2.2.2 Other factors affecting anaerobic granulation

2.2.2.1 Polymer dosing

Polymers such as cationic polymers are known to promote particle agglomeration and have been dosed to accelerate the formation of anaerobic granules. It is reported that the startup period required for the development of granular sludge blanket can be shortened significantly compared to when no polymers are used (El-Mamouni et

al. 1998; Uyanik et al. 2002). In study by Jeong et al. (2006), a large amount of granular sludge was prepared within 5 min by adding organic–inorganic hybrid polymers to the sewage digester sludge. The size of the granular sludge ranged from 1 to 5 mm and its falling velocity was higher than that of the granular sludge from the actual wastewater treatment facility.

However, recent research shows that there is an optimum range for polymer addition and polymer dosing may have negative effect on anaerobic granules under some conditions. Bhunia and Ghangrekar (2008) studied the effect of cationic polymer additives on biomass granulation and COD removal efficiency had been examined in lab-scale upflow anaerobic sludge blanket (UASB) reactors, treating low strength synthetic wastewater. Under thick inoculum conditions, polymer dosing was observed to deteriorate a portion of granules and COD removal efficiency compared to inoculum without polymer dosing.

2.2.2.2 Seeding sludge

Potential seeding sludges for anaerobic granular sludge reactors include manure, septic tank sludge, digested sewage sludge and surplus sludge from anaerobic treatment plants. de Zeeuw (1984) applied digested sewage sludge as seeding sludge, while Wu et al. (1987) used aerobic activated sludge from a sewage treatment plant and primary sludge from an aerobic plant for startup. It is proven that addition of a small amount of granules to non-granular inoculum could stimulate the granulation process (Xu and Tay 2002). This is probably a consequence of supplying a specific inoculum that is responsible for granulation. Inoculation with a large amount of seed granular sludge from a healthy UASB reactor is desirable when it is feasible. UASB systems can also be started-up using existing granules.

2.2.3 Characteristics of anaerobic granules

2.2.3.1 Microstructure

Different types of microstructure for anaerobic granules have been reported. A multilayer model for anaerobic granulation based on the microscopic observations has been proposed (MacLeod et al. 1990; Guiot et al. 1992). According to this model, the microbiological composition of granules is different in each layer. The inner layer mainly consists of methanogens that may act as nucleation centers that are necessary for the initiation of granule development. H_2 -producing and H_2 -utilizing bacteria are dominant species in the middle layer and a mix of species including rods, cocci and filamentous bacteria predominates in the outermost layer.

A distinct layered structure has been discovered in the methanogenic-sulfidogenic aggregates, with sulfate-reducing bacteria in the outer 50 to 100 μm and methanogens in the inner part (Santegoeds et al. 1999). Unlike the initial multilayer model proposed by MacLeod et al. (1990), research shows that UASB granules have large dark non-staining centers in which neither archaeal nor bacterial signals are observed (Rocheleau et al. 1999). These non-staining centers may be formed as a result of the accumulation of metabolically inactive, decaying biomass and inorganic material (Sekiguchi et al. 1999).

Anaerobic granules with a homogeneous non layered structure have also been reported (Grotenhuis et al. 1991; Fang et al. 1995). Filamentous microorganisms were predominant throughout such granules. Some researchers have argued that layered and nonlayered microstructures can be developed with carbohydrates and proteins as substrates, respectively (Fang et al. 1995). It has been suggested that the granular microstructure is dependent on the degradation kinetics of the substrate. In other words, different dominating catabolic pathways may give rise to different granules (Daffonchio et al. 1995; Schmidt and Ahring 1996).

2.2.3.2 Physicochemical properties

Cell surface hydrophobicity

Research suggests that cell surface hydrophobicity plays a crucial role in anaerobic granulation (Tay et al. 2000; Teo et al. 2000; Liu et al. 2003e). Increasing cell surface hydrophobicity causes a decrease in the excess Gibbs energy of the surface and further facilitates cell-to-cell interactions leading to a stable structure. Some environmental factors are known to influence cell surface hydrophobicity. These factors include starvation, oxygen level, selection pressure and the ionic strength of the medium (Rouxhet and Mozes 1990; Castellanos et al. 2000; Liu et al. 2003e, 2004c; Qin et al. 2004a). Biosolids washed out from the UASB reactors have been found to be more hydrophilic than the sludge retained in the reactor (Mahoney et al. 1987). This seems to indicate that in the presence of a selection pressure such as a high liquid upflow velocity, microorganisms having a high surface hydrophobicity can be self-immobilized to form denser aggregates that remain in the reactor. Anaerobic granules tend to become weaker as the surface negative charge increases (Quarmby and Forster 1995). Therefore, it can be concluded that the anaerobic granulation is closely correlated with cell surface properties.

Size

The size of anaerobic granules has a dual effect on the performance of a UASB system. If the granule is too small, it is likely to be easily washed out of the reactor and this leads to operational instability. On other hand, a large size of granules reduces mass transfer within it. In industrial practice, a narrow size distribution of granules is preferred and medium-sized granules with a diameter of 1.0 to 2.0 mm seem the most attractive. In UASB reactors, anaerobic granules can grow up to 2 to 5 mm or larger. The large anaerobic granules in UASB reactors are usually associated with fluffy bacteria.

Density

The density of anaerobic granules indicates their compactness and range in specific gravity from 1.033 to 1.065 (Pereboom and Vereijken 1994; Tay and Yan 1996). The size and density of anaerobic granules depend on many factors including hydrodynamic conditions, COD loading rate, and the microbial species involved. Anaerobic granules with low density can be easily lost with the effluent. The relatively high specific gravity of individual anaerobic granules allows them to settle rapidly. This permits good separation of solids and liquid in a compact separator.

Strength

The strength of anaerobic granules strongly influences the stability of granules. A high strength indicates a more compact and stable structure of the granules. High COD loading rates result in low-strength anaerobic granules (Quarmby and Forster 1995). The strength of anaerobic granules depends on many factors including the microbial diversity, organics loading rate, the feed, exopolysaccharide production, and hydrodynamic shear forces. High-strength anaerobic granules are desirable in industrial applications.

2.3 AEROBIC GRANULATION

Since Mishima et al. (1991) first found aerobic granules in sequencing batch reactors, aerobic granulation technology attracts intense research. Many factors affecting the aerobic granulation were studied thoroughly. Several models of the mechanism of aerobic granulation were proposed, but no consensus was reached for the mechanism because no model can be verified by experimental method yet. Though the mechanism is not completely clear, several essential conditions for the formation of aerobic granules were identified.

2.3.1 Essential conditions for aerobic granulation

2.3.1.1 Organic loading rate

It is demonstrated that aerobic granules can form under a wide organic loading rate (OLR) range of 2.5 to 15 kg COD m⁻³ d⁻¹. OLR also affects the structure of aerobic granules. The mean size of aerobic granules was larger when the organic loading was higher (Moy et al. 2002; Chen et al 2008; Tay et al. 2004b). Aerobic granules cultivated under higher organic loading rate have higher growth rate, loosen structure, lower dry biomass density, physical strength than aerobic granules cultivated under lower organic loading rate.

Moy et al. (2002) found that glucose-fed granules exhibited a loose fluffy morphology dominated by filamentous bacteria at low OLR, while these granules became irregularly shaped, with folds, crevices and depressions at higher OLRs of 6 to 9 COD m⁻³ d⁻¹. Different OLRs were achieved by varying influent COD concentration, while HRTs were kept at the same level.

In study of the effect of high OLR on aerobic granules, Chen et al. (2008) found that the selection and enriching of different bacterial species under different organic loading rates had an important effect on the characteristics and performance of the mature aerobic granules and caused the difference on granular biodegradation and kinetic behaviors. In the study by Chen et al. (2008), different OLRs were achieved by changing influent COD concentration, while HRTs were maintained at the same level. Larger and denser aerobic granules were developed and stabilized at relatively higher organic loading rates with decreased bioactivity in terms of specific oxygen utilization rate and specific growth rate. With the increase of organic loading rate, solid retention time is increased and net sludge production is decreased. Decay rate and true growth yield changed insignificantly, and can be regarded as constants under different organic loading rates.

2.3.1.2 Substrate composition

Aerobic granules have been successfully cultivated with a wide variety of substrates, including glucose, acetate (Moy et al. 2002), ethanol (Yang et al. 2003), phenol (Jiang et al. 2002), and inorganic carbon source (Tay et al. 2002b; Tsuneda et al. 2003). However, granule microstructure and species diversity appear to be related to the type of carbon source. The glucose-fed aerobic granules have exhibited a filamentous structure, while acetate-fed aerobic granules have had a non-filamentous and very compact bacterial structure in which a rod-like species predominated. Nitrifying granules showed an excellent nitrification ability and better stability (Yang et al. 2004b).

2.3.1.3 Sequencing batch reactor operation and aerobic starvation

A SBR operation cycle includes feeding, aeration, settling and withdrawing of effluent. In aeration stage, the substrate is depleted during the first a few minutes, then no external substrate is available and the aerobic granules undergo aerobic starvation until the end of aeration. The cycle of feast famine happens in each cycle of the operation.

Microorganisms are found to be able to change their surface characteristics when starved. Li et al. (2006) studied the influence of starvation phase on the properties and the development of aerobic granules and proposed that aerobic granulation was initiated by starvation phase and then enhanced by anaerobic metabolism. The study systematically evaluated the influence of starvation phase on surface negative charge, relative hydrophobicity, extra-cellular polymer substances (EPS) and the formation mechanism of aerobic granules. Aerobic granules with encouraging settling properties were observed in the reactor about 7 days after the inoculation. The surface negative charge decreased from 0.203 to 0.023 meq g VSS⁻¹ and the relative hydrophobicity increased from 28.8 to 60.3% during the granulation period. Concentrations of protein and carbohydrate decreased from 18.0 to 7.1 mg g VSS⁻¹ and 7.0 to 2.9 mg g VSS⁻¹, respectively in the first period. And from day 13, those

values were observed in the range of 5.8–8.6 and 2.9–5.6 mg g VSS⁻¹, respectively. The EPS especially protein concentrations well correlated with surface charge and relatively hydrophobicity. It was concluded that the amount of EPS should be controlled to form and maintain aerobic granules.

The starvation time also has effect on formation of aerobic granules (Liu and Tay 2008). Liu and Tay (2008) applied different cycle times that led to three different starvation times in repeated cycles of the three reactors. It was found that shorter cycle time with a shorter starvation time speeded up the granulation. This was mainly due to the stronger hydraulic selection pressure at shorter cycle time. However, it was found that granules formed with the shortest starvation time were unstable. Therefore, the starvation time should be long enough to maintain the long-term stability of aerobic granules.

2.3.1.4 Hydrodynamic shear force

A high shear force in terms of superficial upflow air velocity is essential for aerobic granulation. Aerobic granules could only form only when the superficial upflow air velocity is above 1.2 cm s⁻¹ in column SBR. The essential roles of high shear force are displayed in two aspects. First, a high shear force affects the structure of aerobic granules. Tay et al. (2001b) found that aerobic granules developed under higher shear force have rounder, more regular and compact structures. Tay et al. (2003a) found that the density and strength of aerobic granules were correlated with the applied shear force. Second, a high shear force induces higher production of extracellular polysaccharides, which can facilitate the cohesion and adhesion between cells and is crucial to maintain structural integrity of immobilized cells. Shear force was found to be closely related with the production of extracellular polysaccharides, which was found to be correlated with the stability of aerobic granules. High shear force cause aerobic granules produce more extracellular polysaccharides. This may be part of reason why high force make the aerobic granules more compact.

2.3.1.5 Settling time

At the end of every cycle, the biomass is settled before the effluent is withdrawn. The settling time acts as a major hydraulic selection pressure on microbial community. A short settling time preferentially selects for the growth of fast settling bacteria and the sludge with a poor settleability is washed out. Qin et al. (2004b) reported that aerobic granules were successfully cultivated and became dominant only in the SBR operated at a settling time of 5 minutes. Mixtures of aerobic granules and suspended sludge were observed in the SBRs run at settling times of 20, 15 and 10 minutes. The production of extracellular polysaccharides was stimulated and the cell surface hydrophobicity improved significantly at short settling times. These findings illustrate the fact that aerobic granulation is driven by selection pressure and the formation and characteristics of the granules may be controlled by manipulating the selection pressure. Therefore, choice of an optimal settling time is very important in aerobic granulation. Generally, the mature aerobic granules tend to settle within 1 min, leaving a clear supernatant in the reactor (Tay et al. 2001a).

2.3.1.6 Hydraulic retention time

Pan (2003) studied the hydraulic retention time (HRT) on aerobic granulation and found that aerobic granules could form under only the hydraulic retention time between 2 and 12 hours. No aerobic granules were cultivated out of this HRT range until now. Pan (2003) concluded that aerobic granules could not form under too low HRT because too low HRT caused the frequent washout of biomass, while too high HRT provide too weak selection pressure to form aerobic granules. The average size of aerobic granules decreased with the increase of HRT (Pan 2003).

2.3.1.7 Dissolved oxygen

The views on dissolved oxygen are not in consensus in the literatures. Aerobic granules have been usually developed at dissolved oxygen (DO) concentrations of $>2 \text{ mg L}^{-1}$ (Yang et al. 2003), but aerobic granules have formed at DO concentration as low as 0.7 to 1.0 mg L^{-1} in a SBR (Peng et al. 1999). However, McSwain (2004) tried cultivating aerobic granules with different DO and concluded that granule formation requires a high DO concentration during the react phase when a static fill is applied. Aerobic granules can not form when the DO is limiting, even if a high shear force and short settling time is provided to the SBR. Chen et al's (2008) results seem to reconcile the contradiction, they found that the DO was low at the beginning of the aeration stage then increased with the depletion of substrate. Maybe both Peng et al. (1999) and McSwain (2004) ignored that DO is fluctuating in each cycle.

2.3.1.8 Temperature

Aerobic granules are usually cultivated at the methophilic temperatures, which are in the range of 15 to 45°C . Thermophilic aerobic granules have been cultivated in a few cases with special control technique. However, the cultivation of aerobic granules under psychrophilic condition ($<15^\circ\text{C}$) was unsuccessful. Aerobic biological biomass usually flocculates poorly under thermophilic conditions, which are between 45 and 65°C . Daniel et al. (2006) cultivated under the temperature of 55°C a mixture of granular and flocculant biomass resulted when closed reactors were aerated with recirculated reactor headspace gas containing some air. In their study, the conventionally aerated control reactor contained dispersed growth that did not flocculate. The maximum diameters of aerobic granules were from 1.2 to 1.9 mm , and the strength of the aerobic granules was comparable to mesophilic aerobic granules.

Guyen (2004) also cultivated thermophilic aerobic granules under the temperature of 55°C with a special feed schedule, without which aerobic granules could not be cultivated. 50% to 75% of the feed must be pumped to the reactor at the beginning

of the first feed period in a cycle when oxygen was not supplied. The rest of the feed should be added at the beginning of the second feed period when oxygen was supplied. The average diameters of the thermophilic aerobic granules were 1.1 to 1.9 mm and average respect ration is 77% to 83%. Unlike Daniel et al.'s (2006) results, Guven (2004) found thermophilic aerobic granules the settling velocity, removal efficiency strength were only a little comparable with mesophilic aerobic granules.

De Kreuk's (2005) attempted to cultivate aerobic granules at 8°C was not successful, because the sludge in the reactor was subject to severe biomass washout and instable operation. However, start-up at 20 °C and lowering the temperature to 8 °C did not have any effect on granule stability and biomass could be easily retained in the reactor. De Kreuk (2005) concluded that start-up in practice should take place preferentially during warm summer periods, while decreased temperatures during winter periods should not be a problem for granule stability and COD and phosphate removal in a granular sludge system.

2.3.1.9 Reactor configuration

Reactor configuration has an impact on the flow pattern of liquid and microbial aggregates in the reactor (Beun et al. 1999; Liu and Tay 2002). Almost all aerobic granules were produced in cylinder column reactors until now. Most of the cylinder column reactors are traditional SBR reactors, while airlift reactors are applied in a few cases. The SBR should have a high H/D ratio to improve selection of granules by the difference in settling velocity (Beun et al. 1999). The high H/D ratio also enables the area of the reactor to be small if the volume of the reactor is fixed. Under the same amount of aeration, the surface aeration velocity will be higher. Compared with low H/D reactors, the shear force will be bigger and granules are more irregular in shape and size.

2.3.2 Advantages of aerobic granules

In comparison with the irregular, loose, fluffy conventional activated sludge, aerobic granules are superior in the following aspects: (i) regular, smooth round shape and clear outer boundary, which is beneficial to easy solid-liquid separation; (ii) denser and stronger microbial structure; (iii) high biomass retention and excellent settleability; (iv) visibility as separate entities in the mixed liquor (v) capability of withstanding high flow rates; (vi) capability of withstand high organic loading rates; (vii) strong endurance to the toxic substances in wastewater. The excellent settleability of aerobic granules simplifies the separation of treated effluent from the granular sludge.

2.3.2.1 Morphology

Aerobic granules' morphology enables them settle fast. The shapes of aerobic granules are nearly spherical with clear outlines (Peng et al., 1999; Tay et al. 2001a; Zhu and Wilderer 2003). The morphology results from a balance between growth and abrasive detachment caused strong hydrodynamic shear force in aerobic reactors (Liu and Tay 2002; Liu et al. 2003f). Hydrodynamic shear forces are known to control the prevailing size of the suspended biosolids in many situations (Chisti 1999a). The diameters of aerobic granules vary in the range of 0.2 to 5 mm.

2.3.2.2 Settleability

The settleability of aerobic granules determine the efficiency of biomass removal from effluent. The settling velocity of aerobic granules is positively related with granule size and is as high as 30 to 70 m h⁻¹. The high settling velocities of aerobic granules allow the use of relatively high hydraulic loading in the reactors without washout of biomass (Beun et al. 2000b; Tay et al. 2001b). Thus, aerobic granulation can lead to more biomass retention in the reactor and this can enhance the performance and stability of the reactor. The sludge volume index (SVI) of aerobic granules is usually lower than 50 ml g⁻¹, which is much lower than that of conventional activated sludge (Liu et al. 2003e; Qin et al. 2004).

2.3.2.3 Strength and density

The granules with a high physical strength withstand high abrasion and shear force. The physical strength, expressed as integrity coefficient, which is the percentage of residual granules to the total weight of the granular sludge after 5 minutes of shaking at 200 rpm on a platform shaker. The physical strength is higher than 95% for the aerobic granules grown on glucose and acetate (Tay et al. 2002c). The physical strengths of aerobic and anaerobic granules are comparable. Aerobic granules with smaller sizes tend to be denser compared to larger aerobic granules (Toh et al. 2003; Yang et al. 2004a). The high strength of aerobic granules maybe is related with the high specific gravity of aerobic granules are in the ranges of 1.004 to 1.065 (Etterer and Wilderer 2001; Tay et al. 2001a; Yang et al. 2003).

2.3.2.4 Hydrophobicity of cell surface

Cell surface hydrophobicity is an important affinity force in cell self-immobilization and attachment processes (Pringle and Fletcher 1983; Kosaric et al. 1990; Liu et al. 2003a). The role of cell surface hydrophobicity in the formation of aerobic granules is not clear. Liu et al. (2003a) have linked the formation of heterotrophic and nitrifying granules to the cell surface hydrophobicity. The hydrophobicity of granular sludge was nearly two-fold higher than that of conventional bioflocs. A high shear force or hydraulic selection pressure imposed on microorganisms resulted in a significant increase in the cell surface hydrophobicity, while the cell surface hydrophobicity seemed not to be sensitive to the changes in the organic loading rates.

2.3.2.5 Storage stability

The storage stability is important for aerobic granules to survive in non-influent conditions and for using precultured aerobic granules as bioseed. To study the feasibility of transporting stored aerobic granules as bioseeds, Zeng et al. (2007) the storage stability, physicochemical characteristics, and recovering efficiency of

stored aerobic granules. In Zeng et al.'s (2007) study, phthalic acid (PA)-degrading aerobic granules were cultivated and stored for 8 week at 4 °C. The granular size, settling ability and structure integrity were stable during the storage period. After the 8-week storage, the upper 1/3 part of granules stored in the reagent bottle turned to black color, while the lower 2/3 part granules did not significantly change color (brown–yellow). The black and brown–yellow color PA-degrading granules were manually separated and re-inoculated into two identical sequencing batch reactors for reviving the PA degradation capability. After a 7 days operation, both black and yellow granules restored their activities to the levels before storage, in terms of total organic carbon removal efficiency, specific oxygen uptake rate ($59 \text{ mg g VSS}^{-1} \text{ h}^{-1}$), and adenosine triphosphate content ($0.016 \text{ mg g}^{-1} \text{ VSS}^{-1}$). The study demonstrated that aerobic granules grown on a complex substrate could tolerate storage conditions and rapidly restored their bioactivities toward the target pollutant.

Zhu et al. (2003) studied the possibility of keeping aerobic granular sludge reactor under idle phase for long time and its revitalizing. Zhu et al.'s (2003) results revealed that the size, color and sedimentation characteristics of the granular sludge did hardly change during the seven weeks storage period. However, sludge activity in terms of oxygen consumption rate dropped to values as low as $0.17 \text{ mg min}^{-1} \text{ L}^{-1}$. After restarting the reactor, the OCR increased within 1 day to a level of $0.57 \text{ mg min}^{-1} \text{ L}^{-1}$, kept rising at a linear rate in the following days, and reached after 1 week, a value of $5.74 \text{ mg min}^{-1} \text{ L}^{-1}$ typical for the former activity status. These results imply that granular activated sludge can be stored for a considerably long period of time, and brought into service again relatively quickly. After an idle period of 7 weeks, it took less than a week to regain full capacity of the SBR.

In another study by Wang et al. (2008), aerobic granules were stored for seven months and then reactivated successfully. Wang et al. (2008) found that the granule size and structure integrity remained during storage, whereas some cavities and pleats appeared on the surface and further deteriorated the settleability. Extracellular polymeric substances (EPS) significantly decreased within the first month, and then gradually accumulated during the last six months storage.

Accumulation of EPS was an effective strategy for maintaining structural integrity of aerobic granules during long-term storage. During the reactivation, the physical characteristics and microbial activities of aerobic granules were gradually improved. Activities of heterotrophs and nitrifiers can be fully recovered within 16 days and 11 days respectively. Nitrifiers were reinstated faster during reactivation than heterotrophs.

2.3.3 Drawbacks of aerobic granules

The main drawback of aerobic granules is their low activity caused by diffusion limitation. Microbial activity of microorganisms is indicated by the specific oxygen utilization rate (SOUR). Generally, aerobic granules have lower SOUR than activated sludge. Liu et al. (2005a) stated that diffusion limitation is the reason why aerobic granules have low activity. The degree of diffusion limitation can be described by effectiveness factor, which is defined as a ratio of reaction rates of substrate with and without diffusion limitations. Liu et al. (2005a) also pointed that the kinetic behaviours of aerobic granules were size dependent, while the size of granule is determined by a combination of several factors.

2.3.4 Microbial structure and diversity

2.3.4.1 Microbial structure

Confocal laser scanning microscopy (CLSM) has been used with different oligonucleotide probes, specific fluorochromes and fluorescent microspheres for studying the microstructure of aerobic granules (Tay et al. 2002d, 2003a; Toh et al. 2003; Jang et al. 2003; Meyer et al. 2003). The obligate aerobic ammonium-oxidizing bacterium *Nitrosomonas* spp. was found mainly at a depth of 70 to 100 μm from the granule surface, and aerobic granules contained channels and pores that penetrated to a depth of 900 μm below the granule surface. The porosity peaked at depths of 300 to 500 μm from the granule surface (Tay et al. 2002d, 2003a). These channels and pores would facilitate the transport of oxygen and nutrients into

and metabolites out of the granules. Polysaccharide formation peaked at a depth of 400 μm below the granule surface. The anaerobic bacterium *Bacteroides* spp. also detected at a depth of 800 to 900 μm from the granule surface (Tay et al. 2002d), while a layer of dead microbial cells was located at a depth of 800 to 1000 μm (Toh et al. 2003). In order to fully utilize the aerobic microorganisms in the granules, the optimal diameter for aerobic granules should be less than 1600 μm , which is twice the distance from the granule surface to the anaerobic layer (Tay et al. 2002d). Consequently, smaller granules will be more effective for aerobic wastewater treatment as these granules have more live cells within a given volume of granules.

Yang et al. (2004b) observed the mushroom-like structure of aerobic granules developed at high substrate N/COD ratios. The nitrifying population was mainly located at a depth of 70 to 100 μm from the surface of the granule (Tay et al. 2002d). Research has shown that biofilms of mixed bacterial communities can form thick layers consisting of differentiated mushroom-like structures (Costerton et al. 1981) that are similar to structures observed in aerobic granules. There is strong evidence that bacteria sense and move towards nutrients (Prescott et al. 1999). It has been demonstrated that biofilms can form the mushroom-like structures by simply changing the diffusion rate, i.e. the biofilm structure is largely determined by nutrient concentration (Wimpenny and Colasanti 1997). Since nitrifying bacteria are slow-growing, the mushroom-like structures seem to result from the demand of nitrifying population for nutrients. These structures improve the access of the nitrifying population to nutrients. As Watnick and Kolter (2000) noted, in mixed biofilms, bacteria distribute themselves according to who can survive best in the particular microenvironment and the high complexity of the resulting microbial community appears to be beneficial to its stability. Consequently, the distribution of different microbial populations in a granule may have an effect on its stability.

2.3.4.2 Microbial diversity

Microbial diversity of aerobic granules has been studied by molecular biotechnology techniques (Yi et al. 2003; Tay et al. 2002d; Jang et al. 2003; Meyer

et al. 2003; Tsuneda et al. 2003). Heterotrophic, nitrifying, denitrifying, P-accumulating bacteria and glycogen-accumulating bacteria have been identified in aerobic granules developed under different conditions (Jang et al. 2003; Meyer et al. 2003; Tsuneda et al. 2003; Lin et al. 2003; Liu et al. 2003e; Yang et al. 2003). The microbial diversity of aerobic granules is closely related to the composition of culture media in which they are developed and the structure of aerobic granules. Anaerobiosis and dead cells have been reported at the centers of aerobic granules (Tay et al. 2002d). The presence of anaerobic bacteria in aerobic granules is likely to result in the production of organic acids and gases within the granules. These end products of anaerobic metabolism can destroy the granules, or at least diminish their long-term stability.

2.3.5 Aerobic granulation for special wastewater treatment

Process efficiency of large scale treatment plants can be improved by using aerobic granular sludge in ways that allow high conversion rates and efficient biomass separation to minimize the reactor volume. Treatment capacities can be easily varied to accommodate varying loading rates, wastewater composition, and treatment goals by bioaugmentation with specifically developed granules.

2.3.5.1 High strength organic wastewater treatment

The previous cultivation of aerobic granules under high organic loading rate was reported by Moy et al. (2002). In their study, glucose or acetate were applied as the carbon source respectively and increased the organic loading rate gradually from 6 to 9, 12 and 15 kg COD m³ d⁻¹. Glucose-fed granules were found sustained the maximum OLR tested, while acetate-fed granules could not sustain high OLRs and disintegrated when the OLR reached 9 kg COD m³ d⁻¹. However, Moy et al.'s (2002) study did not show whether aerobic granules could be cultivated directly at an organic rate higher than 6 kg d⁻¹.

Chen et al. (2008) reported that compact bacteria-dominated aerobic granules with a mean diameter of 1 mm were formed at a chemical oxygen demand (COD) loading

rate of $6.0 \text{ kg m}^{-3} \text{ d}^{-1}$ within 30 days. However, the compact bacteria-dominated aerobic granules were not stable and transited to large-sized filamentous ones gradually. Zheng et al. (2006) reported that the compact bacteria-dominated aerobic granules were not stable and transited to large-sized filamentous ones gradually.

2.3.5.2 Carbon and nitrogen removal

To achieve carbon and nitrogen removal, granules are not purely aerobic but a large portion of the bacteria in the granules are aerobic. Yang et al.'s (2003) study was the first to show the capability of microbial granules in simultaneous removal of organic carbon and nitrogen from wastewater. The study demonstrated that complete organics and nitrogen removal can be achieved in single granule-based SBR with high efficiency and stable performance. They discovered that heterotrophic, nitrifying, and denitrifying populations could co-exist in microbial granules, while increased substrate N/COD ratio led to significant shifts among three populations in granules. Heterotrophic populations in granules tended to decrease with the increase of substrate N/COD ratio. It was found that dissolved oxygen (DO) concentration had a pronounced effect on the efficiency of denitrification by microbial granules, meanwhile the results also indicated that a certain mixing power would be provided to ensure mass transfer between liquid and granules during denitrification.

It was found that selection of slow-growing nitrification bacteria could improve the stability of aerobic granules (Liu et al. 2004c). Aerobic granules with low growth rates showed strong structure and good settleability in terms of specific gravity, SVI and cell hydrophobicity that further lead to high stability as compared to those having high growth rates. Liu et al.'s (2004c) study verified that aerobic granules stability could be improved at the same time of removing ammonia in wastewater.

Qin and Liu (2006) developed aerobic granules with excellent settleability at different ammonium loadings in four sequencing batch reactors run under alternating aerobic-anaerobic conditions. The aerobic granules were subject to anaerobic conditions in every cycle, which enabled denitrification. Qin and Liu

(2006) also found that heterotrophic, nitrifying and denitrifying populations could co-exist in the aerobic granules. The activity of denitrifying bacteria was highly dependent on the availability of external carbon source in the anaerobic phase. Complete denitrification was achieved with supply of external carbon source, while only partial denitrification was observed with no addition of external carbon source. Their study shows that aerobic granules cultivated under the alternating aerobic–anaerobic condition could efficiently remove organic carbon and completely convert ammonia to nitrogen gas.

2.3.5.3 Aerobic granulation for removing phosphorous

Lin et al. (2003) developed phosphorus-accumulating aerobic granules with the substrate P/chemical oxygen demand (COD) ratio up to 10/100 by weight in sequencing batch reactors. The soluble COD and $\text{PO}_4\text{-P}$ profiles were similar as typical phosphorus-accumulating process, which included concomitant uptake of soluble COD and the release of phosphate in the anaerobic stage and rapid phosphate uptake in the following aerobic stage.

The characteristics of aerobic granules were found related with the phosphorus/COD ratio. The size and SVI of phosphorus-accumulating granules decreased with the increase in substrate P/COD ratio, while the structure of the granules was more compact and denser as the substrate P/COD ratio increased. The phosphorus contents in aerobic granules were between 1.9% and 9.3% by weight, which is comparable with P content in conventional enhanced biological phosphorus removal processes.

2.3.5.4 Simultaneous organic and nutrients removal

Aerobic granules were cultivated successfully for simultaneous chemical oxygen demand (COD), nitrogen and phosphate removal in one sequencing batch reactor. According to de Kreuk et al. (2005), simultaneous nutrient removal was possible, because of heterotrophic growth inside the granules (denitrifying PAO). At low oxygen saturation (20%) high removal efficiencies were obtained; 100% COD removal, 94% phosphate removal and 94% total nitrogen removal (with 100%

ammonium removal). Experimental results strongly suggest that P-removal occurs partly by biologically induced precipitation. Monitoring the laboratory scale reactors for a long period showed that N-removal efficiency highly depends on the diameter of the granules. Selection for slow-growing organisms such as phosphate-accumulating organisms (PAO) was shown to be a measure for improved granule stability, particularly at low oxygen concentrations. Moreover, this allows long feeding periods needed for economically feasible full-scale applications.

2.3.5.5 Aerobic granulation for treatment of domestic wastewater

The use of aerobic granules in wastewater treatment can reduce the land area that is needed for the treatment of sewage. Until now granulation has been mainly studied using artificial wastewater. de Kreuk and van Loosdrecht (2006) studied the possibility of forming aerobic granules on domestic sewage in a sequencing batch reactor using presettled sewage as influent. After 20 days of operation at high chemical oxygen demand (COD) loading heterogeneous aerobic granular structures were observed, with a sludge volume index after 10 min settling of 38 mL g^{-1} and an average diameter of 1.1 mm. Applying a high COD load, by means of high COD concentration or short cycle time, was found to be a critical factor for the formation of aerobic granules on this type of influent. Therefore short cycle times and concentrated wastewaters are preferred to form granules in a sequencing batch reactor when low strength wastewater is used.

2.3.5.6 Phenolic wastewater treatment

Using phenol as the sole carbon source, aerobic granules were successfully cultivated in several studies. Tay et al. (2004a) started the reactor at a loading rate of $1.5 \text{ kg phenol m}^{-3} \text{ d}^{-1}$ with phenol-enriched activated sludge as inoculum. After the aerobic granules were matured, the phenol loading was then adjusted stepwise to a final value of $2.5 \text{ kg phenol m}^{-3} \text{ d}^{-1}$. At such high loading, phenol was completely degraded and high biomass concentration was retained in the reactor. The biomass still had good settling ability, with a sludge volume index of 60.5 mL g^{-1} mixed liquid suspended solids. Granules remained stable in structure and

physiology even at the maximum phenol loading rate tested. In this study, specific phenol degradation rates exceeded $1 \text{ g phenol g}^{-1}\text{VSS d}^{-1}$ (volatile suspended solids) under the phenol concentrations of 500 mg L^{-1} . It is considered that the compact structure of the aerobic granules protected the microbial cells against the phenol toxicity.

However, Adav et al. (2007) reported that an active biomass was accumulated at the granule outer layer in phenol-cultivated aerobic granules, using fluorescent staining and confocal laser scanning microscopy (CLSM). The findings by Adav et al. (2007) may help to verify if the active biomass would be under outer layer protection. In their study, cultivated aerobic granules could degrade phenol at a constant rate of $1176 \text{ mg-phenol g}^{-1}\text{VSS h}^{-1}$ up to $1,000 \text{ mg L}^{-1}$ of phenol. A strain, named *Candida tropicalis*, was isolated in the study, which could degrade phenol at a maximum rate of $390 \text{ mg-phenol g}^{-1}\text{VSS h}^{-1}$ at pH 6 and 30°C , whereas inhibitory effects existed at concentrations $>1,000 \text{ mg L}^{-1}$. The fluorescence in situ hybridization (FISH) and CLSM test suggested that the *Candida* strain was primarily distributed throughout the surface layer of granule. This is why a near constant reaction rate over a wide range of phenol concentration. The mass transfer barrier provided by granule matrix did not determine the reaction rates for the present phenol-degrading granule.

2.4 MASS TRANSFER INSIDE MICROBIAL AGGREGATES

2.4.1 Mass transfer inside activated sludge

Usually, diffusion resistance is ignored when activated sludge is studied, because the activated sludge is small in size and is loose and fluffy in structure. All the activated sludge models, Activated Sludge Model 1 (ASM1) (Henze et al. 1987), Activated Sludge Model 2 (ASM2) (Henze et al. 1995) and Activated Sludge Model 3 (ASM3) (Gujer et al. 1999), do not consider diffusion limitation inside activated sludge.

2.4.2 Mass transfer inside biofilm

Mass transfer has much stronger effects on biofilms than on activated sludge. Most studies on mass transfer inside biofilm were based on mathematical models, because it is almost impossible to measure the parameters inside biofilms by experimental tools.

2.4.2.1 One-dimensional biofilm model

Rittman and McCarty (1981) developed a model for estimating substrate flux into a biofilm of any thickness, which included external mass transfer resistance. With this model, the flux became a direct function of the bulk substrate concentration, which is typically the measured concentration of interest. An explicit solution was available for thick biofilms, and a simple iterative solution was used for thin biofilms. This model had the ability to predict the flux of a single rate-limiting substrate when the biofilm thickness was independently known.

Wanner and Gujer (1985) proposed a one dimensional dynamic models. The model was based on mass conservation laws and consisted of several partial differential equations, describing the growth and advection of bacterial mass. These were coupled with reaction-diffusion equations that governed the dynamics of substrate and bacterial waste products. These equations governed behavior in a one-dimensional spatial region between the substratum and the interface between the biofilm and the bulk fluid. The interface was assumed to move due to growth and advection of the biofilm. The interface position indicated the thickness of the biofilm. The model could be used to predict the concentration of water products and substrate within the biofilm as well as the substrate uptake by the biofilm. This model can be used to simulate both single and multiple species biofilms.

Pritchett (2000) derived another complicated one-dimensional biofilm model, which considered the simultaneous interactions of active biomass, inert biomass, substrate, biomass spreading velocity and liquid-biofilm interface. The model could be

applied to describe quantitatively the effects of different parameters. The model was alternated and used to describe the production of EPS. It is demonstrated that the amount of EPS is significant only when the production rate is above a minimum level. The one-dimensional model was more applicable than the two-dimensional and three-dimensional models emerging in the 1990s. The one-dimensional model needed much less computing resources and showed enough accuracy at the time.

2.4.2.2 Two-dimensional and three-dimensional biofilm model

Two-dimensional and three-dimensional biofilm models have evolved from two approaches, which are cellular automata and traditional numerical solution. Wimpenny (1997) was one of the first to introduce cellular automata to biofilm structure model. In the model, the two-dimensional space is divided into compartments which can hold cells and substrates. This is one of the first stochastic model of biofilm structures. This model has not accounted for the flow of liquid and ignored the convection function in substrate transport. The diffusion law is different from the laws usually used. At last, it is only a qualitative model not quantitative one. But the model paves the way for application of cellular automata into the biofilm modeling.

The models were achieved by Picioreanu et al. (1998). The model solved the concentration profiles inside and outside the three dimensional biofilm using finite difference approximations of diffusion and reaction equations. Biofilm growth was modeled with finite difference, but cell redistribution inside the biofilm was modeled using a discrete approach. Using a discrete scheme for cell redistribution within the biofilm allowed simulating heterogeneity, because cells were given the possibility to colonize new spaces in random directions. The model considered a physical domain that contains of bacteria, substrate and liquid and consists of two different phases. One phase was biofilm phase and the other is liquid phase. In these models, the role of EPS was not considered, which affected the biofilm redistribution tremendously.

Picioreanu (1998) proposed a novel model that combines differential discrete method and cellular automaton together. The model was also one of the few models which could simulate 3-D biofilm structures. In the model, the biofilm was modeled in a discrete way, whereas the nutrient field was solved by using conventional differential equations based on mass balances that contained well-know conversion kinetics and mass transport terms. Cellular automation was also used to simulate the biofilm growth. This model included: (i) liquid flow around the biofilm; (ii) substrate mass transport by diffusion and convection in the liquid phase and by diffusion only in the biofilm-gel matrix; (iii) substrate conversion and biomass growth, and (iv) biomass spreading based on cellular automata.

Pizarro (2001) further developed a two-dimensional Cellular Automation biofilm model. Compared with Wimpenny's (1997) model, this model incorporates more factors. Firstly, the model simulated dynamics of the system using stochastic processes that represent the occurrence of specific events within the biofilm. Secondly, the model has the ability of predicting substrate gradients and fluxes of substrate. Finally, the model also compared the evaluation of substrate gradients and fluxes of substrate with the results obtained by a traditional differential equations model. In addition, two parameters usually considered constant, biomass density and thickness of the boundary layer, are proposed to be replaced by the biomass per unit area and the thickness of the mass transfer limited zone, which lumps biofilm and boundary layer thickness. In this way, the restrictions typically imposed to 1D models are related and an iterative procedure can be used to calculate steady-state flux for heterogeneous biofilms where biomass density and boundary layer thickness are not constant. So model also links 2D model and 1D together.

Lapidou (2003) developed another model which predicts quantitatively the developments of the three composites: active biomass, inert biomass and EPS and the concentrations of two soluble organic components and oxygen. The model indicates the trend that the top of the biofilm is dominated by active biomass and EPS, while the bottom is dominated by residual inert biomass. The top of all biofilms is quite fluffy, and all biomass types show considerable local heterogeneity.

The capacities of this model also expand to calculate the different mechanic characteristics throughout biofilms such as the elastic and isotropic and non homogeneous material.

The biofilm models by traditional numerical simulation also have fast progress. Li (1998) implemented a working model of a fluid-biofilm system in porous media. The model has described the motion of the fluid, the transport equations with convection, diffusion and nonlinear reaction terms to govern the concentration of the dissolved nutrients, and a nonlinear microscale model to simulate the biofilm growth. The model proposed a new scheme to for solving the Navier-Stokes equations. This scheme is superior in the sense that it does not require a small velocity so that it works for those problems that the Stokes approaches do not work well. Second, it is a direct scheme, and interacts on each time step. And the most important, it is a linear scheme, so that at each time step, only linear systems were to be solved.

Visser (1998) also formulated a model that included the interaction of fluid dynamics substrate transport, and biofilm reaction is formulated. Equations modeling the processes of fluid dynamics, substrate transport, and biofilm reaction are solved by the finite difference method, which is different from the Li's finite elements method (Li 1998).

Cogan (2003) proposed a model that accounts for the physical and chemical character of EPS and the interaction between the bulk flow and biofilm growth dynamics. This model has indicated two mechanisms that may cause biofilm heterogeneity. One mechanism involves differential growth of biofilm. If the interface between the biofilm and the bulk region is irregular, bacteria in the peaks of the interface have more ready access to diffusing substrate than those in the troughs. Therefore, these bacteria reproduce at a faster rate, increasing the local network density. Since the network is chemically active, this increase induces an osmotic pressure causing the network to swell. Swelling moves the biofilm interface, reinforcing the nonuniformity. The second mechanism is due to the frictional interaction between the biofilm and the bulk flow .As the bulk fluid moves, it drags

the polymer network along with it. This network displacement induces stress on the network due to tangling and cross-linking interaction within the network. In this manner the network distribution is altered increasing the density of the network in some areas while decreasing it in others. The bulk fluid moves through the regions of low volume fraction more easily, thus the fluid flow is larger there. This reinforces the displacement of network creating channels through the biofilm.

2.4.2.3 Mass transfer inside aerobic granules

The mass transfer of aerobic granules has seldom been studied. Most research reflected the effects of mass transfer, based on outside performance of aerobic granules. Liu et al. (2005a) found size had huge effects on the performance of aerobic granules, because bigger size caused greater diffusion resistance. Gapes et al. (2004) found that when dissolved oxygen was higher, oxygen utilization rate of aerobic granules became higher. No previous research has considered the mass transfer of oxygen and substrate simultaneously.

There is also indirect research into mass transfer into aerobic granules. Using FISH, Tay et al. (2002a) found the penetration depth of oxygen would be 800 μm to 900 μm . Jang et al. (2003) et al. measured the penetration depth of oxygen is 400-500 μm by microelectrode. Based on their experimental observation, Moy et al. (2002) found no anaerobic zone in aerobic granules with a size bigger than 2 mm. Beun et al. (2000) found oxygen could not penetrate into the center of aerobic granules by the simulation tool Aquasim.

2.5 GROWTH KINETICS AND METABOLISM OF AEROBIC GRANULES

The growth kinetics of aerobic granules has been studied by different approaches. Yang et al. (2004a) studied the growth kinetics of aerobic granules cultivated under different organic loading using combination of experimental and modeling tools, and reported the observed growth rate of aerobic granules increased from 0.24 to 0.33 d^{-1} when the size of aerobic granules was increased from 1.65 mm to 1.95 mm.

However, Liu et al.'s (2005a) reported the growth rate of aerobic granules under the same organic loading was negatively correlated with the size of aerobic granules in batch tests. The growth rate decreased from 0.72 to 0.48 d⁻¹ when the size was increased from 0.4mm to 1.2mm. Chen et al. (2008) found the same decreasing trend of growth kinetics with size of aerobic granules as early reported by Liu et al. (2005a). The growth rate was determined to be 0.075 to 0.297 d⁻¹, while the size of aerobic granules was 0.95 to 0.35 mm.

The decay rate of aerobic granules is closed related with the grow kinetics. Liu et al. (2005d) reported the decay rate of 0.023–0.075 d⁻¹ for glucose fed aerobic granules, while Chen et al. (2008) reported the decay rate of 0.065-0.069 d⁻¹ for acetate fed aerobic granules.

Growth yield is an indication of metabolism of aerobic granules. The growth yield for glucose fed aerobic granules was 0.183 to 0.250 mg MLSS mg⁻¹ COD (Liu et al. 2005a), and the growth yield for acetate fed aerobic granules was 0.235 to 0.286 mg MLSS mg⁻¹ COD (Chen et al. 2008). To simplify the measurement and calculation, observed growth yield are used sometimes. The observed growth yield for acetate fed aerobic granules was 0.142 to 0.231 mg MLSS mg⁻¹ COD, which was negatively correlated with size of aerobic granules (Chen et al. 2008).

2.6 THE ROLE OF CALCIUM IN AGGREGATES

2.6.1 The role of calcium in anaerobic granules

2.6.1.1 The effect of calcium on formation of anaerobic granules

The role of Ca²⁺ in anaerobic granulation processes is still uncertain. De Deeuw (1984) reported that the rate of sludge granulation was significantly enhanced at a calcium concentration of 100 mg L⁻¹ in the wastewater. Similarly, Mahoney et al. (1987) observed that granule formation was stimulated by the presence of calcium in a concentration range of 100 to 200 mg. Yu et al. (2001) reported that

introduction of Ca^{2+} at concentrations from 150 to 300 mg L^{-1} enhanced the biomass accumulation and granulation process in UASB reactors. They concluded that the addition of low-concentration calcium to the UASB reactors probably enhanced the three steps of sludge granulation: adsorption, adhesion and multiplication, but it did not lead to a different proliferation of predominant microorganisms in the granules. However, Calcium concentrations exceeding about 500 mg L^{-1} (Guiot et al. 1988; Thiele et al. 1990; Yu et al. 2001) are detrimental to granulation. At high calcium concentrations, problems such as the precipitation of calcium on the surface of granules and accumulation of calcium inside anaerobic granules with consequent reduced microbial activity have been reported (Yu et al. 2001). Research by Teo et al. (2000) showed that an increase in Ca^{2+} concentration from zero to 80 mg L^{-1} substantially improved the strength of anaerobic granules.

2.6.1.2 The effect of calcium on structure of anaerobic granules

Batstone et al. (2002) found that an obvious effect of calcium on the structure of the granules was the core of calcium precipitates. They achieved the estimation of core size according to CO_3^{2-} by fracturing of the granule and SEM imaging. The results indicated the core had a relatively consistent size of 200–400 μm . It seems that as progressive formation of the diameter of the core would result in a variety of core sizes in different granules. It is also observed that the core varied in consistency from a sparse matrix through to a saturated, rock-like mineral. The core may have formed prior to the granule as an amorphous or very sparse CaCO_3 crystal, which acted as a nucleation site for granule formation. During granule growth, calcium probably precipitated within the core, where the crystal surface area was greater than in the microbial region (outer 200–400 μm). The finite granule lifetime produced by core precipitate capacity may help explain the relatively narrow size distribution since few granules were greater than 1.5 mm.

2.6.2 Role of calcium in biofilms

2.6.2.1 The effect of calcium on biofilm formation

Turakhia and Charackli (1988) found that the rate and extent of biofilm accumulation increases with increasing calcium concentration. Rose (2000) also found calcium induced aggregation, allowing association-type kinetics to be used to describe the processes here with a firm degree of confidence.

2.6.2.2 The effect of calcium on biofilm properties

Rose et al. (2000) found that calcium accumulated in the biofilm increased in proportion to the calcium concentration in the water phase. Turakhia and Charackli (1988) reported that the immobilized calcium increased the cohesiveness of the biofilm as reflected by the decreased detachment rate at higher calcium concentrations. However, the activity of bacteria as indicated by specific growth rate and yield determinations, was the same regardless of the calcium concentration. Meanwhile, there was no significant difference in EPS production rate with calcium concentration.

2.6.3 The effect of calcium on aerobic granulation

Jiang et al. (2003) reported that addition of Ca^{2+} accelerated the aerobic granulation process. With addition of $100 \text{ mg L}^{-1} \text{ Ca}^{2+}$, the formation of aerobic granules took 16 days compared to 32 days in the culture without Ca^{2+} added. The Ca^{2+} -augmented aerobic granules also showed better settling and strength characteristics and had higher polysaccharides contents. It has been proposed that Ca^{2+} binds to negatively charged groups present on bacterial surfaces and extracellular polysaccharides molecules and thus acts as a bridge to promote bacterial aggregation. Polysaccharides play an important role in maintaining the structural integrity of biofilms and microbial aggregates such as aerobic granules, as they are known to form a strong and sticky non-deformable polymeric gel-like matrix.

2.7 SLUDGE RETENTION TIME

Sludge retention time (SRT) is one of the most important design and operating parameters that affect the capabilities and performance of biological treatment systems. It determines the types of microorganisms that can grow in a bioreactor, thus affecting the contaminant removal efficiencies and the effluent quality. If the operation SRT is smaller than the minimum SRT that allows for the bacteria to grow, they will be wasted from the bioreactor faster than they grow, a stable population will not develop, and the particular biochemical transformation will not occur. The SRT of a bioreactor is the average time the biomass resides in the biological system. It is controlled operationally by the amount of sludge discharged from the system.

2.7.1 The effect of SRT on carbon removal

One objective of wastewater treatment is the removal of organic pollutants. The effluent organics concentration is influenced by SRT. A number of researchers have reported the performance of conventional activated sludge systems at different SRTs. Bisogni and Lawrence (1971) reported that the soluble COD from bioreactors decreased rapidly from 125 to 58 mg L⁻¹ as the SRT increased from 0.25 to 1 d. At a SRT of 2 d, the effluent COD reached a minimum value of 41 mg L⁻¹, which was maintained until the SRT exceeded 8 d. Beyond SRT of 8 d, the effluent COD increased again, probably as a result of the production of soluble microbial products (Rittman 1987). It appears that there is an optimum SRT where effluent COD concentration is minimal. For instance, Kargi and Uygur (2002) found that the optimum SRT for COD removal was 15 days in sequencing batch reactors.

The existence of an optimum SRT where effluent COD is minimal was also observed other researched who have investigated the effect of SRT. Barker and Stuckey (1999) found that the ratio of effluent soluble microbial product (SMP) to influent organics concentration decreased to a minimum and then increased when SRT was increased, again indicating the existence of optimal SRT minimizing the

production SMP. For aerobic systems, this optimum appears to exist between a SRT of 2 and 15 days (Pribyl et al. 1997). In other words, for a conventional activated sludge system that is operated with SRT greater than 1 d, the influent COD converted SMP increased as the sludge age increased as the sludge age increased. In contrast, researchers working on chemostats (Grady and Williams 1975) showed that the conversion of COD to SMP increased with decreasing SRT.

2.7.2 The effect of SRT on nitrification

SRT has tremendous effect on nitrification because it affects the ability of autotrophic nitrifying bacteria. Nitrifier bacteria grow slower than heterotrophic bacteria. In order to keep nitrifiers in the reactors, the net growth rate of nitrifier must be higher than the reciprocal of the SRT.

A wide range of maximum growth rate of nitrifier was reported as a function of temperature (Randall et al. 1992). For nitrification to occur, the bioreactors are typically design with the SRT of 3-7 days. Chuang et al. (1997) found that SRT should be controlled for longer than 10 days for efficient nitrogen removal in combined activated sludge and biofilm reactors.

2.7.3 The effect of SRT on phosphate removal

Chuang et al. (1997) reported that SRT should be controlled less than 10 days for efficient phosphorus removal in combined activated sludge and biofilm reactors, while it was found that the effluent phosphorus concentration increased notably when SRT was longer than 10 days (Kargi and Uygur 2002).

2.7.4 The effect of SRT on bioflocculation

In conventional activated sludge systems, successful operation depends on the ability to effectively separate the biomass from the treated wastewater in the secondary clarifier. In other words, biomass from the bioreactor must be able to aggregate so form strong and compact flocs that settle rapidly, producing dense sludge for recycle to the bioreactor and a low suspended solids, high-quality supernatant for discharge as treated effluent. Activated sludge settling problems will cause biosolids to be carried into the effluent, resulting in poor effluent quality. Sludge settling problems are generally caused by inadequate bioflocculation and an improper balance between floc-forming and filamentous microorganisms. Dispersed growth results from incomplete flocculation and filamentous microorganisms. Dispersed growth results from incomplete flocculation, and consequently caused high density of dispersed cells in the biomass. Pinpoint flocs result when microorganism flocculate, but inadequate quantities of filamentous microorganisms are present to strengthen the floc particles and make them resistant to mechanical abrasion. As a result, flocs are easily ruptured.

The presence of a large amount of dispersed microorganisms at low SRT is caused by inadequate bioflocculation. Bioflocculation is a complex phenomenon for which mechanism are poorly understood. However, it is agreed upon that extracellular polymeric substances are the key to the aggregation of individual microorganisms into biological flocs (Urbain et al. 1993). EPS consists mainly of polysaccharides and proteins and the possible sources are formation by microbial metabolism, release by cell lysis and to a lesser extent the wastewater itself (Urbain et al. 1993). EPS are produced by protozoa and bacteria (Boossier and Verstaete 1996) found in activated sludge, but the relative importance of the two is unknown. Evidence for the role of protozoa comes from the observation that good bioflocculation and low effluent suspended solids concentration are correlated with their presence (Grady et al. 1999).

2.7.5 The effect of SRT on sludge structure

Liss et al. (2002) found that flocs at lower SRTs (4 and 9 days) to be irregular in shape while flocs at higher SRTs (16 and 20 days) had a more spherical and compact structure. Meanwhile, distinctive differences in floc structure and the arrangement of extracellular polymeric substance (EPS) were revealed. Flocs from higher SRTs were less hydrated and were found to possess a dense EPS layer that covers much of the surface. This EPS layer appears to decrease the floc surface roughness and protects the interior cells from disruption by changes in the external environment. Sludge flocs at higher SRTs were found to be physically more stable than those at lower SRTs.

Liao et al. (2006) found that floc size distribution (>10 microm) could be characterized by a log-normal model for no bulking situations, but a bi-modal distribution of floc size was observed for modest bulking situations. Their results also showed that no clear relationship existed between SRT and median floc size based on frequency. However, sludge flocs at the lower SRTs (4-9 d) were much more irregular and more variable in size with time than those at higher SRTs (16 and 20 d). The level of effluent-suspended solids at lower SRTs was higher than that at higher SRTs.

CHAPTER 3

DIFFUSION OF SUBSTRATE AND OXYGEN IN AEROBIC GRANULE

3.1 INTRODUCTION

Little information is currently available about diffusion profiles of substances inside aerobic granule. Using visualized FISH technique, Tay et al. (2002d) found that the penetration depth of a model dye was about 800 μm from the surface of aerobic granule, while a penetration depth of 700 μm for dissolved oxygen from the surface to aerobic granule was reported by Jang et al. (2003). On the contrary, based on their experimental observation, Moy et al. (2002) found no anaerobic zone in aerobic granules with a size bigger than 2.0 mm. This is probably due to the fact that in the above-mentioned studies, diffusion of dissolved oxygen and utilization of substrate in aerobic granule were not taken into account in a simultaneous way.

In the sense of physical structure, some physical properties of aerobic granules would be similar to those of biofilms, e.g. high density, confined and porous structure (Liu and Tay 2002). It should be realized that the major differences between aerobic granule and biofilm can be attributed to the followings: (i) aerobic granules are the self-aggregated bacteria without assistance of any carriers, and (ii) aerobic granules have the truly three-dimensional structure. Modeling of the substrate diffusion in biofilms has been well studied, e.g. Wanner and Gujer (1985) proposed a one dimensional model for biofilms, and Picioreanu et al. (1998) developed a three dimensional model reflecting the heterogeneous structures of

biofilms. However, little information is known about this issue in aerobic granule so far. In this case, this chapter is aimed at simultaneously modeling diffusion processes of both dissolved oxygen and substrate in aerobic granule, while change in the bulk substrate concentration can also be predicted. As shown in Chapter 2, aerobic granulation is novel environmental biotechnology, and mass transfer is one of the most important issues in all attached growth processes. Obviously, in order to optimize the design and operation of aerobic granular sludge reactor, a sound understanding of mass transfer in aerobic granule is essential. This chapter is thus expected to offer useful information about the optimization of aerobic granular sludge SBR.

3.2 MATERIALS AND METHODS

3.2.1 Cultivation of aerobic granules

Aerobic granules were cultivated in a lab-scale column sequencing batch reactor (SBR) with an internal diameter of 5 cm and a height of 120 cm. SBR was inoculated with activated sludge taken from local wastewater treatment plant. Aerobic granules appeared after two weeks of operation, and matured in week three onwards. Synthetic wastewater used for granule cultivation consisted of sodium acetate 640 mg L⁻¹, NH₄Cl 22.0 mg L⁻¹, K₂HPO₄ 7.5 mg L⁻¹, CaCl₂·2H₂O 9.5 mg L⁻¹, MgSO₄·7H₂O 6.25 mg L⁻¹, FeSO₄·7H₂O 5mg L⁻¹ and microelement solution 1.0 ml L⁻¹. This composition gave a COD concentration of 500 mg L⁻¹, while microelements solution contained: H₃BO₃ 0.05g L⁻¹, ZnCl₂ 0.05g L⁻¹, CuCl₂ 0.03g L⁻¹, MnSO₄·H₂O 0.05 g L⁻¹, (NH₄)₆ MO₇O₂₄·4H₂O 0.05 g L⁻¹, AlCl₃ 0.05g L⁻¹, CoCl₂·6H₂O 0.05 g L⁻¹, NiCl₂ 0.05g L⁻¹ (Liu et al. 2003a). Mature aerobic granules were sorted into different sizes using the wet-sieving method developed by

Pereboom (1994).

3.2.2 Batch experiments

The aerobic granules sorted by size were transferred to beakers with a working volume of 800 ml. The synthetic wastewater as described above was used in the batch experiments. Similar to the parent SBR, initial granule and substrate concentrations were maintained at 6250 mg volatile solids L⁻¹ and 465 mg COD L⁻¹, respectively. The experiments were conducted at 25°C, and dissolved oxygen was kept at saturation level. During the batch experiments, 2ml of samples were taken at different time intervals for COD analysis. COD and volatile solids (VS) were analyzed by standard methods (APHA 1998), and dissolved oxygen concentration was recorded by a dissolved oxygen meter (Model YSI 5000).

3.3 RESULTS

3.3.1 Development of model system

Mature aerobic granules are considered to have an equilibrium or stable size when growth and detachment forces are balanced (Liu and Tay 2002). In the development of the one-dimensional model for aerobic granules, it is assumed here that (i) an aerobic granule is isotopic in physical, chemical and biological properties, such as density, diffusion coefficient; (ii) an aerobic granule is ideally spherical; (iii) no nitrification and anaerobic degradation happen in the process; (iv) aerobic granule responses to the change of bulk substrate concentration so quickly that the response time can be ignored. According to Bailey and Ollis (1986), the mass balance equations between the two layers whose radii are respectively r and $r+dr$ can be written as:

Chapter 3 Diffusion of Substrate and Oxygen in Aerobic Granule

$$D_s \left(\frac{d^2 s}{dr^2} + \frac{2}{r} \frac{ds}{dr} \right) = v \quad (3.1)$$

in which v is the substrate conversion rate, s is substrate concentration. In fact, the substrate conversion rate can be expressed by the Monod type equation:

$$v = \frac{\rho_x \mu}{Y_{x/s}} = \frac{\rho_x}{Y_{x/s}} \mu_{\max} \frac{s}{K_s + s} \quad (3.2)$$

in which ρ_x is biomass density and μ and μ_{\max} are the specific growth rate and the maximum specific growth rate, respectively. Inserting Equation 3.2 into Equation 3.1 gives the following expression:

$$D_s \left(\frac{d^2 s}{dr^2} + \frac{2}{r} \frac{ds}{dr} \right) = \frac{\mu_{\max} s}{K_s + s} \frac{\rho_x}{Y_{x/s}} \quad (3.3)$$

The derivative of s at the center of granule is zero, and the concentration of substrate at the surface of granule equals to the bulk solution, i.e.,

$$\left. \frac{ds}{dr} \right|_{r=0} = 0 \quad (3.4)$$

$$s|_{r=R} = S_{bulk} \quad (3.5)$$

Perez et al. (2005) applied Equation 3.3 to study spherical biofilms, and analytically solved this equation by assuming that the growth rate is zero-order or first order. However, it should be pointed out that such simplified treatment of Equation 3.3 eventually leads to the inaccuracy of the prediction by Equation 3.3, and also limits the application of this equation to a very narrow range. As Equation 3.3 is a non-homogenous equation, in this study a numerical method was developed to completely solve Equation 3.3 without any assumption on it. This approach is based on Finite Difference Method (FDM) (Hoffman 2001). For this purpose, the radius of aerobic granule is divided into n grids, i.e.

$$D_s \left(\frac{s_{i+1} + s_{i-1} - 2s_i}{\Delta r^2} + \frac{s_{i+1} - s_{i-1}}{r \Delta r} \right) = \frac{\mu_{\max} s_i}{K_s + s_i} \frac{\rho_x}{Y_{x/s}} \quad (3.6)$$

This numerical scheme is applied to all situations without simplifying assumptions

Chapter 3 Diffusion of Substrate and Oxygen in Aerobic Granule

and therefore the accuracy of simulation is significantly improved as compared to the approach by Perez et al. (2005). The program was written using Matlab language and run under Matlab 7.0. This allows an easy visualization of the simulation data. Dissolved oxygen is an essential element for the growth of aerobic granule, thus Equation 3.6 can also be extended to oxygen if the set of parameters for substrate are replaced with the set of parameters for dissolved oxygen.

After the substrate concentration is determined, the substrate utilization rate (v_1) by a single aerobic granule can be calculated as:

$$v_1 = \frac{1}{Y_{x/s}} \int_0^R \rho_x \mu(s) 4r^2 dr \quad (3.7)$$

Summing up the substrate utilization rates of all the aerobic granules gives the total substrate utilization rate (v):

$$v = \sum_{i=1}^m \frac{1}{Y_{x/s}} \int_0^{R_i} \rho_x \mu(s) 4r^2 dr \quad (3.8)$$

in which m is the number of aerobic granules in the reactor and R_i is the radius of granule being calculated. It is obvious that an average radius \bar{R} of aerobic granules can be expressed as follows:

$$\bar{R} = \frac{1}{m} \sum_{i=1}^m R_i \quad (3.9)$$

Substituting Equation 3.9 into Equation 3.8 yields

$$v = \frac{m}{Y_{x/s}} \int_0^{\bar{R}} \rho_x \mu(s) 4r^2 dr \quad (3.10)$$

After deformation, Equation 3.10 becomes

$$v = \frac{4\pi \bar{R}^3}{3} \frac{\rho_x}{Y_{x/s}} \frac{m}{\bar{R}} \int_0^{\bar{R}} \frac{\mu(s) 4r^2}{\frac{4}{3}\pi \bar{R}^3} dr \quad (3.11)$$

Chapter 3 Diffusion of Substrate and Oxygen in Aerobic Granule

in which $\frac{4}{3}\pi R^3 \rho_x m$ is equal to the total biomass (XV) in the reactor. Thus, Equation 3.11 reduces to

$$v = \frac{XV}{Y_{x/s}} \int_0^{\frac{R}{3}} \frac{\mu(s)4r^2}{\frac{4}{3}\pi R} dr \quad (3.12)$$

in which V is reactor volume. At a time interval of dt, change of substrate concentration in the reactor can be described by

$$dS_{bulk} = \frac{v}{V} dt = \frac{X}{Y_{x/s}} \int_0^{\frac{R}{3}} \frac{\mu(s)4r^2}{\frac{4}{3}\pi R} dr dt \quad (3.13)$$

In a time period from T_o to T, change in the substrate concentration is governed by the following equation:

$$\Delta S_{bulk} = \frac{X}{Y_{x/s}} \int_{T_o}^T \left(\int_0^{\frac{R}{3}} \frac{\mu(s)4r^2}{\frac{4}{3}\pi R} dr \right) dt \quad (3.14)$$

Thus, at an initial substrate concentration (S_{bulk0}), the bulk substrate concentration at any time t can be calculated as follows:

$$S_{bulk} = S_{bulk0} - \Delta S_{bulk} = S_{bulk0} - \frac{X}{Y_{x/s}} \int_{T_o}^T \left(\int_0^{\frac{R}{3}} \frac{\mu(s)4r^2}{\frac{4}{3}\pi R} dr \right) dt \quad (3.15)$$

As discussed earlier, Equation 3.15 can not be solved analytically, and the method based on the finite difference principle is thus applied to solve this equation in the present study. At each time step, the state is considered pseudo-static, which means that the bulk substrate concentration is constant at each time step, and change of the bulk substrate concentration is a process of mapping, i.e. the substrate concentration is determined by the previous time step. Equation 3.6 is valid for different substrates as long as the parameters are replaced with the specific substrate parameters. In this study, Equation 3.6 was applied to organic substrate and dissolved oxygen under various operation conditions. The parameter used in this study is listed in following Table 3.1.

Chapter 3 Diffusion of Substrate and Oxygen in Aerobic Granule

Table 3.1 Symbols and values of constants used

| Symbol | Description | Value | Unit | References | Symbol | Description | Value | Unit |
|-------------------|-----------------------------------------|----------------------|----------------------------|-----------------------------|--------------------------|-------------------------------------------------|-------|-----------------------|
| D_s | Acetate diffusion coefficient | 2.5×10^{-9} | $\text{m}^2 \text{s}^{-1}$ | Beun et al. (2001) | \bar{R} | Average radius of all granules | | mm |
| D_{fo} | Oxygen diffusion coefficient | 2×10^{-9} | $\text{m}^2 \text{s}^{-1}$ | Beyenal and Tanyolac (1994) | s_i | Substrate concentration at no. i layer | | mg L^{-1} |
| $\mu(s)$ | Growth rate at substrate concentrations | | d^{-1} | | s | Substrate concentration at a point of a granule | | mg L^{-1} |
| μ_{\max} | Maximum growth rate | 2.4 | d^{-1} | Yang et al. (2004a) | ΔS_{bulk} | The change of bulk substrate concentration | | mg L^{-1} |
| K_s | Half rate constant | | mg L^{-1} | Beun et al. (2001) | $S_{\text{bulk}0}$ | Initial bulk substrate concentration | | mg L^{-1} |
| $Y_{x/o}$ | Growth yield of oxygen | 1 | g g^{-1} | | v | Substrate conversion rate | | mg (Ls)^{-1} |
| $Y_{x/s}$ | Growth yield of substrate | 0.3 | g g^{-1} | Liu et al. (2005a) | v_1 | Substrate conversion rate of a granule | | mg (Ls)^{-1} |
| S_{bulk} | Bulk substrate concentration | | mg L^{-1} | | V | Volume of the reactor | | L |
| ρ_x | Biomass density | 32 | g L^{-1} | Liu (2003) | V_{all} | Substrate conversion rate of all granules | | mg (Ls)^{-1} |
| R | The radius of a granule | | mm | | X | Biomass concentration | 6250 | mg L^{-1} |
| r | One dimensional coordinate | | mm | | m | Number of aerobic granules in a reactor | | |
| Δr | The thickness of one layer | | mm | | | | | |

3.3.2. Acetate and oxygen profiles in aerobic granules with different diameters

The initial acetate concentration and granule biomass concentration were kept at $465 \text{ mg COD L}^{-1}$ and 6250 mg L^{-1} volatile solids, respectively, while the initial DO concentration was controlled at 8.3 mg L^{-1} . Figures 3.1 and 3.2 show that for aerobic granules with a respective radius of 0.1 and 0.4 mm, both oxygen and acetate can diffuse into the entire aerobic granules, while for aerobic granules with a radius of 0.5 mm, diffusion limitation of dissolved oxygen appeared (Figure 3.3).

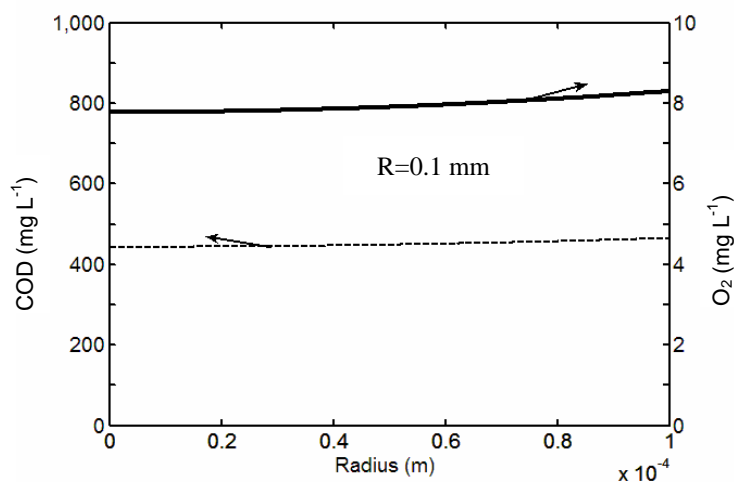


Figure 3.1 Simulated concentration profiles of substrate-COD (dash line) and dissolved oxygen (solid line) in aerobic granule with a radius of 0.1 mm.

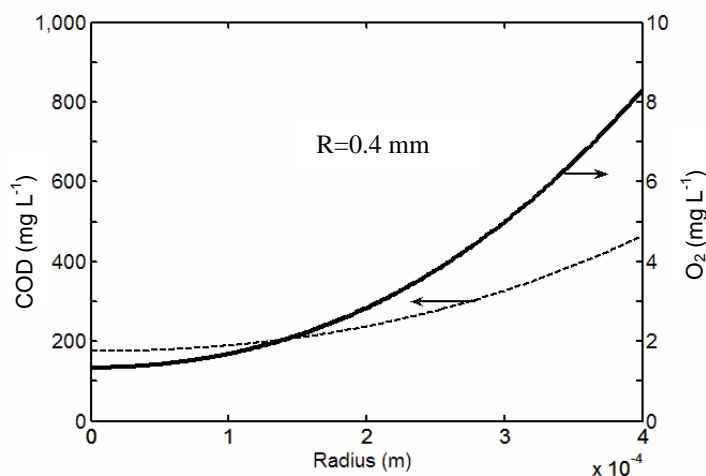


Figure 3.2 Simulated concentration profiles of substrate (dash line) and oxygen (solid line) in aerobic granule with a radius of 0.4 mm.

For aerobic granules with a radius larger than 0.5 mm, oxygen limitation became obvious against the acetate diffusion (Figure 3.3). It appears that the penetration depth of DO decreased from 400 to about 100 μm as the granule radius increases from 0.4 to 1.0 mm (Figures 3.3 to 3.5). After the DO concentration drops to zero, the aerobic activity in granule would be seriously suppressed. This in turn explains a flat acetate diffusion profile observed after the DO was depleted inside the aerobic granules. It seems that in large-size aerobic granules, acetate (organic substrate) is not a limiting factor, but, instead the whole microbial process would be governed by the availability of DO in aerobic granule. Liu et al. (2005a) reported that the substrate removal kinetics of aerobic granules was related to the substrate availability, however it should be pointed out that dissolved oxygen was not taken into account in their study. This may eventually lead to an incomplete conclusion or even misleading.

Chapter 3 Diffusion of Substrate and Oxygen in Aerobic Granule

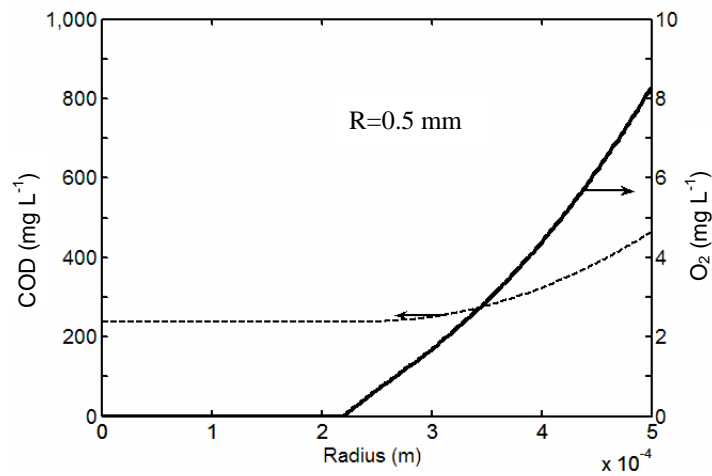


Figure 3.3 Simulated concentration profiles of substrate (dash line) and oxygen (solid line) in aerobic granule with a radius of 0.5 mm.

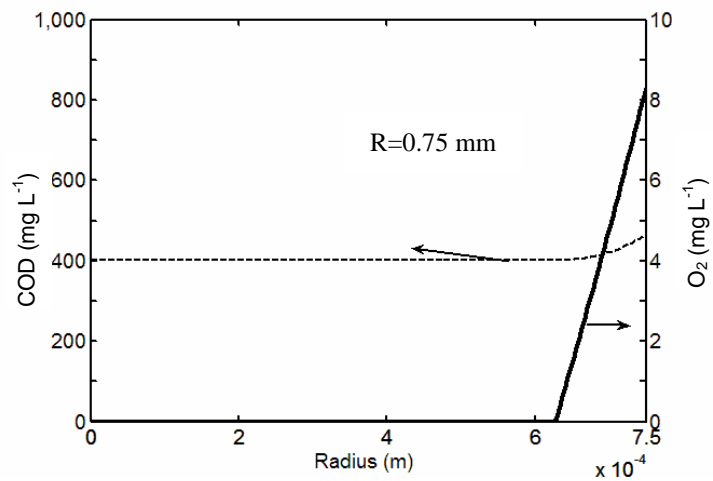


Figure 3.4 Simulated concentration profiles of substrate (dash line) and oxygen (solid line) in aerobic granule with a radius of 0.75 mm.

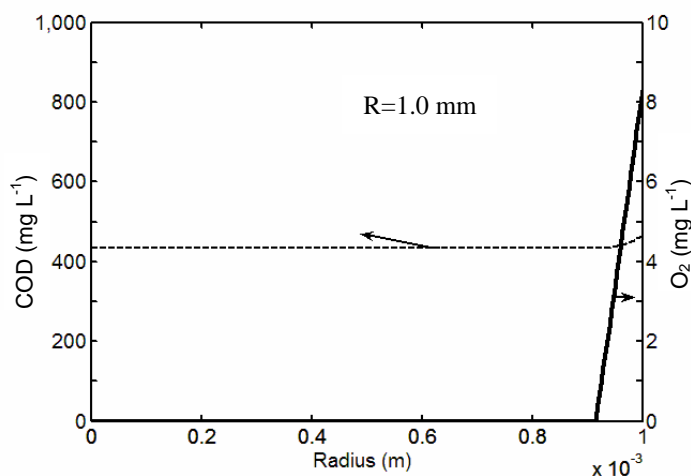


Figure 3.5 Simulated concentration profiles of substrate (dash line) and oxygen (solid line) in aerobic granule with a radius of 1.0 mm.

3.3.3 Diffusion profiles of acetate and DO in aerobic granules at different acetate concentrations

Figures 3.3 and 3.6 to 3.8 show the diffusion profiles of acetate and oxygen in aerobic granules with a radius of 0.5 mm at different acetate concentrations. It can be seen that at the high substrate concentrations of 465 and 300 mg COD L⁻¹, the DO declined quickly in the direction of the granule radius. This is due to the fact that at high substrate concentration, more DO would be required for acetate oxidation, and subsequently it became a limiting factor in the metabolic process of aerobic granules. However, different phenomena were observed at low substrate concentrations (Figures 3.7 and 3.8). In these cases, substrate became the limiting factor over DO in aerobic granule, i.e. DO can penetrate into the center of granules at the lower substrate concentration of 100 and 200 mg COD L⁻¹. These indicate that for a given size of aerobic granule, the microbial metabolism can be limited either by substrate concentration or DO concentration, which is strongly dependent on the level of external substrate concentration in bulk solution.

Chapter 3 Diffusion of Substrate and Oxygen in Aerobic Granule

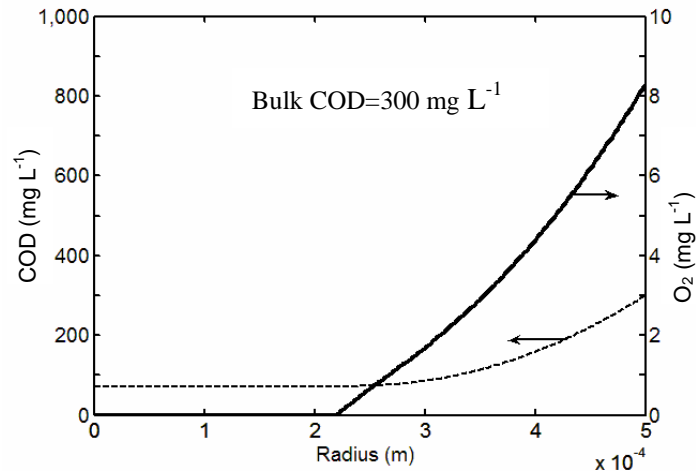


Figure 3.6 Simulated concentration profiles of substrate (dash line) and oxygen (solid line) in aerobic granules with a radius of 0.5 mm at substrate concentration = 300 mg COD L^{-1} .

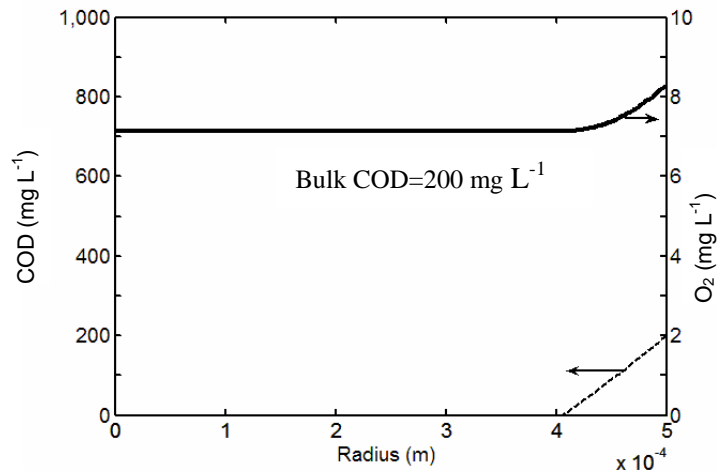


Figure 3.7 Simulated concentration profiles of substrate (dash line) and oxygen (solid line) in aerobic granules with a radius of at substrate concentration = 200 mg COD L^{-1} .

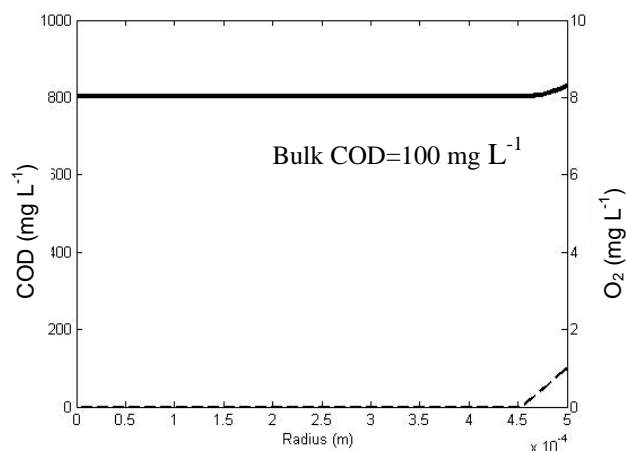


Figure 3.8 Simulated diffusion profiles of substrate (dash line) and oxygen (solid line) in aerobic granules at substrate concentration = 100 mg COD L⁻¹.

3.3.4. Prediction of bulk substrate concentration in aerobic granular sludge SBR

The procedure for simulating the bulk substrate concentration in the course of the reactor operation was described in Figure 3.9. According to Equation 3.14, the substrate conversion rate is proportional to biomass concentration (X) and is inversely related to the yield coefficient at a given granule radius. Figures 3.10-13 show the simulated profiles of the bulk substrate concentration in aerobic granular sludge SBRs with different-sized aerobic granules. For comparison purpose, three set of experiments were also conducted using aerobic granules with different radiuses. Experimental conditions were designed to be the same as those applied in the model simulations, i.e. the initial substrate concentration was 465 mg COD L⁻¹ and the dissolved oxygen was kept at 8.3 ± 0.2 mg L⁻¹ while the granules concentration was maintained a 6250 mg VSS L⁻¹.

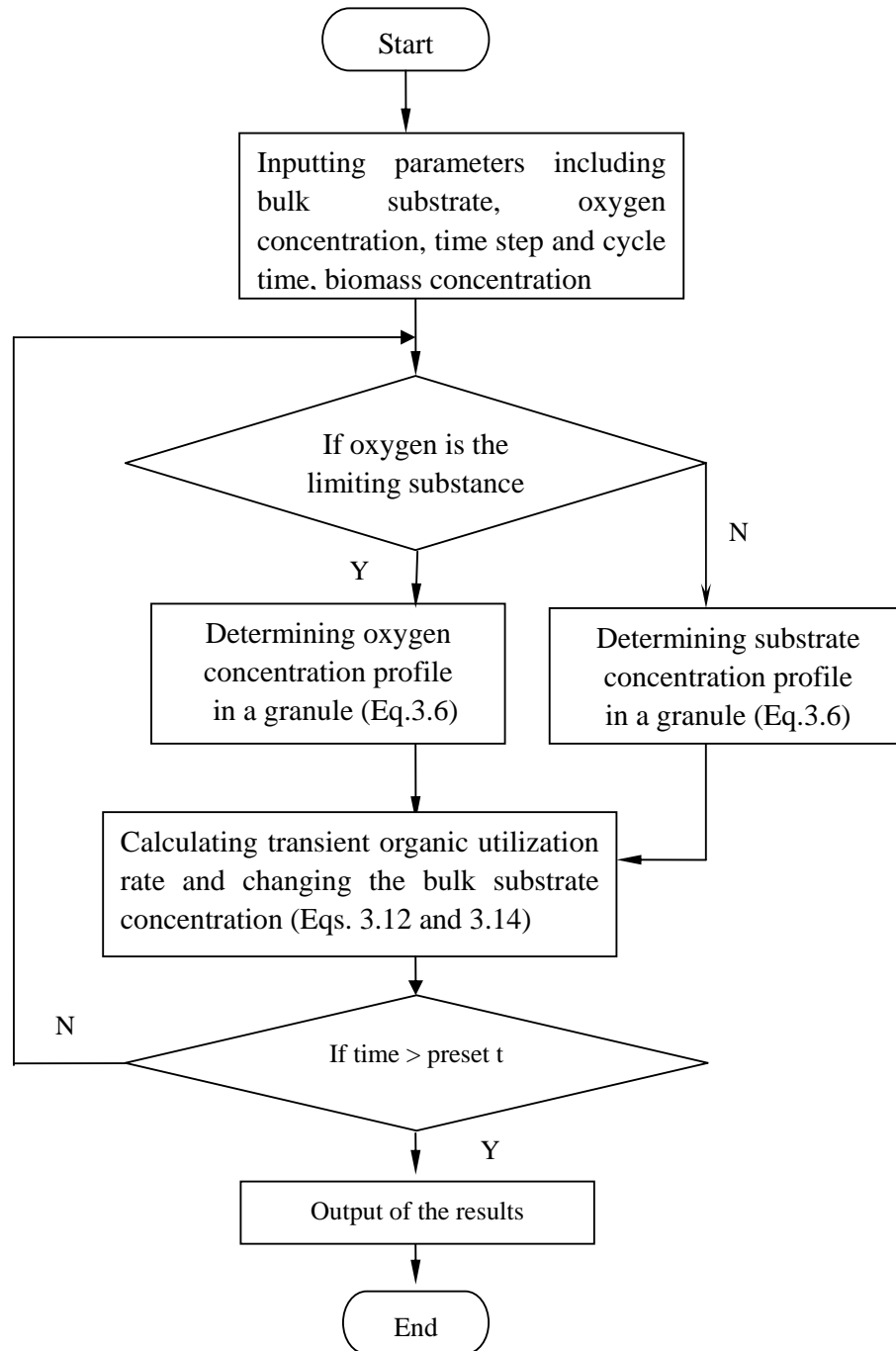


Figure 3.9 Diagram of algorithm used to simulate substrate-time profiles in reactor.

It can be seen in Figures 3.11 to 3.13 that all the simulations are in good agreement with the experimental data. When the granule size was as small as 0.1 mm in radius, nearly no diffusion limitation occurred. In this case, Equation 3.12 reduces to a formulation similar to the activated sludge model (Henze et al. 1987). This point is strongly supported by the simulation results present in Figure 3.10 showing a satisfactory agreement between the predictions by Equation 3.12 and by the activated sludge model when the granule size goes down to the size of bioflocs.

It appears from Figures 3.10-3.13 that under the same operation conditions, the substrate can be removed fast in the SBR with small aerobic granules. For instance, the substrate removal rate by 0.5 mm granules (Figure 3.11) is almost 3 times higher than that by 1.0 mm granules (Figure 3.13). These in turn imply that (i) the reactor with small-size aerobic granules would be more efficient and have a higher treatment capacity than the reactor packed with large-size granules; (ii) the size of aerobic granules needs to be properly controlled in order to maximize their metabolic activity. The breakpoints in Figures 3.11-3.14 indeed represent turning point from oxygen limitation to substrate limitation. Under the condition of the oxygen limitation, the substrate removal rate is mainly determined by the availability of dissolved oxygen, i.e. the substrate removal would be independent of the bulk substrate concentration, this is reason why a pseudo zero-order reaction kinetics is observed in Figures 3.11-3.13 for the substrate removal. In fact, this is pretty consistent with previous experimental observations (Liu 2003; Yang et al. 2004). However, under the substrate limiting condition, Figures 3.11-3.13 show that the substrate removal by aerobic granules tends to decrease with the decrease of the substrate concentration, i.e. it is a function of the substrate concentration.

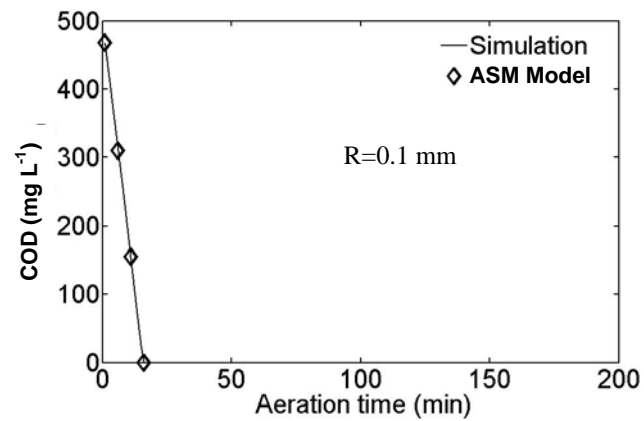


Figure 3.10 Substrate-time profile in aerobic granular sludge SBR dominated by granules with a size of 0.1 mm. -: simulation; \diamond : experimental data.

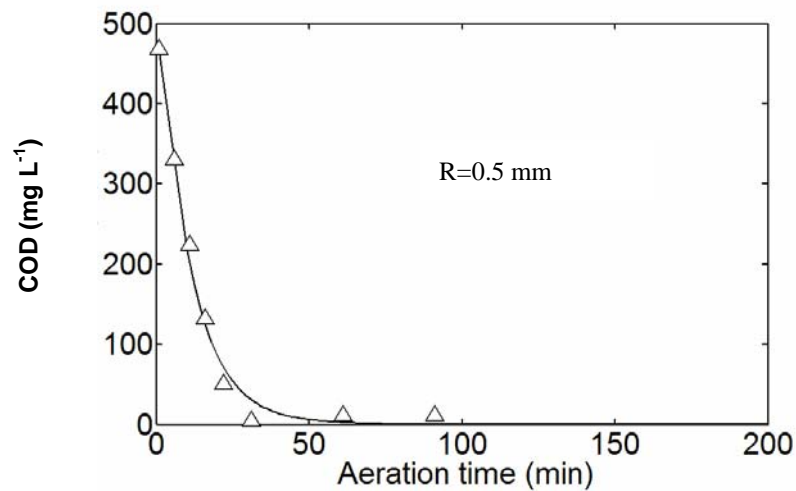


Figure 3.11 Substrate-time profile in aerobic granular sludge SBR dominated by granules with a size of 0.5 mm. -: simulation; Δ : experimental data.

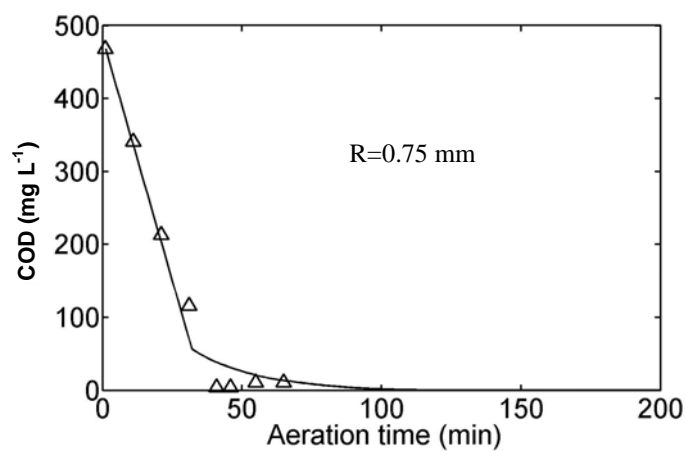


Figure 3.12 Substrate-time profile in aerobic granular sludge SBR dominated by granules with a size of 0.75mm. -: simulation; Δ : experimental data.

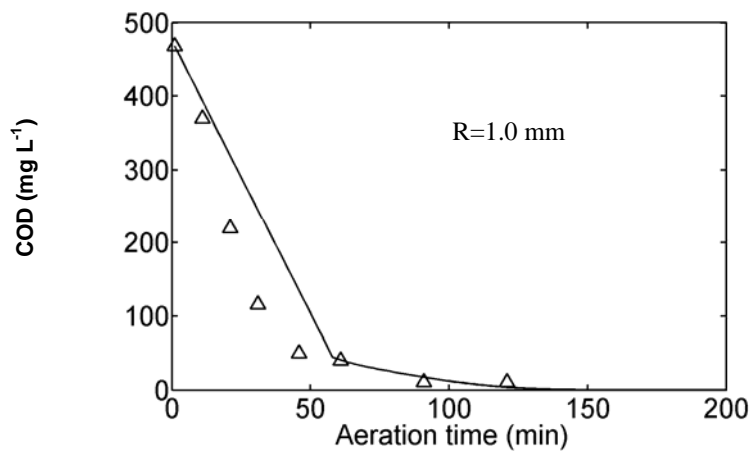


Figure 3.13 Substrate-time profile in aerobic granular sludge SBR dominated by granules with a size of 1.0 mm. -: simulation; Δ : experimental data.

3.4 DISCUSSION

3.4.1 Diffusion of DO and substrate

It should be pointed out that most previous research on aerobic granulation investigated the profiles of DO and substrate separately. For instance, Tay et al. (2002) and Jang et al. (2003) also looked into the diffusion phenomenon in aerobic granule, however, they did not account for the fact that oxygen profile inside an aerobic granule is dynamic and closely related to the substrate profile and metabolic activity as revealed by Figures 3.1 to 3.8. In study of activated sludge by Beun et al. (2001), the oxygen profile in activated sludge floc was considered dynamic, but the interrelation between the oxygen and substrate profiles was also ignored. Beun et al. (1999) concluded that oxygen penetration depth in biofilm cultivated in sequential batch airlift reactor was smaller than the acetate penetration depth. However, this point is valid only when substrate concentration is high as shown in Figure 3.1, while it would be invalid in case where substrate is limiting factor as shown in Figures 3.2-3.4. In addition, in modeling biofilm process, substrate was regarded as the limiting substance without the consideration of dissolved oxygen (Picioreanu et al. 1998; Laspidou 2003). As shown in Figures 3.1 to 3.8, diffusions of substances (e.g. substrate and dissolved oxygen) in aerobic granule are a dynamic process, and are interrelated as well. Consequently, the integrated approach developed in this study offers a more reasonable tool for the study of diffusion phenomenon in aerobic granule.

As discussed earlier, the substrate removal kinetics of aerobic granules would be size-dependent (Figures 3.11 to 3.13). In order to look into the interaction of diffusion and reaction in aerobic granule, the effectiveness factor (η) is thus introduced and defined as a ratio of reaction rates of substrate with and without

diffusion limitations, i.e.

$$\eta = \frac{\text{rate with diffusion resistance}}{\text{rate without diffusion resistance}} = \frac{\text{observed rate}}{\text{intrinsic rate}} \quad (3.18)$$

In case where diffusion resistance is negligible, η is close to unity, while η will approach zero if diffusion resistance dominates over reaction. According to Figures 3.1-3.8, the intrinsic rates of substrate removal can be represented by that computed at the granule radius of 0.1 mm (i.e., no limitations of both substrate and dissolved oxygen). The values of η can thus be theoretically calculated from Figures 3.1 to 3.4. A η -granule radius diagram was generated and shown in Figure 3.14. At a granule radius smaller than 0.4 mm, no significant change in η is observed. However, the effective factor decreases quickly with the further increase of radius of granules, indicating that the mass transfer resistance began to play an important role in the overall reaction of aerobic granules. In fact, these are consistent with Figure 3.1 very well. Liu et al. (2005a) experimentally determined η values of acetate-fed aerobic granules with different radius. It can be seen in Figure 3.14 that both theoretical and experimental values are in good agreement.

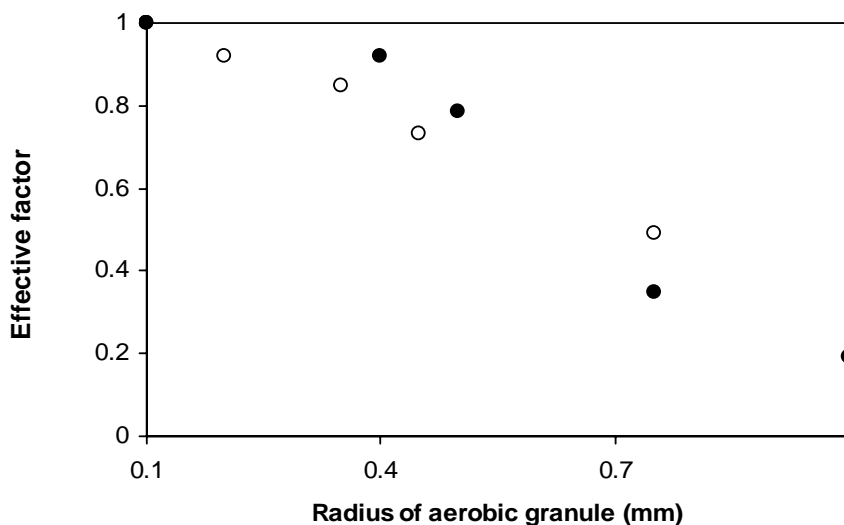


Figure 3.14 Effectiveness factor-granule radius diagram. ●: theoretical data; ○: experimental data from Liu et al. (2005a).

3.4.2 Microbiological implications

3.4.2.1 Aerobic and anaerobic zones in aerobic granule

For aerobic granules in substrate solution, when the radius becomes bigger than 0.5 mm (Figures 3.3 to 3.5), the DO diffusion limitation would occur and dissolved oxygen became a major limiting factor of metabolic activity of aerobic granule. Previous research also showed that the diffusion limitation of oxygen occurred when aerobic granules grew to a radius approximately 0.7 mm (Jang et al. 2003) and 0.8mm (Tay et al. 2002d) respectively. Under the substrate-free condition, the DO diffusion limitation is not significant in aerobic granules with radius smaller than 1.0 mm (Figures 3.6 to 3.8). These seem to imply that in big aerobic granules, aerobic and anaerobic zones would coexist in a layered manner, i.e., the outer layer of granule would be aerobic, while its inner part would be subject to anaerobic growth. In fact, the presence of anaerobic bacteroides in aerobically grown microbial granules has been reported (Tay et al. 2002d). As shown in Figures 3.3 to 3.5, organic substrate was not a limiting factor in large-size aerobic granules. On the contrary, the microbial process would be dominated by the availability of DO in aerobic granule. Toh et al. (2003) detected a layer of dead microbial cells located at a depth of 800 to 1000 μm below the granule surface where the aerobic activities were highly suppressed. Chiu et al. (2007) studied DO diffusion in aerobic granules grown on by phenol and acetate as carbon source, respectively, and found that most DO was consumed by an active layer with a depth of less than 125 to 375 μm from the granule surface, indicating that no aerobic oxidation could occur beneath this active layer. This study and previous studies clearly show that small aerobic granules would be more effective for aerobic wastewater treatment as they have more live cells within a given volume of granules and the optimal diameter for aerobic granules would be less than 0.5 mm.

Oxygen transfer limitation can influence the structure and stability of aerobic granules. The presence of anaerobic bacteria in the center of aerobic granules was likely to result in the production of organic acid and gases within the granules, which further diminished long-term stability of aerobic granules. Moreover, extracellular polysaccharide (EPS) in the centre of granule would be anaerobically degraded as potential energy source, and the biomass in the granule centre would undergo anaerobic decay. It has been shown that a significant portion of EPS produced by aerobic granules can be degraded by their own producers (Wang et al. 2007). These in turn would lead to a porous and weak structure of aerobic granule. Granules would undergo breakup due to a low oxygen concentration, and it is even impossible to form stable granules from activated sludge at a low oxygen concentration (Mosquera-Corral et al. 2005). Consequently, the simulated DO profiles clearly reveal a layered aerobic and anaerobic structure of aerobic granules.

3.4.2.2 Variable DO demand in feast and famine phases

Basically, a cycle of SBR consists of feast and famine phases (Tay et al. 2001a; Liu 2003). The feast phase means the external substrate is available, while the famine phase represents a period in which there is no longer external substrate. As shown in Figures 3.3 to 3.5, under the substrate-sufficient condition, DO only partially penetrate into aerobic granules with a depth less than 500 μm from the granule surface. Under famine conditions, the oxygen can penetrate deeper in aerobic granules (Figures 3.6 to 3.8) than in feast period (Figures 3.3 to 3.5). These imply that for aerobic granules in SBRs with a typical radius from 0.5 to 1.0 mm, a low oxygen concentration might be sufficient enough for penetrating the entire granule in the famine period. This leads to a reasonable consideration that the oxygen demand in the famine period could be much lower than that in the feast period, i.e., the oxygen supply by air aeration can be reduced substantially in the famine period.

Obviously, a considerable amount of aeration-associated energy would be saved if a reduced aeration strategy is adopted in the famine phase of SBR operation.

Previous study shows that the reduced aeration rate in famine period would not pose significant effect on granule size, SVI and effluent quality during a short-term operation (Liu et al. 2006). Mosquera-Corral et al. (2005) also found the reduction of oxygen supply not only reduced the energy demand, but also increased the nitrogen removal efficiency. However, it should be realized that aerobic granules developed at the low oxygen concentration would not be stable, and filamentous growth would eventually encouraged (Mosquera-Corral et al. 2005; Liu et al. 2007). Consequently, a long-term operation is strongly needed before any consolidate conclusion can be drawn with regard to the reduced aeration in the famine phase of aerobic granular sludge SBR.

3.4.2.3 Nitrification-denitrification in aerobic granule

The nitrogen removal through conventional nitrification-denitrification pathway requires on alternative aerobic and anaerobic conditions. As discussed earlier, aerobic granule has a layered structure comprising aerobic and anaerobic zones from the surface to the center of aerobic granule. Thus, aerobic granule may have a great potential for simultaneous nitrification and denitrification even the DO concentration the bulk solution is high (Figures. 3.3 to 3.5). Ammonia oxidizing bacteria were found to exist primarily in the upper and middle layers of the granule, and most of the nitrification is likely to occur from the surface to 300 μm into aerobic granule, while nitrate produced seemed to be removed by denitrification in the granules (Jang et al. 2003). Liu et al. (2007) used a microelectrode fabricated using photolithography to detect the DO profile in nitrifying granule and found that the active part of the nitrifying granule was situated at the upper layer of 150 μm

from the surface of aerobic granules. In conventional denitrification process, organic carbon is required as electron donor, meaning that COD is needed for denitrification in the anaerobic zone of aerobic granule. In this study, it is found that for a SBR dominated by aerobic granules bigger than 0.5 mm, the DO was found to be the bottleneck which limits the utilization of organic substrate, i.e. the organic substrate could penetrate into deeper zone of aerobic granule than DO (Figures 3.3 to 3.5). These imply that denitrification in the anaerobic zone of aerobic granule is possible. Previous study clearly shows that organic carbon-oxidizing, nitrifying and denitrifying bacteria can co-exist in aerobic granules developed at different substrate N/COD ratios, and simultaneous aerobic COD removal, nitrification and denitrification were observed in an aerobic granular sludge reactor (Yang et al. 2004b).

3.5 CONCLUSIONS

A one-dimensional model for aerobic granules was developed and was successfully applied to aerobic granular sludge SBR. Following conclusions can be drawn from this study.

- (i) A new FDM-based numerical method was developed by which the simulation models can be completely solved without adding in any extra assumption in numerical analysis;
- (ii) Diffusions of substrate and dissolved oxygen were synchronously simulated by the proposed models under various conditions. It was found that diffusions of substrate and oxygen in aerobic granule would be a dynamic process, and were closely interrelated. This means that both must be considered together in future optimization of aerobic granular sludge SBR.
- (iii) Simulation of the overall performance of aerobic granular sludge SBR showed that dissolved oxygen would be a main limiting factor of the metabolic activity of aerobic granule;

Chapter 3 Diffusion of Substrate and Oxygen in Aerobic Granule

- (iv) Smaller aerobic granules exhibited higher metabolic activity in terms of the substrate removal rate;
- (v) For a SBR dominated by aerobic granules bigger than 0.5 mm in radius, dissolved oxygen would be the bottleneck which limits the substrate utilization rate.

It is expected that the model system developed in this study can provide an effective and useful tool for predicting and optimizing the performance of aerobic granular sludge reactor.

CHAPTER 4

MECHANISM OF CALCIUM ACCUMULATION IN ACETATE-FED AEROBIC GRANULE

4.1 INTRODUCTION

Calcium content in mature anaerobic granules was found to be much higher than that in seeding sludge (Yu et al. 2001). High calcium concentration was considered to be favorable for anaerobic granulation, and it would help to enhance the physical structure of anaerobic granules, leading to an increased density of anaerobic granules as well as a high resistance to shear stress (Yu et al. 2001; Batstone et al. 2002). Two hypotheses have been put forward to explain the calcium accumulation in anaerobic granule: (i) calcium is bound with EPS to form the EPS- Ca^{2+} -EPS cross-linkage; and ii) calcium is precipitated with carbonate and further form CaCO_3 (Yu et al. 2001; Wloka et al. 2004). Calcium accumulation was also observed in biofilms. Calcium was supposed to provide binding ligands for bacterial attachment (Rose 2000), and this hypothesis was further verified by Körstgens et al. (2001) and Wloka et al. (2004).

A high calcium content has been reported in acetate-fed aerobic granules even though the calcium concentration in the culture medium was very low (Qin et al. 2004a; Wang et al. 2005). So far, little is known about the mechanism behind the excessive accumulation, chemical form and spatial distribution of calcium ion in the acetate-fed aerobic granules. In this chapter, experiments were specifically designed to determine the form and location of calcium ion in acetate-fed aerobic granules,

while the model system developed in Chapter 3 was applied to correlate calcium accumulation with reaction- and diffusion-related phenomena in the acetate-fed aerobic granule.

4.2 MATERIALS AND METHODS

4.2.1 Cultivation of aerobic granules

The stable mature aerobic granules were harvested from the column sequencing batch reactor (SBR) as described in Chapter 3. Synthetic wastewater used in the cultivation of aerobic granules had the following composition: 2560 mg L⁻¹ sodium acetate as the sole carbon source; and NH₄Cl, 200 mg L⁻¹; K₂HPO₄, 45 mg L⁻¹; CaCl₂·H₂O, 30 mg L⁻¹; MgSO₄·7H₂O, 25 mg L⁻¹; FeSO₄·7H₂O, 20 mg L⁻¹. This gives a volumetric loading rate of 6 kg COD m⁻³ d⁻¹ and an initial calcium concentration of 4.65 mg L⁻¹.

4.2.2 Elemental analysis

The elemental composition (Ca, Mg, P, Fe, Al) of acetate-fed aerobic granule was determined by Inductively Coupled Plasma Emission Spectrometer (ICP, PerkinElmer Optima 2000). To analyze the amount of carbonate ion in acetate-fed aerobic granules, 3 ml of 1 M hydrochloric acid solution was added to 50 ml of 2 g SS L⁻¹ granules. Carbon dioxide gas produced was online measured by the carbon dioxide sensor equipped with the respirometer (Columbus Instruments Micro-Oxymax) as illustrated in Figure 4.1, while change in inorganic carbon in the liquid phase was determined by Total Organic Carbon Analyzer (TOC, Shimadzu TOC-Vcsh) before and after the experiment. Thus, the content of carbonate in the acetate-fed aerobic granules was calculated from the sum of the carbon dioxide gas

produced and increased inorganic carbon in the liquid phase. In addition, suspended solids (SS), volatile solids (VS), specific oxygen utilization rate (SOUR), sludge volume index (SVI), dissolved oxygen (DO), granule specific gravity and pH were also measured according to standard methods (APHA 1998). All measurements were done in triplicates.

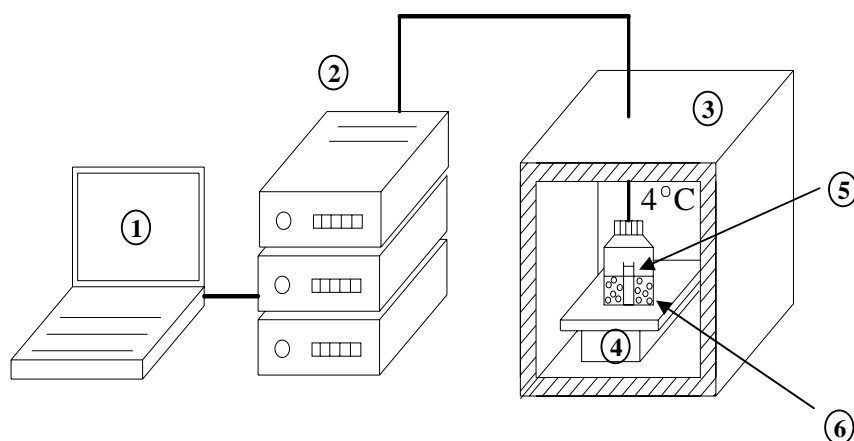


Figure 4.1 Respirometer system for analysis of carbonate in the acetate-fed aerobic granule: 1. computer for data collection; 2. respirometer; 3. fridge; 4. shaker; 5. acid containing vial; 6. reaction bottle.

4.2.3 Calcium mapping by EDX

The calcium distribution in acetate-fed aerobic granule was investigated using a scanning electron microscope (SEM, JSM 6360, JEOL, Tokyo Japan) as well as Energy Dispersive X-ray spectroscopy (EDX) analysis for mapping calcium distribution in aerobic granule. The carbonate location in aerobic granule was determined by chemical titration method as described above, and evolution of

bubbles was visualized by Image Analyzer (IA, Quantimet 500, Leica Cambridge Instruments).

4.3. Model development

4.3.1 Ionic equilibrium of carbonate ion

In the sense of chemistry, the CaCO_3 formation is determined by its ionic concentration product:

$$[\text{Ca}^{2+}][\text{CO}_3^{2-}] = K_{\text{sp},\text{CaCO}_3} \quad (4.1)$$

in which $K_{\text{sp},\text{CaCO}_3}$ is the CaCO_3 solubility product constant. Calcium carbonate will form only when the concentration product of calcium and carbonate is greater than value of $K_{\text{sp},\text{CaCO}_3}$. On the other hand, acetate can be oxidized in a way such that:



$$\text{and} \quad K_{\text{a1}} = \frac{[\text{HCO}_3^-][\text{H}^+]}{[\text{CO}_2]} \quad (4.4)$$



$$\text{and} \quad K_{\text{a2}} = \frac{[\text{CO}_3^{2-}][\text{H}^+]}{[\text{HCO}_3^-]} \quad (4.6)$$

Thus, the overall reaction for carbonate can be expressed as



It should be pointed out that dissolution of CO_2 produced in Equation 4.2 is subject

Chapter 4 Mechanism of Calcium Accumulation in Acetate-Fed Aerobic Granule

to the well-known Henry's law:

$$P_{\text{CO}_2} = K_{\text{h,CO}_2} [\text{CO}_2] \quad (4.8)$$

in which P_{CO_2} is the partial pressure of CO_2 in gas phase, $[\text{CO}_2]$ is molar concentration of dissolved carbon dioxide in the liquid phase, and $K_{\text{h,CO}_2}$ is the Henry's constant for carbon dioxide.

4.3.2 Diffusion kinetics of substances in aerobic granule

It has been demonstrated in Chapter 3 that the diffusion kinetics of substances in aerobic granule can be described by Equation 3.1, which is recalled here as Equation 4.9.

$$D_s \left(\frac{d^2 s}{dr^2} + \frac{2}{r} \frac{ds}{dr} \right) = R_s \quad (4.9)$$

in which D_s and R_s are the diffusion coefficient and mass conversion rate of a specific substance. According to Eq. 4.9, the respective mass balance equations for O_2 , H^+ , HCO_3^- and CO_3^{2-} in aerobic granules can be written as:

$$D_{\text{O}_2} \left(\frac{d^2 C_{\text{O}_2}}{dr^2} + \frac{2}{r} \frac{dC_{\text{O}_2}}{dr} \right) = R_{\text{O}_2} \quad (4.10)$$

$$D_{\text{H}^+} \left(\frac{d^2 C_{\text{H}^+}}{dr^2} + \frac{2}{r} \frac{dC_{\text{H}^+}}{dr} \right) = R_{\text{H}^+} \quad (4.11)$$

$$D_{\text{HCO}_3^-} \left(\frac{d^2 C_{\text{HCO}_3^-}}{dr^2} + \frac{2}{r} \frac{dC_{\text{HCO}_3^-}}{dr} \right) = R_{\text{HCO}_3^-} \quad (4.12)$$

$$D_{\text{CO}_3^{2-}} \left(\frac{d^2 C_{\text{CO}_3^{2-}}}{dr^2} + \frac{2}{r} \frac{dC_{\text{CO}_3^{2-}}}{dr} \right) = R_{\text{CO}_3^{2-}} \quad (4.13)$$

In Chapter 3, it was shown that the dissolved oxygen would be a rate-limiting factor in aerobic granules. In this case, the oxygen utilization rate can be described by the

Chapter 4 Mechanism of Calcium Accumulation in Acetate-Fed Aerobic Granule

well known Monod equation:

$$R_{O_2} = \frac{\rho_x}{Y_{x/O_2}} \mu_{\max} \frac{C_{O_2}}{K_{O_2} + C_{O_2}} \quad (4.14)$$

in which ρ_x is biomass density, Y_{x/O_2} is the growth yield of oxygen, K_{O_2} is the dissolved oxygen-based half constant, μ_{\max} is the maximum specific growth rate. According to Equation 4.2, the oxygen utilization rate and the H^+ consumption rate are interrelated by Equation 4.15:

$$R_{O_2} = 2R_{H^+ \text{ (consumption)}} \quad (4.15)$$

Similarly, the following relationship can be obtained from Equations 4.3 and 4.7 for H^+ , HCO_3^- and CO_3^{2-} :

$$R_{H^+ \text{ (production)}} = R_{HCO_3^-} + 2R_{CO_3^{2-}} \quad (4.16)$$

Thus, the net consumption rate of H^+ , namely R_{H^+} in Equation 4.11 can be expressed as follows:

$$R_{H^+} = R_{H^+ \text{ (consumption)}} - R_{H^+ \text{ (production)}} \quad (4.17)$$

The DO concentration at the granule surface can be reasonably assumed to be equal to its bulk concentration, and its change rate in the granule center should be close to zero in consideration of the symmetrical distribution of DO in the granule center, i.e.,

$$C_{O_2} \Big|_{r=R} = C_{\text{bulk}, O_2} \quad (4.18)$$

$$\frac{dC_{O_2}}{dr} \Big|_{r=0} = 0 \quad (4.19)$$

Likewise, C_{H^+} at the granule surface is assumed to be equal to the bulk H^+ concentration, and derivative of C_{H^+} at the center of granule is supposed to be zero. Hence,

$$C_{H^+} \Big|_{r=R} = C_{\text{bulk}, H^+} \quad (4.20)$$

Chapter 4 Mechanism of Calcium Accumulation in Acetate-Fed Aerobic Granule

$$\left. \frac{dC_{H^+}}{dr} \right|_{r=0} = 0 \quad (4.21)$$

In this study, Equations 4.10 to 4.13 were numerically solved by Matlab 7.0 based on the method developed in Chapter 3. All the kinetic constants used are summarized in Table. 4.1.

Chapter 4 Mechanism of Calcium Accumulation in Acetate-Fed Aerobic Granule

Table 4.1 Symbols and values of constants used

| Symbol | Description | Value | Units | References |
|-----------------|--------------------------------------|------------------------|--------------|-----------------------------|
| D_{O_2} | Diffusion coefficient of O_2 | 2×10^{-9} | $m^2 t^{-1}$ | Beyenal and Tanyolac (1994) |
| D_{H^+} | Diffusion coefficient of H^+ | 1.19×10^{-9} | $m^2 t^{-1}$ | Flora et al. (1995) |
| $D_{HCO_3^-}$ | Diffusion coefficient of HCO_3^- | 1.19×10^{-10} | $m^2 t^{-1}$ | Flora et al. (1995) |
| $D_{CO_3^{2-}}$ | Diffusion coefficient of CO_3^{2-} | 1.23×10^{-10} | $m^2 t^{-1}$ | Flora et al. (1995) |
| μ_{max} | Maximum specific growth rate | 2.4 | d^{-1} | |
| ρ_x | Biomass density | 32 | $g L^{-1}$ | |
| K_{CaCO_3} | Solubility product constant | $10^{-8.47}$ | | CRC (2003) |
| K_{h,CO_2} | Henry's law constant of CO_2 | $10^{1.47}$ | | Metcalf & Eddy (1991) |
| K_{a1} | 1st step dissociation constant of | $10^{-6.35}$ | | CRC (2003) |
| K_{a2} | 2nd step dissociation constant of | $10^{-10.33}$ | | CRC (2003) |
| P_{CO_2} | Partial CO_2 pressure in air | 0.033 | % | Metcalf & Eddy (1991) |
| C_{O_2} | Dissolved oxygen concentration | | M | |
| C_{H^+} | H^+ concentration | | M | |
| $C_{HCO_3^-}$ | HCO_3^- concentration | | M | |
| $C_{CO_3^{2-}}$ | CO_3^{2-} concentration | | M | |
| R_{CaCO_3} | $CaCO_3$ formation zone | | mm | |
| s | Substance concentration in granule | | | |
| r | Distance to granule center | | mm | |
| R_s | Substance utilization rate | | | |
| R_{O_2} | O_2 utilization rate | | mg | |
| R_{H^+} | H^+ consumption rate | | $M d^{-1}$ | |
| $R_{HCO_3^-}$ | HCO_3^- production rate | | $M d^{-1}$ | |
| $R_{CO_3^{2-}}$ | CO_3^{2-} production rate | | $M d^{-1}$ | |

4.4 RESULTS

4.4.1 Chemical form of calcium accumulated in acetate-fed aerobic granule

Figure 4.2 shows the major inorganic components of acetate-fed aerobic granule. It can be seen that both Ca^{2+} and CO_3^{2-} are dominant over the other inorganic components, such as Mg, P, Fe and Al which are indeed negligible. According to Figure 4.2, the molar ratio of granule calcium to carbonate was estimated as 1:1.16, indicating that most calcium ions in aerobic granule would exist in the form of calcium carbonate. The formation of calcium carbonate in aerobic granule implies that the concentration product of Ca^{2+} and CO_3^{2-} in aerobic granule must be greater than the solubility product constant of calcium carbonate.

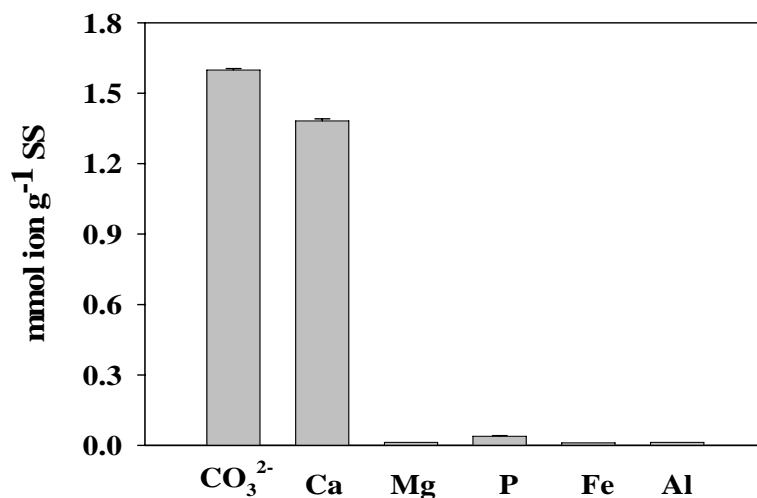


Figure 4.2 Ionic compositions of the acetate-fed aerobic granules.

4.4.2 Calcium distribution in acetate-fed aerobic granules

Fresh acetate-aerobic granules with a SOUR of $64 \text{ mg O}_2 \text{ g}^{-1} \text{ VS h}^{-1}$; SVI of 52 ml g^{-1} and a mean diameter of 1.4 mm were sectioned for SEM-EDX analysis (Figure 4.3). Figures 4.3 clearly show that the calcium was mainly accumulated in the core part of aerobic granule, while the granule shell was nearly calcium free. The IA analysis further revealed white deposits localized at $300 \text{ }\mu\text{m}$ from the granule surface (Figure 4.3c). After hydrochloric acid was added to the zone of white deposits (Figure 4.3c), gas bubbles were immediately generated (Figure 4.3d). The gas phase analysis by the online carbon dioxide sensor (Figure 4.1) confirmed that the bubbles generated were carbon dioxide (Figure 4.3d). These observations provide further visualized evidence that calcium mainly existed in the form of CaCO_3 in the acetate-fed aerobic granules, which is in good agreement with the stoichiometric analysis (Figure 4.2).

The pH and CO_3^{2-} profiles in aerobic granule were simulated along the granule radius using the models presented earlier (Figure 4.4). For aerobic granule with a radius of 0.7 mm , the pH and CO_3^{2-} profiles can be divided into two regimes, i.e. in the depth of $300 \text{ }\mu\text{m}$ from the granule surface, a significant decline in both pH and carbonate concentrations was found, while at the depth of $300 \text{ }\mu\text{m}$ from the granule surface to the centre of the granule, the profiles of pH and carbonate concentration nearly remained constant at the maximum levels. In fact, a similar pH profile was also observed in the acetate-fed anaerobic granule (de Beer et al. 1992).

Theoretically, the maximum calcium concentration in granule would be equal to its bulk concentration, i.e. about $1.16 \times 10^{-4} \text{ mol L}^{-1}$. According to Equation (4.1), the required minimum CO_3^{2-} concentration for the formation of CaCO_3 was thus estimated as $2.9 \times 10^{-5} \text{ mol L}^{-1}$. In view of the CO_3^{2-} profile in Figure 4.4, it is

Chapter 4 Mechanism of Calcium Accumulation in Acetate-Fed Aerobic Granule

reasonable to consider that CaCO_3 will be mainly formed in the region with a depth below $300\text{ }\mu\text{m}$ from the granule surface, i.e. $r < R_{\text{CaCO}_3}$ zone (Figure 4.4). Such a theoretical prediction is in good agreement with the experimental observation as shown in Figure 4.3.

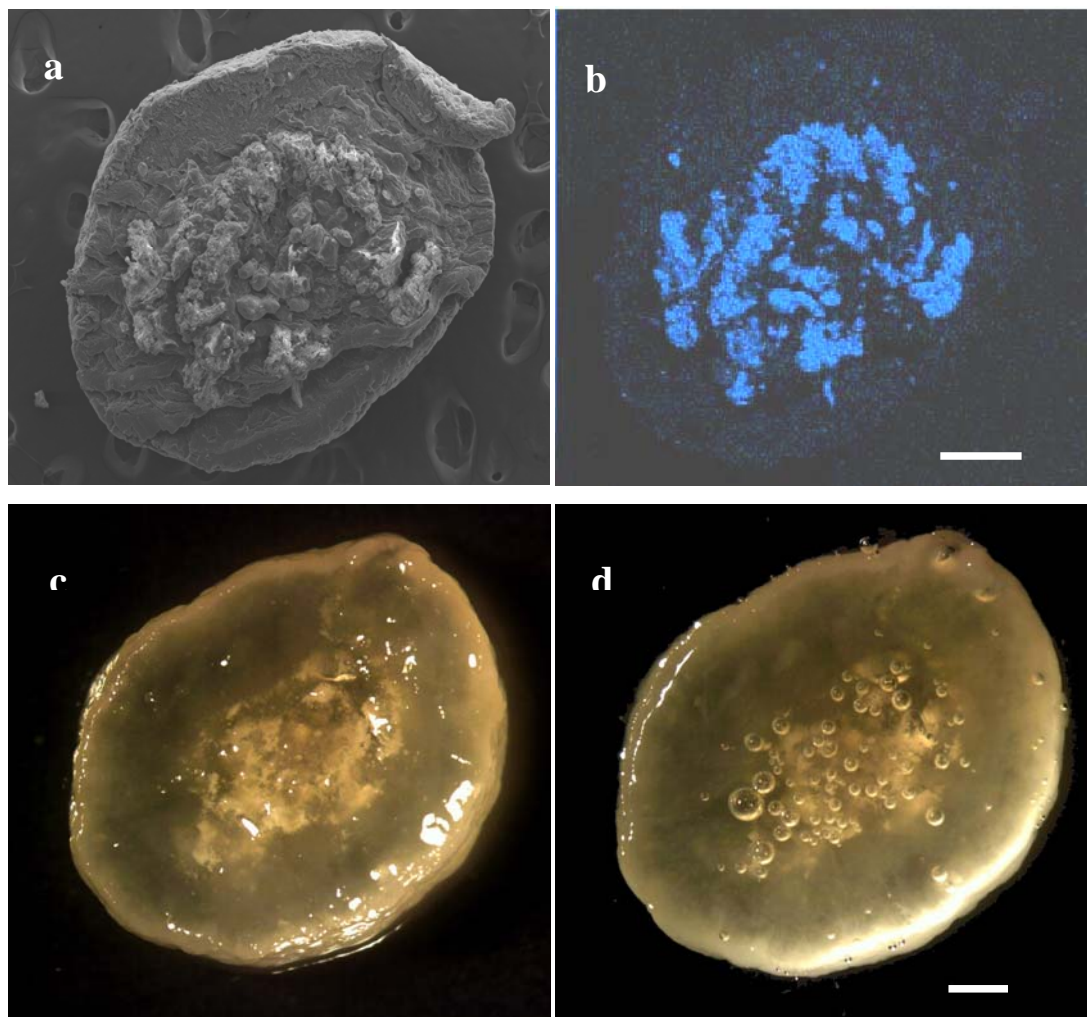


Figure 4.3 a: Cross-section view of the acetate-fed aerobic granule by SEM; b: the EDX mapping for calcium indicated by *blue color*, bar: $100\text{ }\mu\text{m}$; c: IA cross-section view of the acetate-fed aerobic granule; d: generation of gas bubbles during the acid-granule reaction, bar: $200\text{ }\mu\text{m}$.

4.4.3 Granule size-dependent CaCO_3 formation in acetate-fed aerobic granule

It appears from Figures 4.2 and 4.3 that calcium in the form of CaCO_3 would preferably be accumulated in the core part of granule, while a nearly calcium free outer shell of aerobic granule was found. A basic question of how this would happen remains unanswered so far. Figure 4.5a shows the calcium contents in aerobic granules with various sizes. It appears that the calcium content of aerobic granule is proportionally related to the granule size, e.g. the calcium content in aerobic granule with a radius of 1.4 to 2.0 mm is almost 10 times higher than that in aerobic granules with a radius of 0.1 to 0.2 mm. Changes in the ash content of aerobic granule over time further reveals that the ash content was very low at the initial stage of aerobic granulation, but it sharply increased on the 8th day in response to a significant increase in granule size, and gradually stabilized at the level of about $0.4 \text{ g g}^{-1} \text{ SS}$ after 40 days (Figure 4.5b). These seem to imply that calcium would continue to accumulate in aerobic granule even after the formation of aerobic granule.

In this study, the volume fraction of the R_{CaCO_3} region in aerobic granule (Figure 4.4), i.e. $(R_{\text{CaCO}_3}/R)^3$, was simulated for aerobic granules with various radiuses in the range of 0.5 to 2 mm (Figure 4.6). It appears that the formation of calcium carbonate would be negligible in aerobic granule smaller than 0.5 mm in radius, while calcium carbonate would start to form only in aerobic granules larger than 0.5 mm in radius. This in turn provides a plausible explanation for the observed size-dependent CaCO_3 formation in aerobic granules (Figure 4.5). Such theoretical estimate is pretty consistent with the measured calcium and ash contents in aerobic granules (Figure 4.6).

Chapter 4 Mechanism of Calcium Accumulation in Acetate-Fed Aerobic Granule

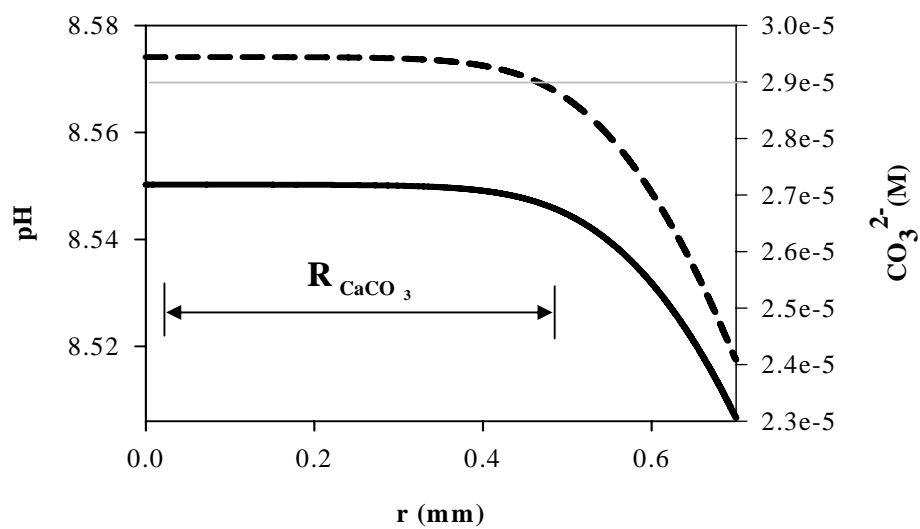


Figure 4.4 Simulation profiles of pH (—) and CO_3^{2-} (---) in the acetate-fed aerobic granule.

Chapter 4 Mechanism of Calcium Accumulation in Acetate-Fed Aerobic Granule

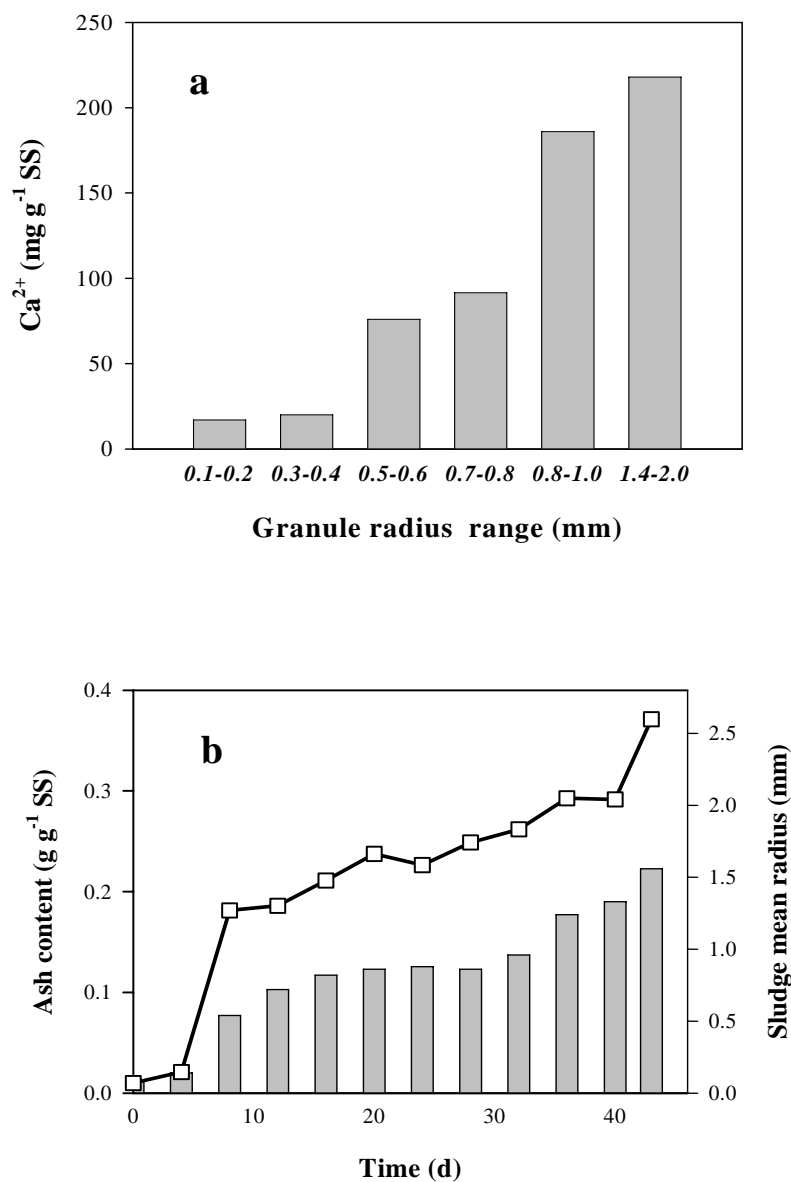


Figure 4.5 Size-dependent calcium and ash contents in the acetate-fed aerobic granules. a: calcium contents in aerobic granules with different radius ranges; b: ash content (*line*) and corresponding sludge mean radius (*bar*) in the course of aerobic granulation.

Chapter 4 Mechanism of Calcium Accumulation in Acetate-Fed Aerobic Granule

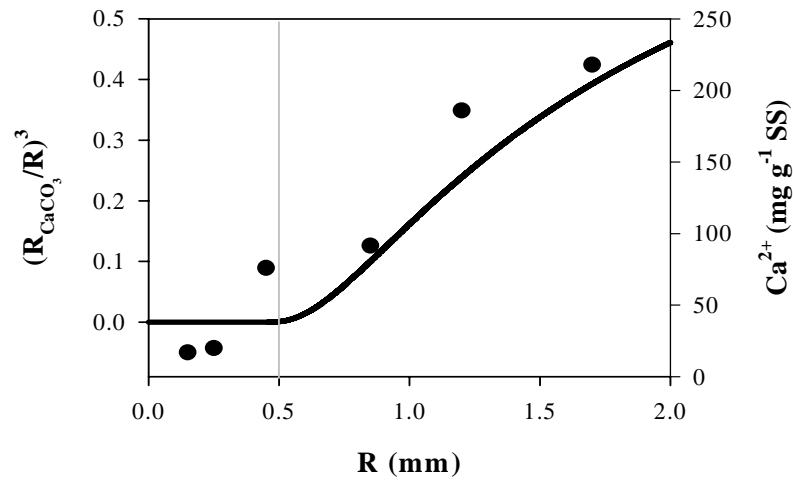


Figure 4.6 Comparison of the simulated and experimentally measured $CaCO_3$ as well as ash contents in the acetate-fed aerobic granule. —: $(R_{CaCO_3}/R)^3$ simulation; ●: calcium content.

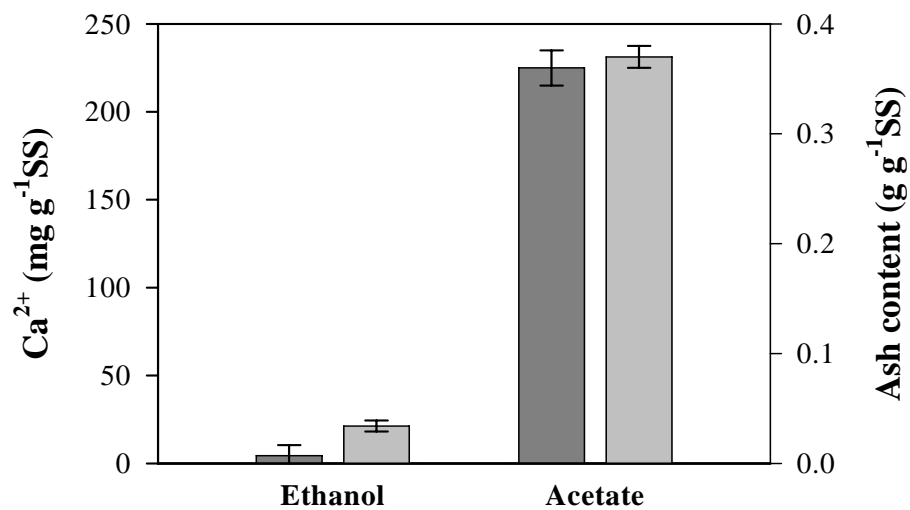


Figure 4.7 Comparison of calcium (*left*) and ash (*right*) contents in the ethanol- (Liu et al. 2003) and acetate-fed aerobic granules.

4.5 DISCUSSION

Both microscopic observation and chemical analysis showed the accumulation of calcium in the form of CaCO_3 , and that the accumulation was mainly situated in the central part of acetate-fed aerobic granule (Figures 4.2 to 4.4). Moreover, the formation of CaCO_3 was only found in aerobic granules with a mean radius larger than 0.5 mm (Figures 4.5 and 4.6). These may indicate that the formation of calcium carbonate in the acetate-fed aerobic granules would be determined by the granule size. As can be seen in Equations 4.10 to 4.13, diffusion of metabolites in aerobic granule is size-dependent. Moreover, it appears from Equations 4.2, 4.3 and 4.5 that the metabolites, such as alkalinity and carbon dioxide produced by acetate oxidation, would further react to produce carbonate. As the result of mass diffusion, Equation 4.13 reveals that the carbonate gradient along the granule radius was established towards the bulk solution so as to diffuse the carbonate out of the granule. This means that the highest carbonate concentration would be found inside aerobic granule (Figure 4.4). It should be realized that this carbonate gradient would increase with the size of aerobic granule. Thus, a large aerobic granule would have a high carbonate concentration in its central part. Figure 4.6 clearly indicated that only in the acetate-fed aerobic granule with a radius larger than 0.5 mm, the inside carbonate concentration would be high enough for the formation of CaCO_3 .

Compared to the acetate-fed aerobic granules, Figure 4.7 showed that the calcium and ash contents were very low in aerobic granules grown on ethanol as sole carbon source. This is mainly due to the fact that alkalinity in the form of hydroxide ion was produced during the biological oxidation of acetate as illustrated in Equation 4.2, while no hydroxide ion can be generated in the oxidation of ethanol. In this case, calcium would not be accumulated in the ethanol-fed aerobic granules no matter what the granule size would be (Figure 4.7). In fact, the experimental

evidence point to the fact that a crystal CaCO_3 core is not necessarily required for aerobic granulation.

Extensive accumulation of calcium has also been found in biofilms and anaerobic granules (Batstone et al. 2002; Kemner et al. 2004). In the study of biofilm and anaerobic granulation in UASB reactor, Ca^{2+} has been often considered to bridge negatively charged sites on extracellular biopolymers, thus enhance the matrix stability of attached microbial community (Bruus et al. 1992; Korstgens et al. 2001; Wloka et al. 2004). According to this hypothesis, extra calcium has often been introduced into the medium for enhanced formation of biofilm and anaerobic granules (Huang and Pinder 1995; Yu et al. 2001). However, it appears from Figures 4.2 and 4.3 that calcium detected in the acetate-fed aerobic granules was mainly in the form of calcium carbonate rather than linked to extracellular polymeric substances. Batstone et al. (2002) put forward a hypothesis that pre-formation of a crystal CaCO_3 core would be prerequisite of anaerobic granulation. However, increasing evidence shows that microbial granulation is a cell-to-cell self immobilization process mainly driven by selection pressures (Liu et al. 2005), i.e. calcium may play a very minor role in microbial granulation process. This indeed is supported by previous studies on aerobic and anaerobic granulation (Guiot et al. 1988; Thiele et al. 1990; El-Mamouni et al. 1995; Van Langerak et al. 1998).

4.6 CONCLUSIONS

This study offers in-depth insights into the mechanisms of calcium accumulation in acetate-fed aerobic granules. It was found that almost all calcium accumulated in acetate-fed aerobic granules was in the form of CaCO_3 . Moreover, the accumulated calcium carbonate was mainly situated in the central part of acetate-fed aerobic granule. It was demonstrated that the accumulation of calcium was closely related

Chapter 4 Mechanism of Calcium Accumulation in Acetate-Fed Aerobic Granule

to the size-dependent diffusion limitation of oxygen inside aerobic granules. For instance, the calcium accumulation was shown to be size dependent, i.e., the calcium accumulation was only found in aerobic granules with the size larger than 0.5 mm.

CHAPTER 5

STOICHIOMETRIC ANALYSIS OF DOC FLUX INTO STORAGE AND GROWTH IN AEROBIC GRANULES

5.1 INTRODUCTION

Microorganisms can be classified into two gross groups with respect to their colony morphology, namely suspended and immobilized microbial growths. Suspended microorganisms, represented by activated sludge, demonstrate loose consortia structure and tiny colony size, thus they may have instant access to ambient resources. In contrast, immobilized microorganisms, such as biofilm, aerobic and anaerobic granules, live in a lower than ambient resource condition because their highly compact structure causes severe mass diffusion limitation (Caldwell and Lawrence 1986; Alphenaar et al. 1993; Liu et al. 2005a). Microorganisms living in suspended and immobilized cultures indeed exhibit different physiological behaviors, which may help to explain the possible discrepancy between the kinetics and metabolisms of these two groups of microorganisms. So far, numerous investigations have been dedicated to looking into the metabolic and kinetic behaviors of biofilms.

Aerobic granules are dense bacterial spheres formed through cell-to-cell self-immobilization which is driven by selection pressure (Liu et al. 2005c). Their superiorities over conventional activated sludge flocs entitle them a promising alternative form of microorganisms for advanced wastewater treatment. Unlike the intensive research that has been done with biofilm and anaerobic granules, very limited information is currently available about the metabolic and kinetic behaviors of aerobic granules with different sizes. Therefore, this chapter mainly focused on these two aspects.

5.2 MATERIALS AND METHODS

Precultivation of aerobic granules was described in Chapter 3. Synthetic substrate used consisted of sodium acetate 820 mg L⁻¹, NH₄Cl 22.0 mg L⁻¹, K₂HPO₄ 7.5 mg L⁻¹, CaCl₂·2H₂O 9.5 mg L⁻¹, MgSO₄·7H₂O 6.25 mg L⁻¹, FeSO₄·7H₂O 5mg L⁻¹ and micronutrient solution 1.0 ml L⁻¹. The micronutrient solution contained: H₃BO₃ 0.05g L⁻¹, ZnCl₂ 0.05g L⁻¹, CuCl₂ 0.03g L⁻¹, MnSO₄·H₂O 0.05 g L⁻¹, (NH₄)₆MO₇O₂₄·4H₂O 0.05 g L⁻¹, AlCl₃ 0.05g L⁻¹, CoCl₂·6H₂O 0.05 g L⁻¹, NiCl₂ 0.05g L⁻¹.

Matured aerobic granules were harvested and further sorted into four-size categories using the wet-sieving method developed by Pereboom (1994), i.e. 0.75 mm, 1.5 mm, 2.4 mm and 3.4 mm, respectively. The mean sizes of the four groups of aerobic granules were further determined by IA technique (Image-Pro Plus, v 4.0, Media Cybernetics).

A respirometer (MicroOxymax, Columbus, USA) was used to study metabolism of aerobic granules with different mean sizes. The respirometer was equipped with online oxygen and carbon dioxide probes, which allow determination of the oxygen utilization and carbon-dioxide production (Figure 5.1). The sorted aerobic granules were put into the four chambers of respirometer with 50 ml substrate that had 240 mg L⁻¹ dissolved organic carbon (DOC) and other necessary nutrients as presented above. The initial MLSS concentrations in the four chambers were controlled at the same level of 2.0 g L⁻¹. The DOC concentration was analyzed by TOC analyzer (Shimadzu, TOC-Vcsh, USA). The elemental compositions of aerobic granules were determined by CHNS analyzer (CHNS analyzer, 2400 II, PerkinElmer, USA) and inductively coupled plasma emission spectrometer (ICP, Optima 2000, PerkinElmer, USA). The other measurements were all done according to standard methods (APHA 1998).

Chapter 5 Stoichiometric Analysis of DOC Flux into Storage and Growth in Aerobic Granules

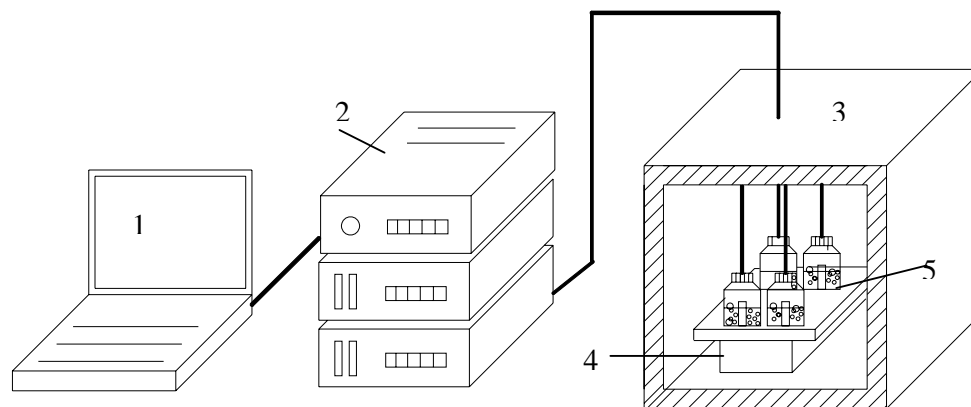


Figure 5.1 Respirometer system. 1. Computer for data collection; 2. Respirometer equipped with oxygen and carbon dioxide probes; 3. Evaporation condensing machine; 4. Shaker; 5. Reaction vessel.

5.3 RESULTS AND DISCUSSION

5.3.1 Respirometric profiles of aerobic granules with different sizes

In this study, the respirometer (Figure 5.1) was used to determine carbon flux in the cultures of aerobic granules with different sizes of 0.75 to 3.4 mm. Figures 5.2 to 5.5 show the profiles of oxygen utilization rate (OUR) and carbon dioxide production rate (CPR) for aerobic granules with different sizes, meanwhile utilization of external DOC is also presented in the same figures. Regardless of the granule mean size, three metabolic phases can be differentiated in Figures 5.2 to 5.5: (I) a quick reduction in the external DOC concentration is observed, and this DOC reduction is associated with a maximum OUR as well as a maximum CPR. In this phase, external organic carbon would likely be converted to storage materials first; (II) after depletion of the external DOC, aerobic granules further grow on the stored

Chapter 5 Stoichiometric Analysis of DOC Flux into Storage and Growth in Aerobic Granules

materials derived from phase one. As the result, a low OUR and CPR are recorded; (III) by the end of phase II, most stored materials are likely consumed, and microbial metabolism comes into the endogenous respiration which leads to a minimum OUR.

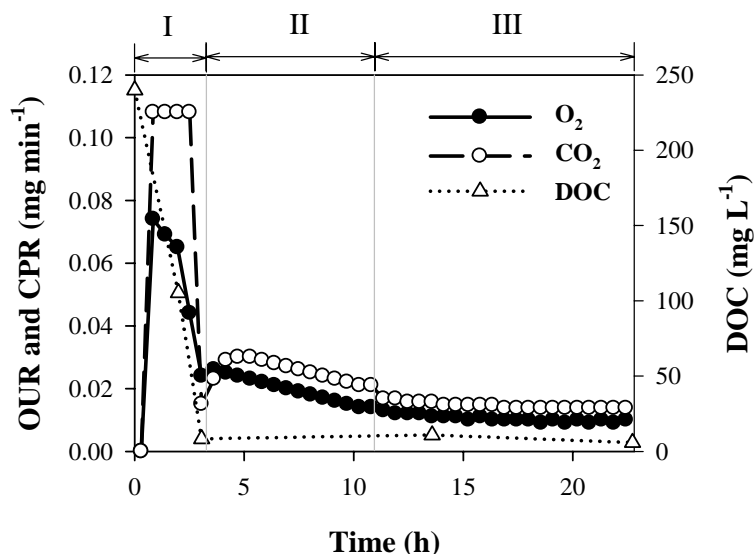


Figure 5.2 Changes in OUR, CPR and DOC concentration during respirometric test of aerobic granules with a mean size of 0.75 mm.

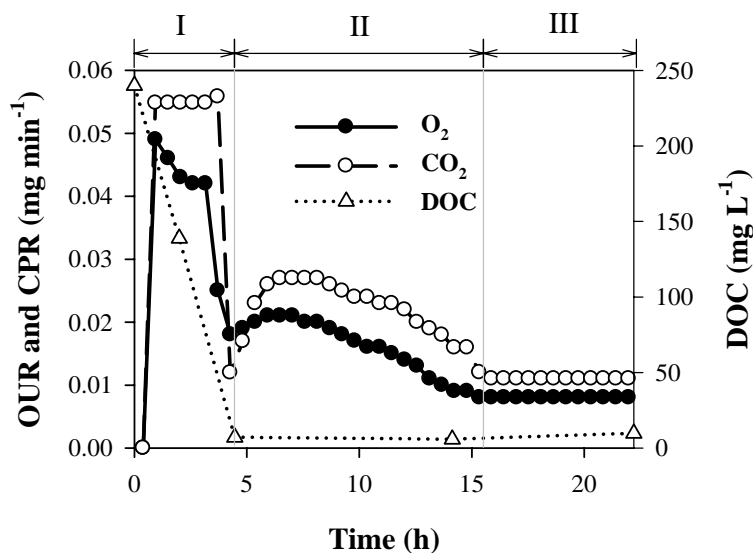


Figure 5.3 Changes in OUR, CPR and DOC concentration during respirometric test of aerobic granules with mean size of 1.5 mm.

Chapter 5 Stoichiometric Analysis of DOC Flux into Storage and Growth in Aerobic Granules

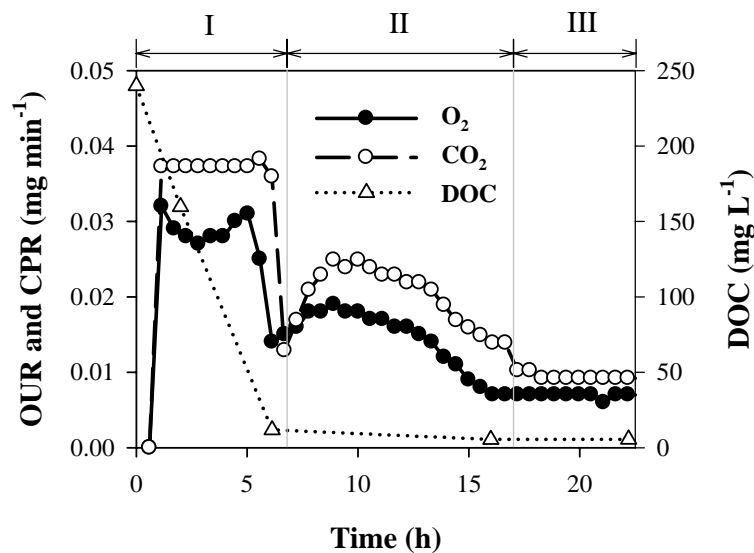


Figure 5. 4 Changes in OUR, CPR and DOC concentration during respirometric test of aerobic granules with a mean size of 2.4 mm.

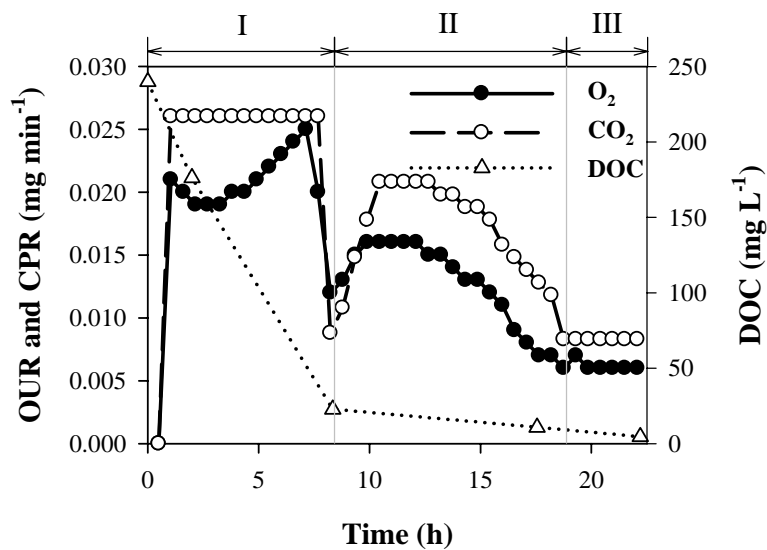


Figure 5. 5 Changes in OUR, CPR and DOC concentration during respirometric test of aerobic granules with a mean size of 3.4 mm.

Chapter 5 Stoichiometric Analysis of DOC Flux into Storage and Growth in Aerobic Granules

It appears that the OURs of smaller aerobic granules were higher than those of bigger granules in all the three phases. For instance, in phase I, the OUR of aerobic granules with the size of 0.75 mm was almost three times higher than that of aerobic granules with the size of 3.4 mm. This can be properly explained by the results presented in Chapter 3, i.e. diffusion of substrate and oxygen in aerobic granules smaller than 0.4 mm would not be a limiting factor in the observed biodegradation process of external organic substrate. The higher OUR of smaller aerobic granules is due to the less diffusion limitation inside smaller aerobic granules. These in turn will result in a higher microbial activity in terms of OUR and CPR as observed in Figures 5.2 to 5.5.

5.3.2 Carbon flux in aerobic granules with different sizes

According to the results given in Figures 5.2 to 5.5, carbon fluxes in the cultures of aerobic granules with different sizes can be determined. As shown in Figures 5.6 to 5.9, the carbon fluxes into each form of bioproducts appear to be independent of the granule size, despite very distinctive transformation rates observed in Figures 5.2 to 5.5. It can be seen in Figures 5.6 to 5.9 that in phase I, around 60% of the substrate-DOC was first transformed into cellular storage material, while the rest 40% was oxidized to carbon dioxide as energy source. Subsequently, in phase II, about half of the storage material was ultimately synthesized into new cells, and the remaining part was oxidized into carbon dioxide.

Chapter 5 Stoichiometric Analysis of DOC Flux into Storage and Growth in Aerobic Granules

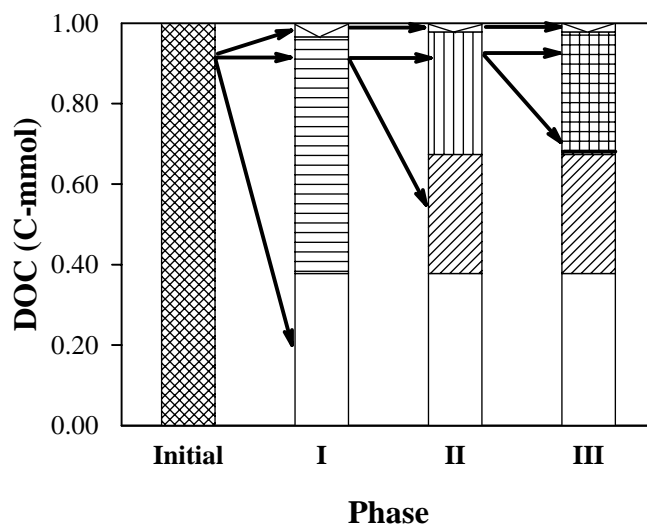


Figure 5.6 Carbon fluxes in the culture of aerobic granules with the mean size of 0.75 mm. : substrate; : cellular storage; : CO₂ produced in phase I; : biomass synthesized in phase II; : CO₂ produced in phase II; : biomass after decay in phase III; : CO₂ produced in phase III; : residual DOC.

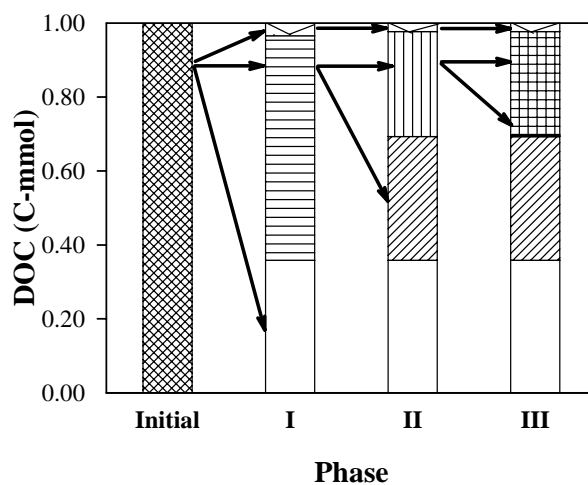


Figure 5.7 Carbon fluxes in the culture of aerobic granules with the mean size of 1.5 mm, : substrate; : cellular storage; : CO₂ produced in phase I; : biomass synthesized in phase II; : CO₂ produced in phase II; : biomass after decay in phase III; : CO₂ produced in phase III. : residual DOC.

Chapter 5 Stoichiometric Analysis of DOC Flux into Storage and Growth in Aerobic Granules

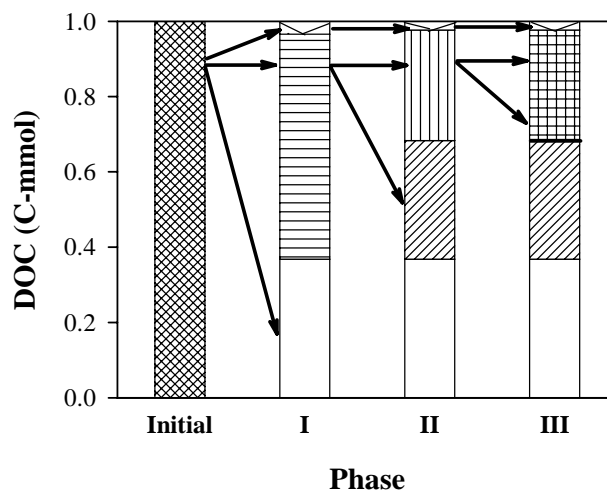


Figure 5.8 Carbon fluxes in the culture of aerobic granules with the mean size of 2.4 mm, : substrate; : cellular storage; : CO₂ produced in phase I; : biomass synthesized in phase II; : CO₂ produced in phase II; : remained biomass after decay in phase III; : CO₂ produced in phase III. residual DOC.

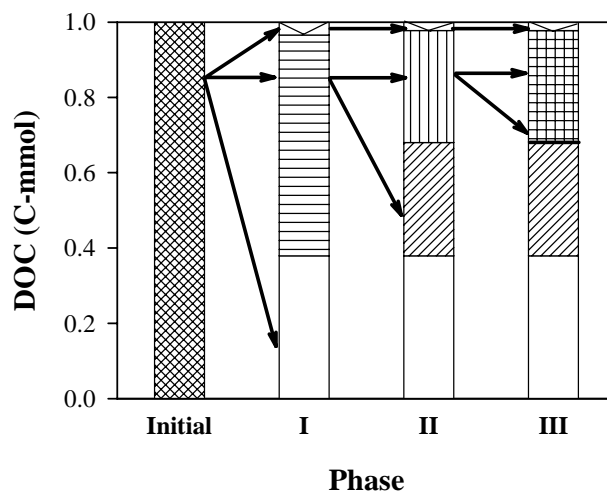


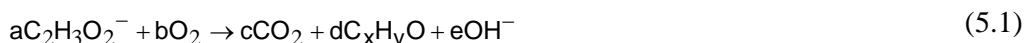
Figure 5.9 Carbon fluxes in the culture of aerobic granules with the mean size of 3.4 mm, : substrate; : cellular storage; : CO₂ produced in phase I; : biomass synthesized in phase II; : CO₂ produced in phase II; : biomass after decay in phase III; CO₂ produced in phase III. residual DOC.

5.3.3 Stoichiometric analysis of metabolisms of aerobic granules

Storage material has been reported in activated sludge process, and most storage materials are found to be in the form of poly- β -hydroxybutyrate (PHB), especially in microbial cultures fed with acetate. According to activated sludge model No. 3 (ASM3) (Gujer et al. 1999), organic substrate will be firstly transformed into storage materials which are subsequently metabolized into new biomass, meanwhile some portion of dissolved organic carbon will be oxidized to provide energy required for substrate conversion and microbial growth as well. The results shown in Figures 5.2 to 5.5 are consistent with the ASM3 model. Based on the ASM3 model, a series of stoichiometric analyses of DOC degradation during the respirometric experiments was conducted for each metabolic phase observed in Figures 5.2 to 5.6.

Phase I: Conversion of external DOC to storage materials

As discussed earlier, the external DOC was quickly converted to storage materials in this phase. Such a conversion process of the external DOC to the storage material can thus be described as follows:



in which a, b, c, d and e represent the respective actual molar numbers of reactants and products measured from the respirometric experiments of aerobic granules (Figures 5.2 to 5.5), while x and y are the molecular ratio of carbon and hydrogen to oxygen in the formula of storage material produced. In addition, the mass balance equation for phase I reaction can be derived for each element (e.g. C, H, O).

Phase II: microbial growth on storage materials

In this phase, aerobic granules grew on the storage material derived from Phase I. The elemental composition of aerobic granules was predetermined by the CHNS analyzer and ICP (Inductively Coupled Plasma) emission spectrometer as described in Section 5.2. It was found that the elemental compositions of aerobic granules with different sizes were about the same, which could be expressed as $\text{C}_{5.9}\text{H}_{10}\text{O}_{3.4}\text{N}$. Thus, microbial growth in Phase II can be depicted in a way such that:

*Chapter 5 Stoichiometric Analysis of DOC Flux into Storage and Growth in
Aerobic Granules*



in which f, g, h, i and j are the actual molar numbers of oxygen, ammonia consumed and carbon dioxide, biomass and water produced in the reaction.

According to Equation 5.1, the following mass equations can be obtained:

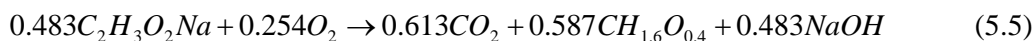
$$\begin{aligned} \text{C: } 2a &= x \times d + c \\ \text{H: } 3a &= y \times d + e \\ \text{O: } 2a + 2b &= 2c + d + e \\ \text{Charge: } a &= e \end{aligned} \quad (5.3)$$

Similarly, it appears from Equation 5.2 that

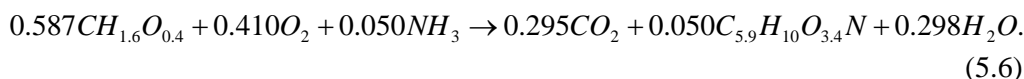
$$\begin{aligned} \text{C: } x \times d &= 2h + 5.9i \\ \text{H: } y \times d + 2f &= 2h + 3.4i + 2j \\ \text{O: } d + 2f &= 2h + 3.4i + j \\ \text{N: } g &= i \end{aligned} \quad (5.4)$$

As mentioned earlier, a is the actual number of moles of acetate determined by TOC analyzer. The b and c represent the actual numbers of moles of oxygen and carbon dioxide measured in phase I, and f and h are the actual number of moles of oxygen and carbon dioxide measured in phase II, respectively.

Following is an example of how the coefficients involved in Equations 5.1 and 5.2 would be derived for aerobic granules with the size of 0.75 mm. The values of a, b, c, f and h can be experimentally determined from Figures 5.2 and 5.6, i.e. a=0.483, b=0.254, c=0.613, f=0.411 and h=0.295. Using software Mathematica 5.2, Equations 5.3 and 5.4 can be solved simultaneously for the rest unknowns. Consequently, the transformation of DOC to the storage materials in Phase I can be expressed as



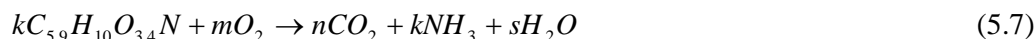
and the oxidation of the stored material to new biomass is given by



*Chapter 5 Stoichiometric Analysis of DOC Flux into Storage and Growth in
Aerobic Granules*

To better illustrate the storage and biosynthesis reactions based on one mol of external acetate, both the sides of Equations 5.5 and 5.6 are divided by 0.483, and the resultant reactions are summarized in Table 5.1 for aerobic granules with a mean size of 0.75 mm. The reactions for aerobic granules with other sizes can also be derived in a similar way and presented in Table 5.1.

The reaction of phase III can be expressed as follows:



in which k, m, n, k and s are the respective number of moles of decayed biomass, oxygen consumed, carbon dioxide, ammonia water produced. Values of m and n can be obtained from the respirometric tests. Similar to Phases I and II, the rest coefficients can be calculated from the mass balance equation on each element involved in Eq. 5.7 as given in Table 5.1.

It appears from Table 5.1 that the storage materials produced by aerobic granules have a similar chemical composition regardless of the sizes of aerobic granules. It was further found that the storage material synthesized by aerobic granules indeed is very close to poly- β -hydroxybutyrate (PHB) (Table 5.2). In fact, the accumulation of PHB was observed in the N-removal aerobic granules, and PHB was stored in bacteria situated in deeper layers of aerobic granules (Beun et al. 2001).

In the activated sludge process, the storage material is often observed in feast period, and is then utilized in famine period (Beun et al. 2000a; Dircks et al. 2001). Previous research showed that the storage material would predominantly be PHB when acetate was used as sole carbon source (Beccari et al. 2002). As shown in Table 5.3, PHB has been found to be the main storage material in most of activated sludge cultures, especially when acetate is used as the substrate, while in case where glucose is used as substrate, glycogen is possibly formed as an alternative of storage materials.

Chapter 5 Stoichiometric Analysis of DOC Flux into Storage and Growth in Aerobic Granules

Table 5.1 Reaction stoichiometry of aerobic granules with different sizes.

| Size of aerobic granules | Phase | Reactions |
|--------------------------|-----------|---------------------------------------------------------------------------------------------------------------------|
| 0.75 mm | Phase I | $C_2H_3O_2Na + 0.526O_2 \rightarrow 0.783CO_2 + 1.217CH_{1.6}O_{0.4} + NaOH$ (5.10) |
| | Phase II | $1.217CH_{1.6}O_{0.4} + 0.85O_2 + 0.103NH_3 \rightarrow 0.611CO_2 + 0.103C_{5.9}H_{10}O_{3.4}N + 0.614H_2O$ (5.11) |
| | Phase III | $C_{5.9}H_{10}O_{3.4}N + 5.92O_2 \rightarrow 5.97CO_2 + NH_3 + 3.3H_2O$ (5.12) |
| 1.5 mm | Phase I | $C_2H_3O_2Na + 0.557O_2 \rightarrow 0.743CO_2 + 1.257CH_{1.6}O_{0.5} + NaOH$ (5.13) |
| | Phase II | $1.257CH_{1.6}O_{0.4} + 0.877O_2 + 0.095NH_3 \rightarrow 0.694CO_2 + 0.095C_{5.9}H_{10}O_{3.4}N + 0.671H_2O$ (5.14) |
| | Phase III | $C_{5.9}H_{10}O_{3.4}N + 5.90O_2 \rightarrow 5.90CO_2 + NH_3 + 3.4H_2O$ (5.15) |
| 2.4 mm | Phase I | $C_2H_3O_2Na + 0.448O_2 \rightarrow 0.762CO_2 + 1.238CH_{1.6}O_{0.5} + NaOH$ (5.16) |
| | Phase II | $1.238CH_{1.6}O_{0.4} + 0.998O_2 + 0.092NH_3 \rightarrow 0.694CO_2 + 0.092C_{5.9}H_{10}O_{3.4}N + 0.667H_2O$ (5.17) |
| | Phase III | $C_{5.9}H_{10}O_{3.4}N + 5.88O_2 \rightarrow 5.90CO_2 + NH_3 + 3.36H_2O$ (5.18) |
| 3.4 mm | Phase I | $C_2H_3O_2Na + 0.467O_2 \rightarrow 0.785CO_2 + 1.215CH_{1.6}O_{0.5} + NaOH$ (5.19) |
| | Phase II | $1.215CH_{1.6}O_{0.4} + 0.892O_2 + 0.100NH_3 \rightarrow 0.63CO_2 + 0.100C_{5.9}H_{10}O_{3.4}N + 0.560H_2O$ (5.20) |
| | Phase III | $C_{5.9}H_{10}O_{3.4}N + 5.85O_2 \rightarrow 5.9CO_2 + 3.5H_2O + NH_3$ (5.21) |

Chapter 5 Stoichiometric Analysis of DOC Flux into Storage and Growth in Aerobic Granules

Table 5.2 Composition of storage materials in aerobic granules with different sizes.

| Mean size of aerobic granules (mm) | Composition |
|------------------------------------|---------------------------------|
| 0.7 | $\text{CH}_{1.6}\text{O}_{0.4}$ |
| 1.5 | $\text{CH}_{1.6}\text{O}_{0.5}$ |
| 2.4 | $\text{CH}_{1.6}\text{O}_{0.3}$ |
| 3.4 | $\text{CH}_{1.5}\text{O}_{0.3}$ |
| PHB | $\text{CH}_{1.5}\text{O}_{0.5}$ |

Chapter 5 Stoichiometric Analysis of DOC Flux into Storage and Growth in Aerobic Granules

Table 5.3 Yield coefficients obtained in this study and reported in literatures. All units in C-mol C-mol⁻¹.

| $Y_{x/s}$ | $Y_{sto/s}$ | $Y_{x/sto}$ | $Y_{co2/s}$ | Condition | Substrate | Storage | Culture | References |
|--------------|--------------|-------------|-------------|-----------|-----------|----------|------------------------|-----------------------|
| 0.41 | 0.62 | 0.63 | 0.59 | Aerobic | Acetate | PHB | Activated sludge | (Beun et al. 2000a) |
| 0.47 | 0.60 | - | 0.53 | Aerobic | Acetate | PHB | Activate sludge | (Carucci et al. 2001) |
| 0.15 | 0.47 | - | 0.38 | Aerobic | Acetate | PHB | Alcaligenes eutrophus | (Shi et al. 1997) |
| 0.35 | 0.48-0.68 | - | 0.65 | Anoxic | Acetate | PHB | Activated sludge | (Third et al. 2003) |
| 0.12 | 0.37 | - | 0.63 | Aerobic | Acetate | PHB | Thiothrix (CT3 strain) | (Majone et al. 2007) |
| 0.53 | 0.74 | 0.68 | 0.24 | Aerobic | Acetate | PHB | Activated sludge | (Sin et al. 2005) |
| 0.02 to 0.43 | 0.40 to 0.83 | - | - | Aerobic | Acetate | PHB | Activated sludge | (Serafim et al. 2004) |
| 0.05 | 0.88 | - | 0.07 | Aerobic | Glucose | Glycogen | Activated sludge | (Dircks et al. 2001) |
| 0.024 | 0.74 | - | 0.23 | Aerobic | Glucose | Glycogen | Activated sludge | (Dircks et al. 2001) |
| | | 0.44 | 0.66 | | | PHB-like | | |
| 0.27 to 0.30 | 0.61 to 0.63 | to | to | Aerobic | Acetate | material | Aerobic granules | This study |
| | | 0.50 | 0.72 | | | | | |

*Chapter 5 Stoichiometric Analysis of DOC Flux into Storage and Growth in
Aerobic Granules*

5.3.4 Conversion of DOC to storage material

As discussed earlier, in phase I, part of the external DOC was first converted into the storage materials, while the rest was oxidized to carbon dioxide. The conversion yield ($Y_{sto/s}$) of the external DOC to the storage material in Phase I can be obtained from Table 5.1. Figure 5.10 shows a nearly constant $Y_{sto/s}$ of about 0.6 C-mmol C-mmol⁻¹. This in turn implies that the conversion yield of the external DOC to the storage material would be independent of the size of aerobic granules. The $Y_{sto/s}$ values of aerobic granules obtained in this study are comparable with that reported in the literature, e.g. a conversion yield of 0.62 C-mmol C-mmol⁻¹ was obtained in the activated sludge culture fed with acetate as sole carbon source (Beun et al. 2000a).

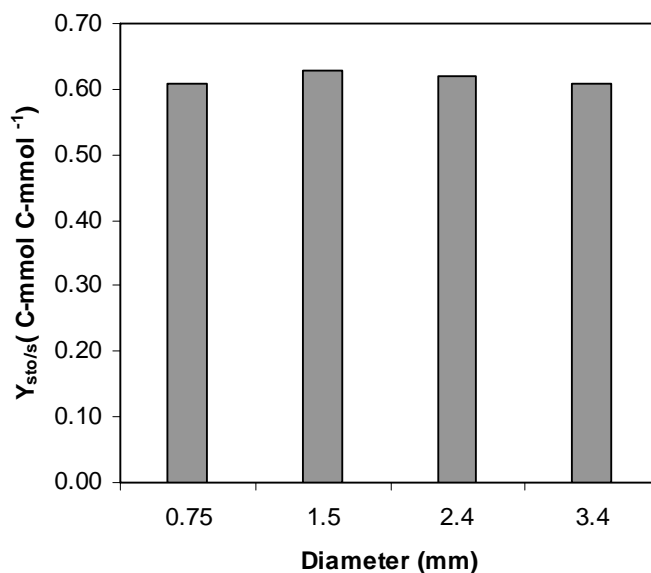
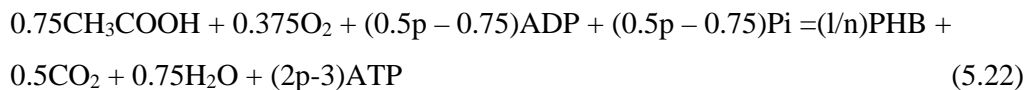


Figure 5.10 Conversion yield of DOC to storage material in aerobic granules with different sizes.

Chapter 5 Stoichiometric Analysis of DOC Flux into Storage and Growth in Aerobic Granules

Yamane (1993) estimated the theoretical yield of PHB from the biochemical pathway which accounts for recyclings or regenerations of $\text{NADP}^+ / (\text{NADPH} + \text{H}^+)$ and $\text{NAD}^+ / (\text{NADH} + \text{H}^+)$. According to Yamane (1993), when acetic acid is the carbon source, isocitrate dehydrogenase is the most possible enzyme to regenerate NADPH, and the net reaction becomes



in which PHB has the formula $(\text{CH}_{1.5}\text{O}_{0.5})_n$. The theoretical conversion yield of PHB can be estimated as $0.67 \text{ C-mol C-mol}^{-1}$. It appears that the conversion yield of PHB in aerobic granules is close to this theoretical value. It has been reported that the conversion of acetate to PHB in a laboratory activated sludge SBR was dissolved oxygen-dependent, e.g. at the lower DO supply rates, a higher proportion of the acetate was preserved as PHB ($Y_{\text{sto/s}} = 0.68 \text{ C-mol C-mol}^{-1}$) than at higher DO supply rates ($Y_{\text{sto/s}} = 0.48 \text{ C-mol C-mol}^{-1}$) (Third et al. 2003). The DO diffusion limitation in aerobic granules has been experimentally and theoretically demonstrated in Chapter 3. Therefore, the DO-dependent PHB conversion may reasonably explain the high conversion yield of acetate to PHB in the culture of aerobic granules in which DO limitation is often encountered.

5.3.5 Conversion of storage material to new biomass

In Phase II, aerobic granules would grow on the storage material. The growth yields of aerobic granules ($Y_{\text{x/sto}}$) on the storage material can be calculated from Table 5.1. It was found in Figure 5.11 that the values of $Y_{\text{x/sto}}$ fell into a very narrow range of 0.44 to $0.50 \text{ C-mmol C-mmol}^{-1}$ for aerobic granules with different sizes. These in turn imply that aerobic granules grown on acetate with different sizes would exhibit similar growth behaviors. As summarized in Table 5.3, the growth yield of activated sludge on PHB was reported to be about $0.653 \text{ C-mmol C-mmol}^{-1}$ (Van Aalst-van Leeuwen et al. 1997), while a lower yield of $0.248 \text{ C-mmol C-mmol}^{-1}$ was also obtained by Beun et al. (2000a).

Chapter 5 Stoichiometric Analysis of DOC Flux into Storage and Growth in Aerobic Granules

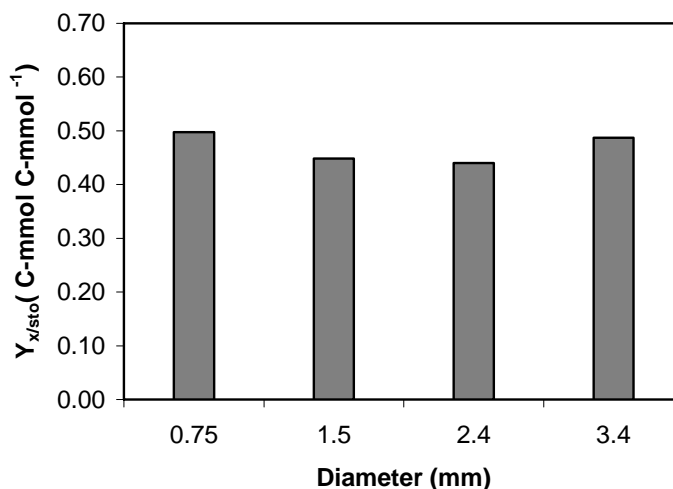


Figure 5.11 Growth yields of biomass on storage material for aerobic granules with different sizes.

5.3.6 Specific consumption rate of storage material

In Phase II, the average specific storage consumption rate can be calculated as follows:

$$q_{sto} = \frac{C_{sto}}{X t_{p2}} \quad (5.23)$$

in which C_{sto} is the storage material consumed in phase II, t_{p2} is the duration of phase II, and X is the amount of total biomass. In this calculation, the storage material consumed is assumed to be equal to the storage material produced in phase I.

For instance, q_{sto} by aerobic granules with the mean size of 0.75 mm can be determined as follows:

*Chapter 5 Stoichiometric Analysis of DOC Flux into Storage and Growth in
Aerobic Granules*

$$q_{sto} = \frac{0.588 \text{ mmol}}{(7.75 \text{ h}) \times (0.1 \text{ g})} = 0.758 \text{ C-mmol h}^{-1} \text{ g}^{-1} \text{ biomass} \quad (5.24)$$

in which 0.588 mmol is the storage utilized in phase II and equals to the storage produced in phase I as shown in Figure 5.6. The time interval used in Equation 5.24 was determined from Figure 5.2.

Figure 5.12 shows that the storage consumption rate varies in a very narrow range with the size of aerobic granules. Aerobic granules with the smallest size of 0.75 mm have the highest specific cellular storage consumption rate, while aerobic granules with the size bigger than 0.75 mm have the comparable specific cellular storage consumption rates. For the activated sludge, according to data by Beun et al. (2000a) and using Equation 5.23, the average PHB consumption rate by activated sludge was estimated as $0.57 \text{ C-mmol g}^{-1} \text{ MLSS h}^{-1}$, which is comparable with the q_{sto} values given in Figure 5.12 for aerobic granules. It is reasonable to conclude that the storage consumption rate of aerobic granules is close to that of activated sludge.

Chapter 5 Stoichiometric Analysis of DOC Flux into Storage and Growth in Aerobic Granules

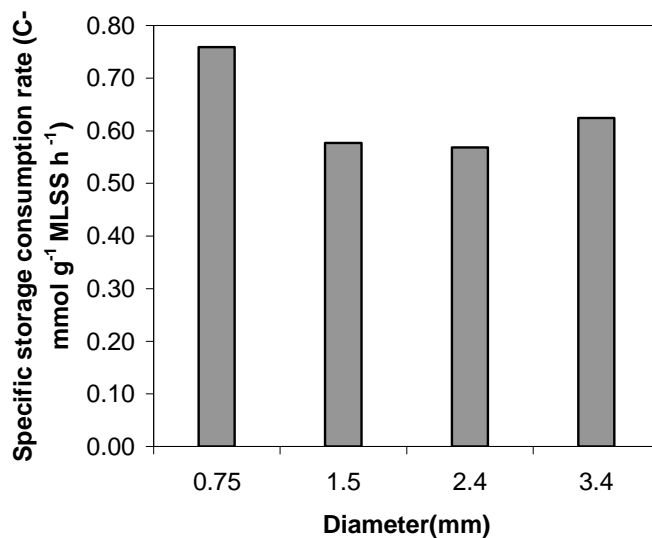


Figure 5.12 Specific storage consumption rates in phase II for aerobic granules with different sizes.

5.3.7 Overall growth yield of aerobic granules

The overall growth yield ($Y_{x/s}$) of aerobic granules in phases I and II can be calculated as follows:

$$Y_{x/s} = Y_{sto/s} Y_{x/sto}. \quad (5.25)$$

It appears from Figure 5.13 that the overall growth yields of aerobic granules with different sizes were found to be quite constant, around 0.3 (C-mol C-mol⁻¹). It can be seen that about 30% of the external acetate-DOC was ultimately converted to new biomass of aerobic granules. The $Y_{x/s}$ values of aerobic granules obtained in this study fall into the yield range of those PHB synthesizing microbial cultures, i.e. 0.13 to 0.53 C-mol C-mol⁻¹ when acetate was used as substrate (Table 5.3).

Chapter 5 Stoichiometric Analysis of DOC Flux into Storage and Growth in Aerobic Granules

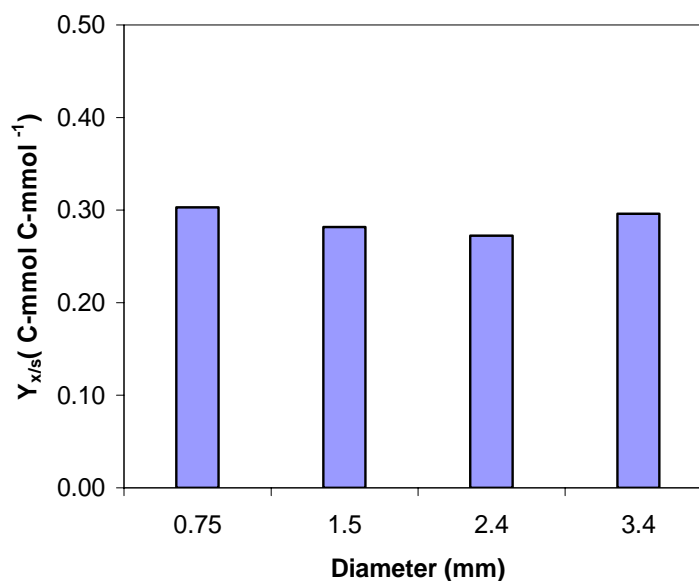


Figure 5.13 The observed growth yields of aerobic granules with different sizes.

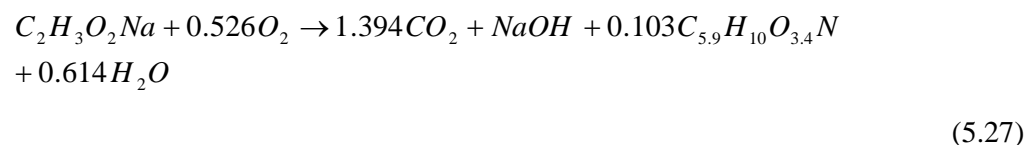
5.3.8 Overall growth rate of aerobic granules

The overall growth rate of aerobic granules is the average value of phases I and II. According to Canziani et al. (2006), the growth rate μ_{obs} can be calculated as follows:

$$\mu_{obs} = \frac{\Delta MLSS}{MLSS \cdot t_{12}} \quad (5.26)$$

in which $\Delta MLSS$ is the biomass increased in phases I and II, $MLSS$ is the mixed liquid suspended solid, t_{12} is the total duration of phase I and II.

Based on the given initial input of DOC, $\Delta MLSS$ for each size of aerobic granules can be estimated from equations in Table 5.1. For instance, in case of aerobic granules with the mean size of 0.75 mm, combination of Equations. 5.10 and 5.11 gives



*Chapter 5 Stoichiometric Analysis of DOC Flux into Storage and Growth in
Aerobic Granules*

It appears from Equation 5.24 that every 2 mols of DOC consumed can form 0.103 mol of new biomass. As shown in Figure 5.6, in the culture of aerobic granules with the mean size of 0.75 mm, 0.966 mmol DOC was utilized, thus $0.966 \times 0.103/2$ mmol of new biomass would be produced, i.e. $\Delta MLSS = 0.966 \times 0.103/2$ (mmol-biomass) $\times 149.2$ (mg/mol) = 7.46 mg in which 149.2 is the molecular weight of biomass. According to Eq. 5.19, the overall growth rate of aerobic granules with the mean size of 0.75 mm can be calculated as follows:

$$\mu_{obs} = \frac{7.46 \text{ mg}}{(100 \text{ mg}) \times (10.81 \text{ h})} = 0.0069 \text{ h}^{-1} = 0.161 \text{ d}^{-1} \quad (5.28)$$

It can be seen in Figure 5.14 that smaller aerobic granules show higher growth rate than bigger granules, e.g. the growth rate of the smallest granules is about 1.5 times higher than that of the biggest aerobic granules. As shown in Figure 5.14, the overall growth rates (μ_{obs}) of aerobic granules with different sizes varied from 0.097 to 0.161 d^{-1} . Chen et al. (2008) reported that the observed growth rates of acetate-fed aerobic granules fell into a very wide range of 0.075 to 0.274 d^{-1} . Using the respirometric method similar to that used in this study, the specific growth rate for acetate-fed activated sludge was found to be in the range of 0.05 to 0.264 d^{-1} (Beun et al. (2000a).

Chapter 5 Stoichiometric Analysis of DOC Flux into Storage and Growth in Aerobic Granules

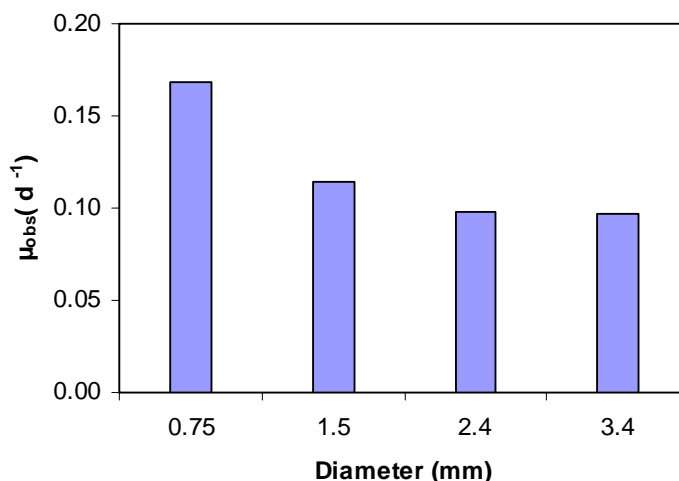


Figure 5.14 Overall growth rates of aerobic granules with different sizes.

Evans and Liu (2003) examined the influence of hydrodynamic forces on the overall behaviors of activated sludge, and found that the observed growth rates varied in a wide range of 0.96 to 4.8 d⁻¹, while in study of the specific growth rate of mixed activated sludge with the limiting substrate of phosphorus in both batch cultures, the specific growth rate was found to be as high as 0.092 to 0.617 h⁻¹ at 25°C, equivalent to 2.2 to 14.8 d⁻¹ (Wu and Okrutny 2004). These indicate that the growth rate of activated sludge is much higher than the growth rate of aerobic granules, i.e. activated sludge in the form of suspended sludge can grow faster than aerobic granules. This is probably due to the aggregated structure of aerobic granules that serves as a diffusion barrier of substrate and nutrients for microbial growth. In fact, Rozen et al. (2001) reported that the growth profile of a thin biofilm with a thickness less than 11 μm was similar to that of the same planktonic bacteria, and they further concluded that in case where diffusion limitation would be negligible, i.e. if bacteria are not embedded in a thick and dense biofilm, the growth of bacteria in biofilm may resemble their growth in suspension. In addition, Wentland et al. (1996) also found that biofilms with a thickness of 20 μm had high average specific growth rates greater than 1 h⁻¹, however biofilms with a thickness bigger than 200 μm grew slowly at a rate smaller than 0.15 h⁻¹. Aerobic granules are

Chapter 5 Stoichiometric Analysis of DOC Flux into Storage and Growth in Aerobic Granules

formed through microbial self aggregation and finally organized in structured communities enmeshed in an exopolysaccharide matrix. Thus, similar to biofilms, aerobic granules can also be differentiated from their suspended counterparts by generation of an extracellular polymeric substance (EPS) matrix, reduced growth rates, and the regulation of specific genes via cellular signaling (Liu and Tay 2002; Wang et al. 2007).

5.3.9 Endogenous respiration of aerobic granules

It was observed in Figure 5.15 that in the endogenous respiration phase (Phase III), the OUR remained nearly constant regardless of the sizes of aerobic granules. The decay rate (k_d) can be determined from Equation 5.12, 5.15, 5.18, 5.21 and the experimentally measured OUR in Phase III:

$$k_d = \frac{149.2}{\alpha \times 32} \times \frac{OUR}{MLSS} \quad (5.29)$$

in which α is the number of moles of oxygen in the reaction of endogenous respiration (Table 5.1), and OUR is the measured oxygen utilization rate in phase III, and MLSS is the total biomass.

For the aerobic granules with the mean size of 0.75mm,

$$k_d = \frac{149.2}{5.92 \times 32} \times \frac{0.011 \text{ mg min}^{-1}}{100 \text{ mg}} = 7.8 \times 10^{-5} \text{ min}^{-1} = 0.11 \text{ d}^{-1} \quad (5.30)$$

It can be seen in Figure 5.15 that the k_d values of aerobic granules with different tended to decrease from 0.114 to 0.069 d^{-1} with the increase in the size of aerobic granules, i.e. smaller aerobic granules have higher decay rate than bigger granules. These values are consistent with those reported in the literature, e.g. the k_d values of acetate-fed aerobic granules varied in the range of 0.023 to 0.075 d^{-1} (Liu et al. 2005d; Chen et al. 2008). In Activated Sludge Model No. 1, by default, heterotrophic and autotrophic decay rates are often present to 0.24 and 0.1 d^{-1} at 15°C, respectively. In addition, the decay rates of heterotrophic biofilms have been reported to be 0.25 and 0.27 d^{-1} (Rittmann and McCarty 1980; Jin and Huang 1994). These seem to imply that the decay rates of aerobic granules are very low compared to values for activated sludge and biofilms. It has been observed that dissolve

*Chapter 5 Stoichiometric Analysis of DOC Flux into Storage and Growth in
Aerobic Granules*

oxygen would be a limiting substance in the cultures of aerobic granules (Chapter 3). In fact, previous study showed that at the lower level of dissolved oxygen, the lower decay rate would be observed (Avcioglu et al. 1998).

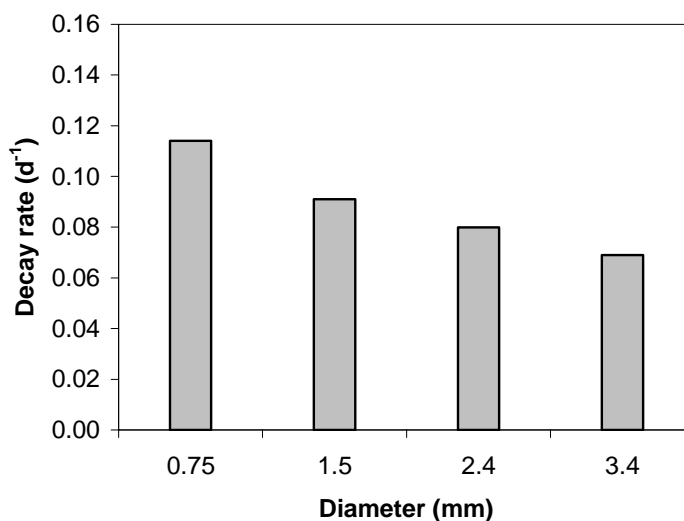


Figure 5. 15 Specific biomass decay rate (k_d) of aerobic granules with different size

5.4 CONCLUSION

Metabolisms of aerobic granule were found to comprise three phases: (i) a quick reduction in the external DOC concentration associated with a maximum OUR as well as a maximum CPR. In this phase, external organic carbon would likely be converted to storage materials first; (ii) after depletion of the external DOC, aerobic granules further grew on the stored materials derived from phase I. As the result, a low OUR and CPR were recorded; (iii) by the end of phase II, most stored materials were consumed, and microbial metabolism came into the endogenous respiration leading to a minimum OUR.

The conversion yields of external acetate-DOC to storage material, the growth yields of biomass to storage, and growth yields of biomass on external acetate were not strongly related to the sizes of aerobic granules. The stoichiometric analyses

*Chapter 5 Stoichiometric Analysis of DOC Flux into Storage and Growth in
Aerobic Granules*

further revealed that the metabolisms of aerobic granules would be independent of their physical sizes. However, the reaction kinetics are size-dependent, i.e. smaller aerobic granules would have higher growth rates as well as higher decay rates than bigger aerobic granules.

CHAPTER 6

THE EFFECT OF SLUDGE RETENTION TIME ON AEROBIC GRANULATION

6.1 INTRODUCTION

Sludge retention time (SRT) is one of the most important design and operation parameters in the activated sludge process. It has been known that SRT may have remarkable effect on bioflocculation of activated sludge. Basically a SRT of 2 days is often required for the formation of flocculated activated sludge with good settling ability (Ng 2002), while the optimum SRT for good bioflocculation and low effluent COD was found to be in the range of 2 and 8 days (Rittman 1987). It has been believed that a SRT shorter than 2 days favors the growth of dispersed bacteria that in turn would result in increased SVI and effluent COD concentration.

Nearly all aerobic granular sludge reactors are operated in a sequencing mode without intentional control of SRT. For instance, Beun et al. (2000b) found that the SRT increased from 2 days to 30 days, and then dropped to 17 days, finally the SRT stabled at 9 days along with the formation and maturation of aerobic granules in sequencing batch reactor (SBR). So far, there is no research available in the literature with regard to the essential role of SRT in the formation of aerobic granules in SBR, i.e., the effect of SRT on aerobic granulation remains unknown. It has been shown that aerobic granulation in a SBR is driven by hydraulic selection pressure in terms of minimum settling velocity of bioparticles (Liu et al. 2005c). This means that to study the effect of SRT on aerobic granulation in SBR, the interference of hydraulic selection pressure needs to be avoided. For this purpose, this chapter aimed to show if SRT is essential for aerobic granulation in case where hydraulic selection pressure is absent, and it is expected to offer in-depth insights into the mechanism of aerobic granulation as well as operation strategy for successful aerobic granulation in SBR.

6.2 MATERIALS AND METHODS

6.2.1 Experimental set-up and operation

Five columns (127 cm in height and 5 cm in diameter), each with a working volume of 1.96 L, were operated as sequencing batch reactors, namely R1, R2, R3, R4 and R5, which were seeded with the activated sludge taken from a local municipal wastewater treatment plant. R1 to R5 were run at a respective SRT of 3, 6, 9, 12 and 40 days, while the other operation conditions were kept the same, i.e. 4 h of total cycle time, 5 min of filling, 30 min of settling and 5 min of effluent withdrawal. The remaining time in each cycle was the aeration period. In the last 2 min of aeration, a certain volume of the mixed liquor was discharged out of the reactor in order to maintain the desired SRT. Fine air bubbles were introduced at a flow rate of 3.0 L min^{-1} through a dispenser located at the bottom of each reactor. At the end of the settling phase, supernatant was discharged from an outlet located at 0.6 m height from the reactor bottom. A hydraulic retention time of 8 h was maintained in the reactors. The sequential operation of the reactors was automatically controlled by timers, while two peristaltic pumps were employed for influent feeding and supernatant withdrawal. The cultivation medium was the same as described in Chapter 5 (Section 5.2).

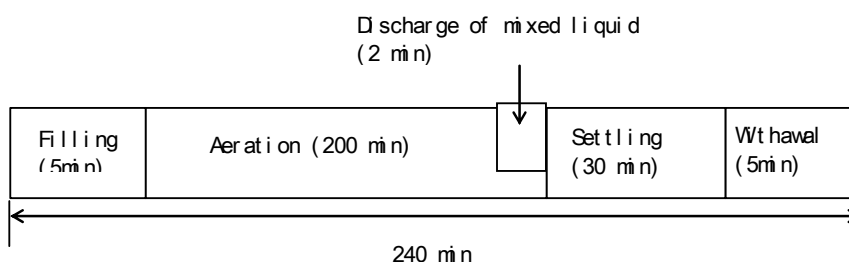


Figure 6.1 Diagram of cyclic operation stages in R1 to R5.

6.2.2 Control of SRT

In order to control SRT, the mixed liquor was discharged from SBR during aeration, i.e., discharge of the mixed liquor was done in the last two minutes of each aeration period (Figure 6.1). For a desired SRT, the corresponding volume of mixed liquor to be discharged can be calculated from the following formula:

$$SRT = \frac{VX}{6(V_e X_e + V_s X)} \quad (6.1)$$

in which V is the volume of the reactor, 6 is the number of cycles per day, X_e is the suspended solid concentration in the supernatant after settling, X is biomass concentration in the complete-mix reactor equal to biomass concentration in the discharged mixed liquor, while V_e and V_s are the volume of discharged supernatant after sludge settling, and the volume of discharged mixed—liquor in each cycle, respectively. Equation 6.1 can be rearranged to

$$V_s = \frac{V}{6SRT} - \frac{V_e X_e}{X}. \quad (6.2)$$

To achieve a desirable SRT, Equation 6.2 can be used to estimate the corresponding volume of the mixed liquor to be discharged.

6.2.3 Analytical methods

Biomass concentrations in terms of total solids (TS) and volatile solids (VS), and sludge volume index (SVI) were determined by standard methods (APHA, 1998). The size of sludge was measured by a laser particle size analyser (Malvern Mastersizer Series 2600, Malvern), or an image analyser (IA) (Image-Pro Plus, v 4.0, Media Cybernetics). Cell surface hydrophobicity was determined using the method developed by Rosenberg et al. (1980). In this method, hexadecane (2.5 ml) was used as the hydrophobic phase, and cell surface hydrophobicity was expressed as the percentage of cells adhering to the hexadecane after 15 minutes of partitioning.

6.2.4 Bacterial tests

6.2.4.1 Pretreatment of biosample

45 ml of mixed liquor was collected from each SBR, and was then transferred into a sterile 50 ml centrifuge tube. The sample was centrifuged for 15 minutes at 4500 rpm. The supernatant was removed, and the sludge harvested was resuspended in 45 ml of 0.85% saline. The sample suspended in saline was mounted to a mortar, and was grinded by the pestle till it was completely disintegrated. These were all done in a laminar flow hood in order to prevent potential contamination, while aseptic technique was practiced at every step. In addition, the centrifuge tube, saline, the mortar and pestle were all autoclaved at 121°C for 20 minutes for sterilization before use.

6.2.4.2 Nutrient agar preparation

Nutrient Agar was used as the growth medium for microbial isolation. For this purpose, 28 g of nutrient agar was dissolved in 1 liter of reverse osmosis water, and was then autoclaved at 121°C for 20 minutes. After autoclaving, the agar was left to cool at room temperature for 15 minutes, and it was then poured out into Sterilin© disposable Petri dishes.

6.2.4.3 Spread plate method

900 µl of saline was pipetted into a number of Eppendorf tubes for serial dilution. After the sample had been dispersed, the suspension was stirred, and 100 µl of the sample was taken out. This volume of sample was added to a sterile 1.5 mL Eppendorf tube containing 900 µL of sterile 0.85% saline, and it was further diluted by serial dilution into Eppendorf tubes, each containing 900 µl of sterile saline. Serial dilution was carried out from 10^{-1} to 10^{-8} for each sample. From tubes with dilution factors of 10^{-3} to 10^{-8} , 100 µl of the sample from each dilution was inoculated into a plate of nutrient agar respectively. The sample was then spread

around the plate uniformly with the aid of a spreader, which was then covered and placed in a 30°C incubator. Duplicates were done for each dilution.

6.2.4.4 Isolation of bacteria

After 5 days of the incubation at 30°C, the total bacterial number per plate was counted. Plates that did not have a total count of between 25–250 colonies were discarded. From the plates that had 25–250 colonies, colonies with similar morphologies were grouped together and numbered. Within each group, 3 colonies were picked out and each was subcultured into a plate containing nutrient agar, respectively. Triplicates were done in order to minimize variation within each group.

6.2.4.5 Identification by biochemical kits

API 20 NE kit (bioMérieux) was used for microbial identification. Fresh subcultures of microorganisms from each plate of isolate were inoculated as per the manufacturers' instructions. Each plate was tested twice with the kit to ensure valid results. Numerical profiles obtained from the test were determined by the API software, using API database version 6.

6.3. RESULTS

6.3.1 General observation by image analysis

Figure 6.2 shows the morphology of the seed sludge inoculated to all the SBRs. On day 3 after the start-up of SBRs, some microbial aggregates with a regular shape appeared in R1 run at the SRT of 3 days (Figure 6.3), while very few regular-shape aggregates were observed on day 4 and day 5 in the SBRs operated at the SRTs of 6 to 40 days (Figures 6.5, 6.7, 6.9, 6.11). After the first a few days, the evolution of sludge morphology became insignificant in R1 to R5 until the reactors were stabilized in terms of constant biomass and effluent concentrations after 30-day operation. At the steady state, it was found that aerobic granules with a size bigger

Chapter 6 The Effect of Sludge Retention Time on Aerobic Granulation

than 0.35 mm only accounted for a very small fraction of total biomass in SBRs, i.e., bioflocs were absolutely the dominant form of microorganisms in all the five SBRs operated at the SRT of 3 to 40 days (Figures 6.4, 6.6, 6.8, 6.10, 6.12).

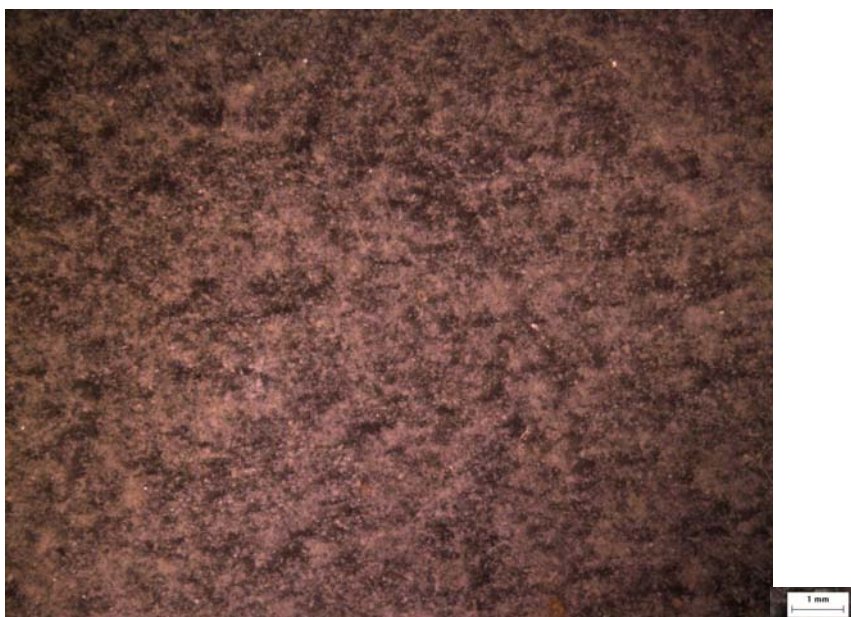


Figure 6.2 Morphology of seed sludge.

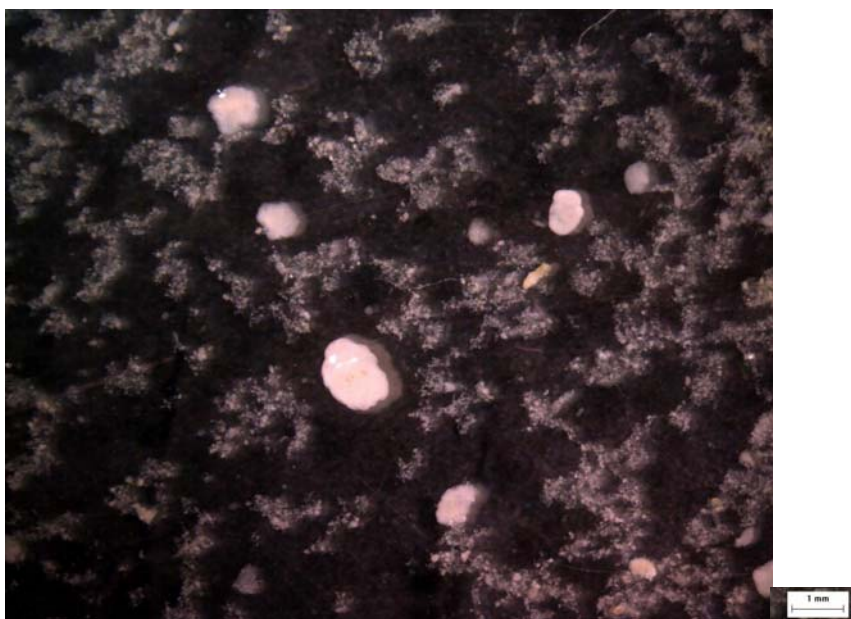


Figure 6.3 Morphology of sludge cultivated in R1 on day 3.

Chapter 6 The Effect of Sludge Retention Time on Aerobic Granulation



Figure 6.4 Morphology of sludge cultivated in R1 on day 30.

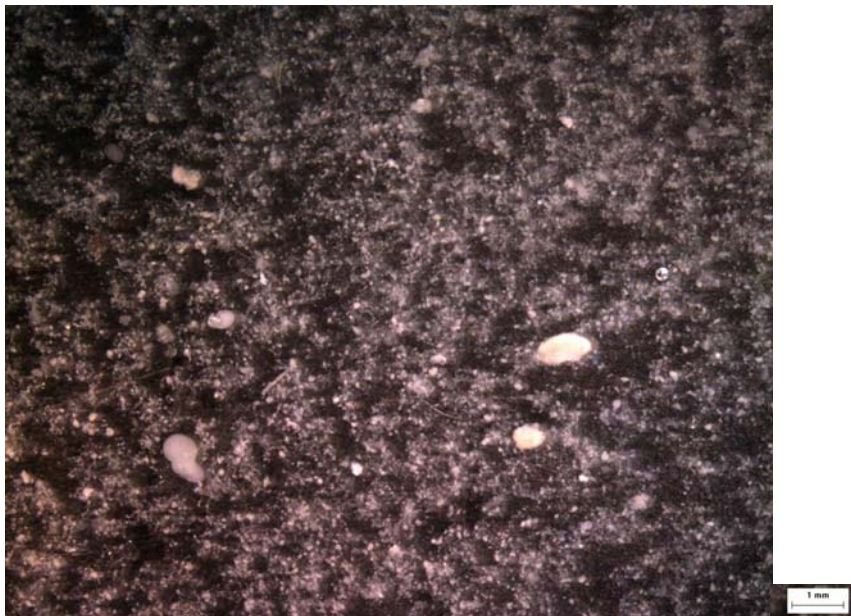


Figure 6.5 Morphology of sludge cultivated in R2 on day 4.

Chapter 6 The Effect of Sludge Retention Time on Aerobic Granulation



Figure 6.6 Morphology of sludge cultivated in R2 on day 30.



Figure 6.7 Morphology of sludge cultivated in R3 on day 4.

Chapter 6 The Effect of Sludge Retention Time on Aerobic Granulation

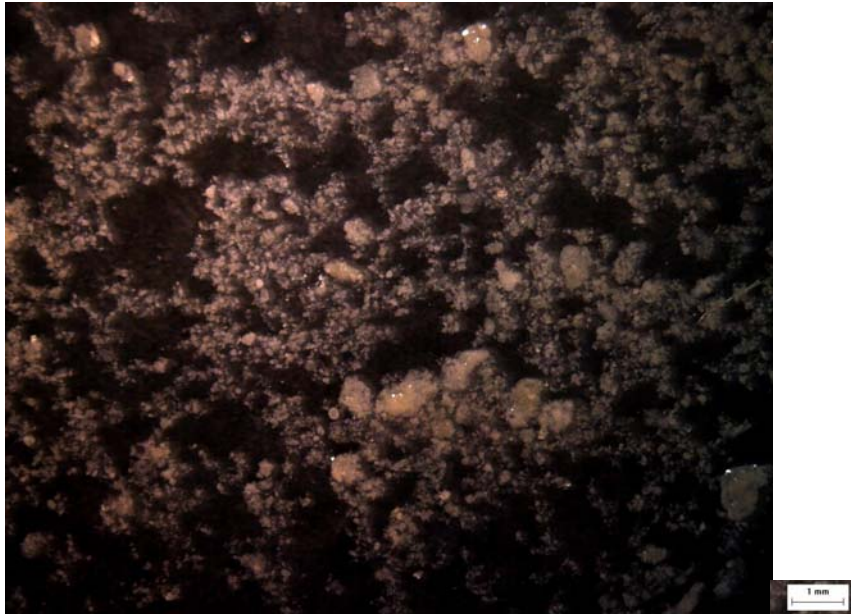


Figure 6.8 Morphology of sludge cultivated in R3 on day 30.



Figure 6.9 Morphology of sludge cultivated in R4 on day 4.

Chapter 6 The Effect of Sludge Retention Time on Aerobic Granulation

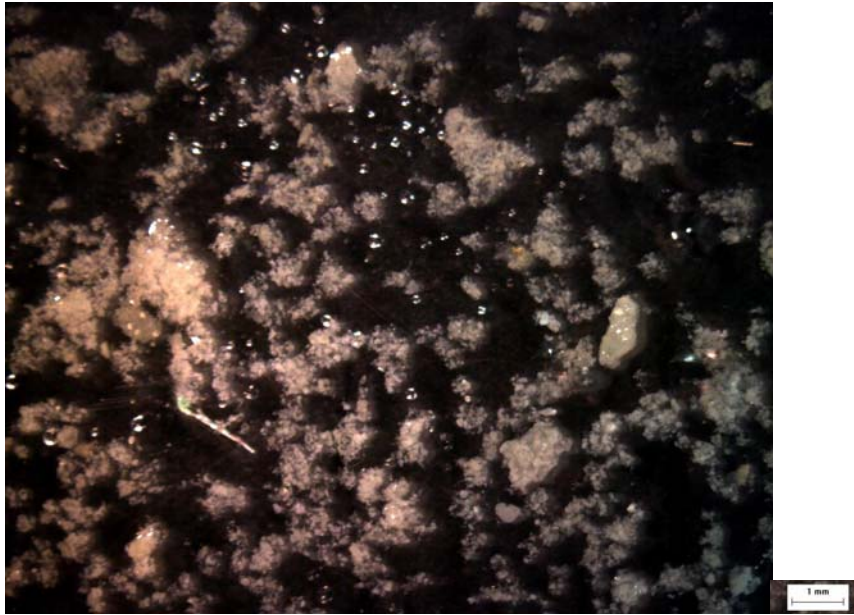


Figure 6.10 Morphology of sludge cultivated in R4 on day 30.

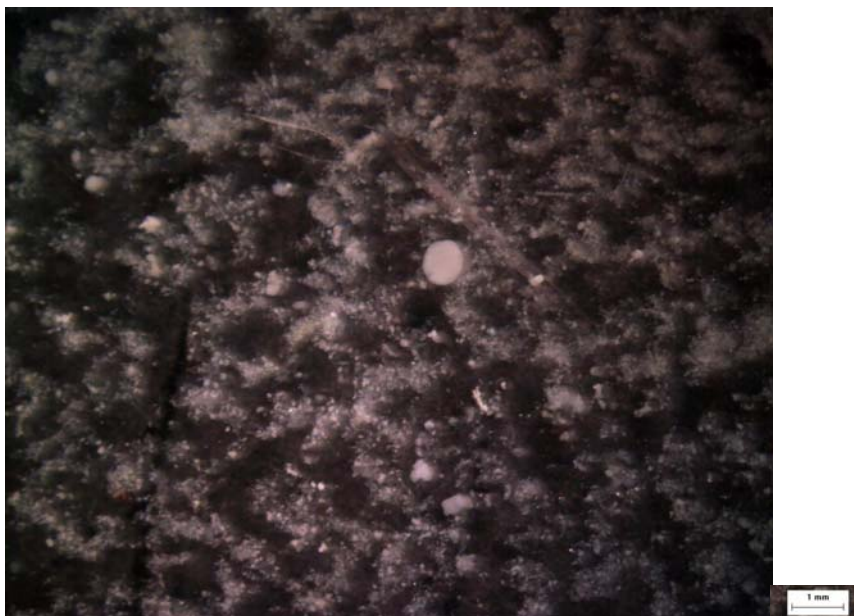


Figure 6.11 Morphology of sludge cultivated in R5 on day 5.

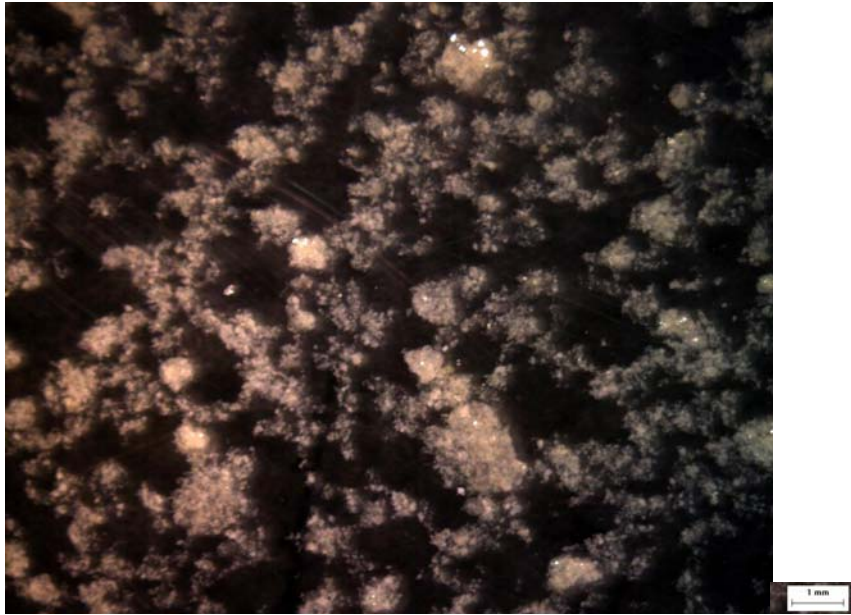


Figure 6.12 Morphology of sludge cultivated in R5 on day 30.

6.3.2 Evolution and distribution of sludge size

Figures 6.13 shows the size evolution of microbial aggregates in R1 to R5 operated at different SRTs. The average size of the seed sludge was about 75 μm . A significant increase in aggregate size was observed in the first four days of operation in all the SBRs. From day 4 onwards, the average size of aggregates gradually stabilized in five SBRs run at the SRTs of 3 to 40 days.

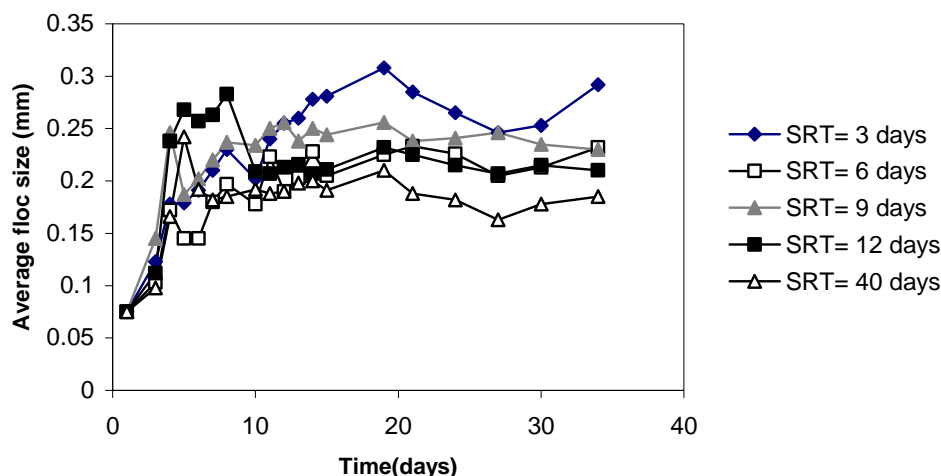


Figure 6.13 Changes in aggregate size in the course of operation of SBRs.

During 35 days of operation, no aerobic granular sludge blanket was developed in five SBRs operated at the large SRT range of 3 to 40 days. As shown in Figures 6.4, 6.6, 6.8, 6.10 and 6.12, only a few aerobic granules with round shape were found after 30-days of operation, while relatively a large quantity of tiny aggregates seemed dominant in the sludge community cultivated at different SRTs.

The size distribution of aggregates was determined on day 30 (Figure 6.14). The peak values of the size distribution fell into a narrow range of 150 to 350 μm for R1 to R5. These seem to indicate that the SRT in the range studied would not have remarkable effect on the formation of aerobic granules. According to Figure 6.14, the fraction of aerobic granules defined as microbial aggregates with a mean size bigger than 350 μm and a round shape (Qin et al. 2004a) can be calculated. Figure 6.15 clearly shows that the fractions of aerobic granules in R1 to R5 are comparable and remain at the level of about 20% by volume. These in turn imply that bioflocs would be dominant form of biomass present in R1 to R5.

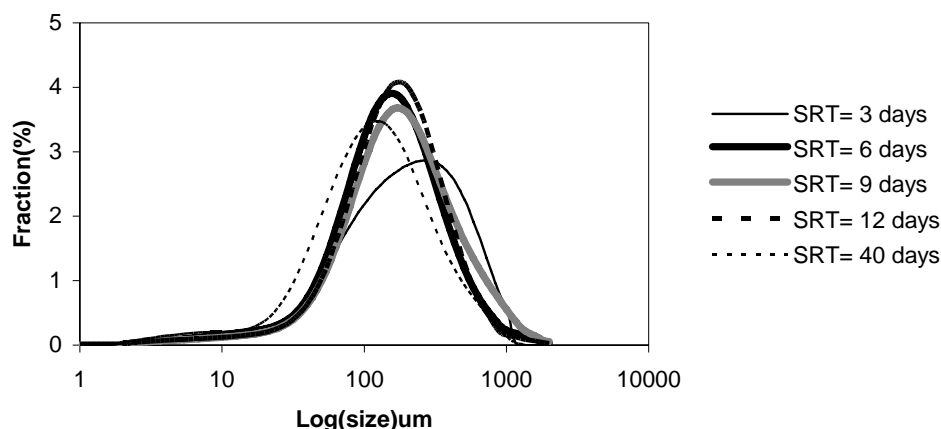


Figure 6.14 Size distribution of aggregates cultivated at different SRTs.

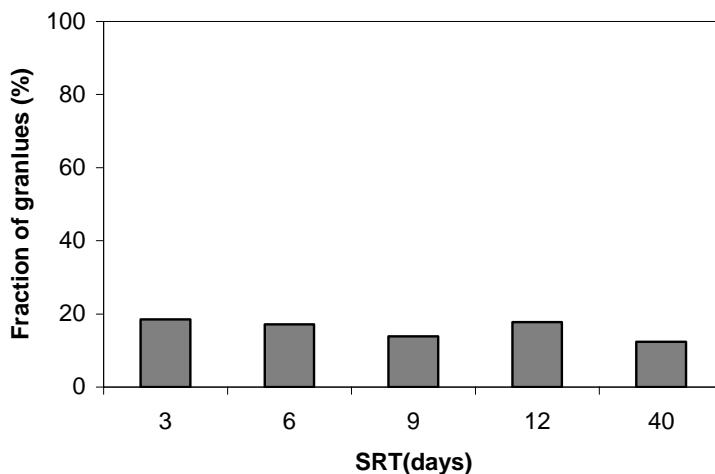


Figure 6.15 Fraction of aerobic granules in the SBRs run at different SRTs.

6.3.3 Settleability of sludge

Changes in the sludge volume index (SVI) at different SRTs were determined in the course of SBR operation (Figure 6.16). The SVI observed in all the reactors tended to decrease rapidly in the first 10-days of operation, and gradually approached a stable level of around 50 ml g^{-1} in all cases. In addition, a horizontal comparison across the SRTs also shows that the SVI of sludge cultivated at the SRT of 40 days decreased more slowly than those developed at the relatively short SRTs.

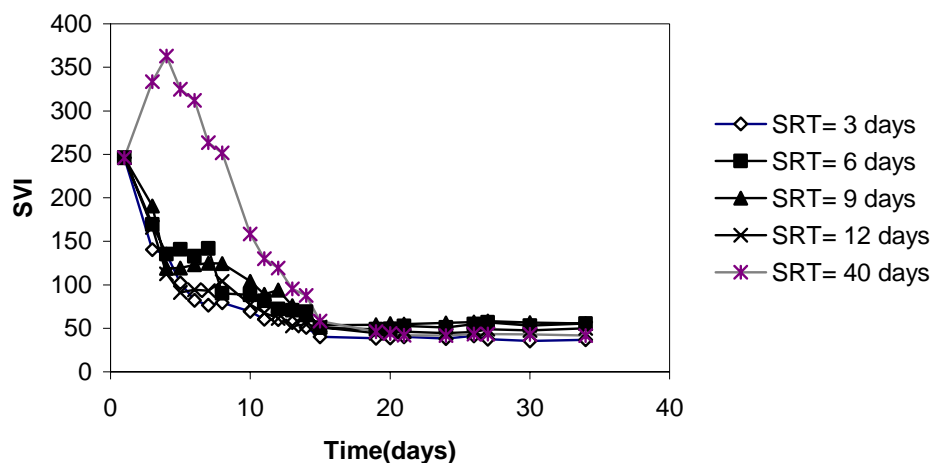


Figure 6.16 Changes in SVI in course of SBR operation at different SRTs.

6.3.4 Biomass concentration

The biomass concentration in terms of MLSS was measured along with the reactor operation (Figure 6.17). The biomass concentrations in R1 to R5 gradually increased up to a stable level. It was found that the biomass concentration at steady state was proportionally related to the SRT applied, i.e., a longer SRT would lead to a higher biomass accumulation.

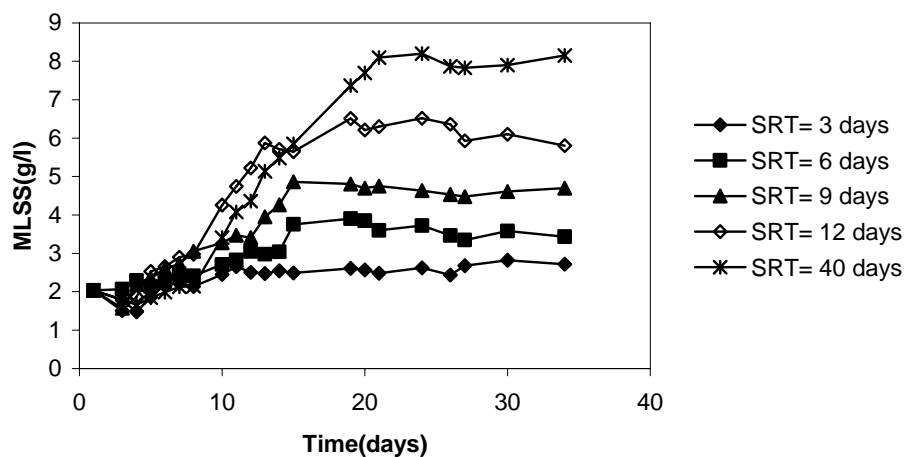


Figure 6.17 Biomass concentration versus operation time.

6.3.5 Substrate removal kinetics

The TOC profiles within one cycle were determined after 21 days of operation in R1 to R5 (Figure 6.18). A fast TOC degradation was observed in all five SBRs, i.e., nearly all input TOC was removed during the first 20 minutes. These eventually lead to a long famine period which has been believed to favor aerobic granulation in SBR (Tay et al. 2001a). Fig. 6.18 also reveals that the calculated TOC removal rate is proportionally related to the SRT applied, i.e., a higher TOC removal rate is observed at a longer SRT. However, the lower specific TOC removal rate is observed at higher SRT. This can be reasonably explained by the differences in biomass concentrations as shown in Figure 6.17.

Chapter 6 The Effect of Sludge Retention Time on Aerobic Granulation

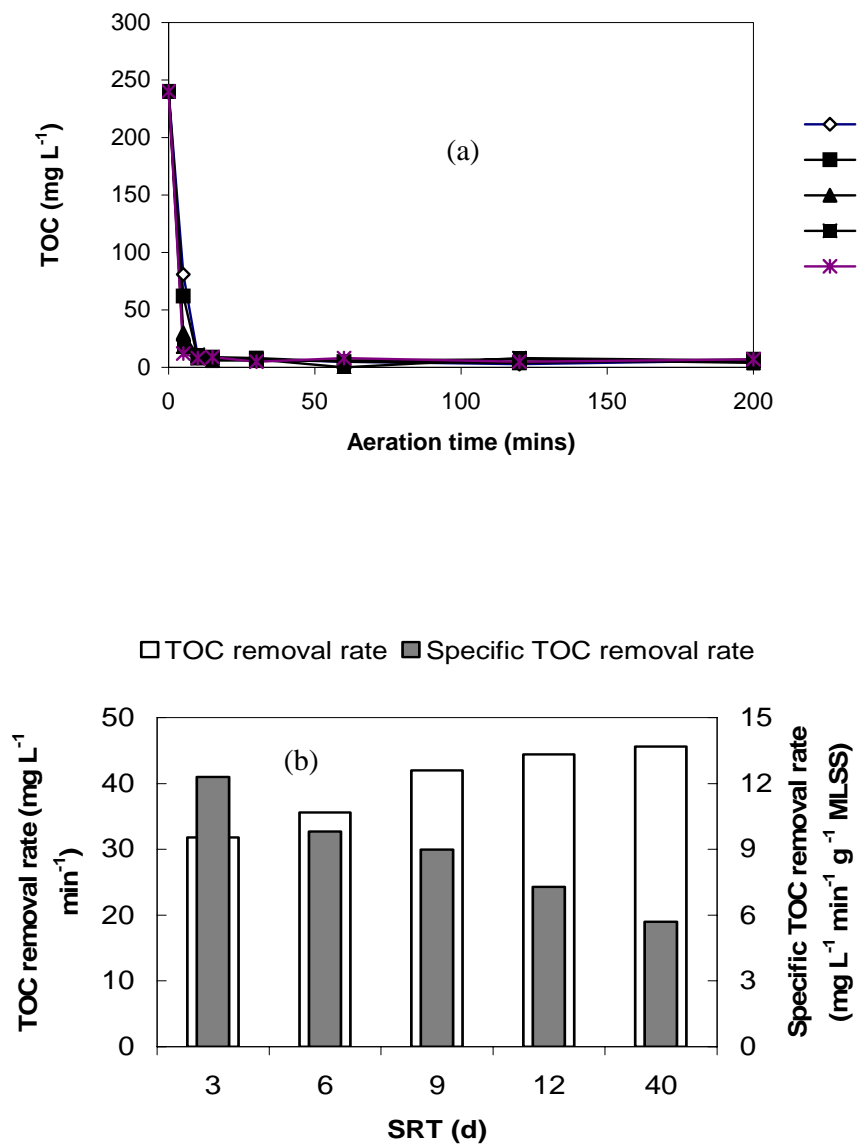


Figure 6.18 (a) TOC profile on day 30 in a cycle; (b) TOC removal kinetics versus SRT.

6.3.6 Cell surface hydrophobicity

The cell surface hydrophobicities of sludges cultivated at different SRTs are shown in Figure 6.19. Only the cell surface hydrophobicity of sludge developed at the SRT of 3 days seems slightly higher than that of the seed sludge, whereas the cell surface hydrophobicities of sludges cultivated at the SRTs longer than 3 days are pretty comparable with that of the seed sludge. These mean that the SRT in the range studied would not have remarkable effect on the cell surface hydrophobicity.

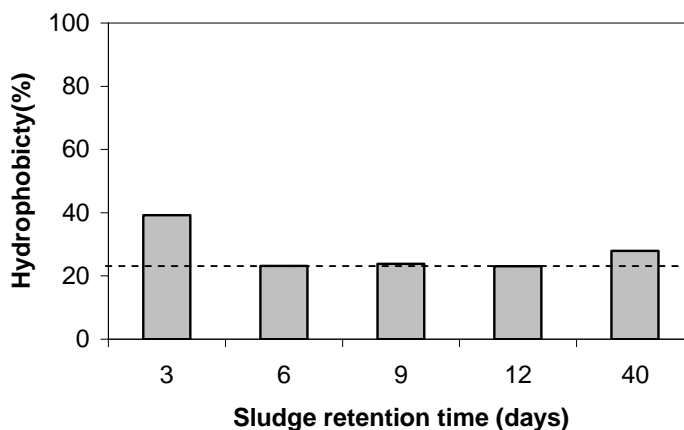


Figure 6.19 Cell surface hydrophobicity of sludges cultivated at different SRTs, and dashed line represents the seed sludge.

6.3.7 Shift in microbial population

The sludges cultivated in R2 and R3 were sampled on day 3, 10, 17, 24 for microbial analysis. Basically, 12 species, namely No.1 to No. 12, were isolated from all the sludge samples. All the isolates are listed in Table 6.1. It was found that the isolates No. 1, 5 and 8 were very close to the strain *Brevundimonas vesicularis*, while the isolates No. 4, 7 and 9 could belong to the strain *Comamonas testosteroni*. Because of limitation of biokits (API 20 NE), the isolates No. 10, 11 and 12 could not be identified and further study is needed in this regard.

Chapter 6 The Effect of Sludge Retention Time on Aerobic Granulation

Table 6.1 shows the population shifts of the sludges in R2 and R3 at day 3, 10, 17, 24 respectively. In the sludge developed in R2, isolate No. 10 was the most dominant species on day 3. On day 10, isolate No. 10 kept dominant, meanwhile isolate No. 7 appeared. On day 17, number of isolate No. 10 decreased, while isolates No. 11 and 12 became dominant even though they were not detected in the previous days. Isolate No. 4 disappeared. On day 24, isolate No. 11 and 12 kept dominant.

In R3, isolate No. 10 was found to be the dominant species on day 3 and day 10 (Table 6.1), then decreased in day 17, and finally disappeared on day 24. Isolates 11 and 12 were not detected on day 3 and 10, but they were dominant on day 17 and 24. Isolate No.7 began to appear on day 10 (Figure 6.22) and isolate No. 9 began to appear on day 17.

The population of the most dominant species in the sludge from R2 was always higher than that of the sludge from R3 except in day 17. At last, the population of same species in both sludge in the sludge from R2 exceeded that in the sludge from R3 (Figure 6.23). Both of the sludge had 8 species in total, of which 6 species were the same.

Chapter 6 The Effect of Sludge Retention Time on Aerobic Granulation

Table 6. 1 Distribution of microbial isolates identified in the course of operation of R2 and R3.

| Isolate No. | Closest relative | No. of species in R2 (10 ⁸ CFU g ⁻¹ dry biomass) | | | | No. of species in R3 (10 ⁸ CFU g ⁻¹ dry biomass) | | | |
|-------------|-------------------------------------|---------------------------------------------------------------------------|--------|--------|--------|---------------------------------------------------------------------------|--------|--------|--------|
| | | Day 3 | Day 10 | Day 17 | Day 24 | Day 3 | Day 10 | Day 17 | Day 24 |
| 1 | <i>Brevundimonas vesicularis</i> | 66.5 | 14.5 | 9.3 | 15.3 | 17.2 | 11.7 | 13.3 | 6.4 |
| 2 | <i>Ochrobactrum anthropi</i> | 29.6 | 6.2 | 26.7 | 11.1 | 27.1 | 6.7 | 13.3 | 7.1 |
| 3 | <i>Chryseobacterium indologenes</i> | 0.0 | 0.0 | 62.7 | 25.0 | 39.4 | 11.7 | 0.0 | 0.0 |
| 4 | <i>Comamonas testosterone</i> | 22.2 | 10.4 | 0.0 | 0.0 | 39.4 | 11.7 | 0.0 | 0.0 |
| 5 | <i>Brevundimonas vesicularis</i> | 0.0 | 0.0 | 16.0 | 0.0 | 0.0 | 16.8 | 16.8 | 9.5 |
| 6 | <i>Sphigobacterium spiritivorum</i> | 32.0 | 14.5 | 29.3 | 34.7 | 29.6 | 16.8 | 0.0 | 0.0 |
| 7 | <i>Comamonas testosterone</i> | 0.0 | 35.3 | 37.3 | 26.4 | 0.0 | 8.4 | 88.7 | 13.5 |
| 8 | <i>Brevundimonas vesicularis</i> | 0.0 | 0.0 | 80.0 | 40.3 | 14.8 | 23.5 | 10.6 | 12.7 |
| 9 | <i>Comamonas testosterone</i> | 17.2 | 8.3 | 0.0 | 0.0 | 0.0 | 0.3 | 7.1 | 0.8 |
| 10 | Not identified | 96.1 | 104.0 | 17.3 | 0.0 | 71.4 | 72.1 | 10.6 | 0.0 |
| 11 | Not identified | 0.0 | 0.0 | 82.7 | 61.1 | 0.0 | 0.0 | 35.5 | 20.6 |
| 12 | Not identified | 0.0 | 0.0 | 86.7 | 61.1 | 0.0 | 0.0 | 42.6 | 21.4 |

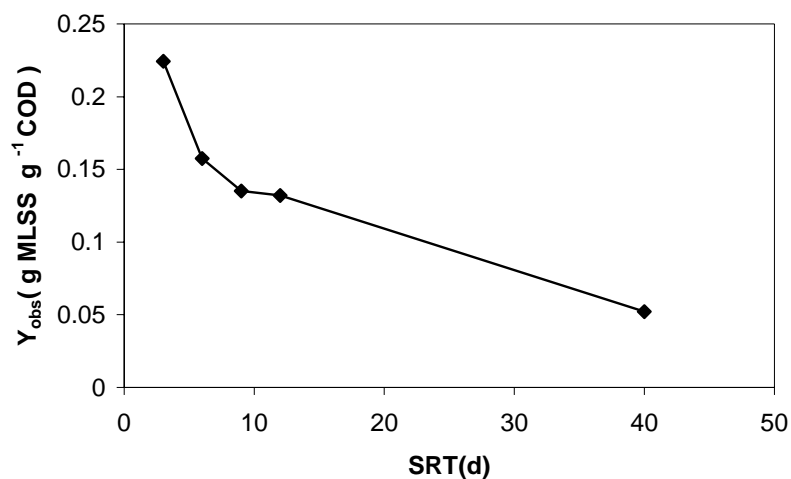
6.4 DISCUSSION

Existing evidence shows that the formation and structure of aerobic granules are associated very closely with cell surface hydrophobicity which can initiate cell-to-cell aggregation that is a crucial step towards aerobic granulation (Liu et al. 2004b). It is observed in Fig. 6.19 that the cell surface hydrophobicities of the sludges cultivated at the SRT of 3 to 40 days are pretty comparable with that of the seed sludge. These seem to imply that the SRT in the range studied would not induce significant changes in cell surface hydrophobicity, and the low cell surface hydrophobicity observed in turn may partially explain unsuccessful aerobic granulation in SBR. In addition, Liao et al. (2001) reported that hydrophobicities of sludges in terms of contact angle only increased from 25 to 35 degrees as the SRT was prolonged from 4 to 20 days. In addition, all the data obtained at the SRT of 40 days showed that the properties of sludge in terms of biomass concentration, size and SVI were all stable after 20 days of operation (Figures 6.16 and 6.17). In this case, no granulation would be expected, and it was decided to terminate the experiment for the SRT of 40 days after 35 days of operation.

In the field of environmental engineering, the observed growth yield (Y_{obs}) is calculated as follows:

$$Y_{obs} = \frac{\Delta X}{\Delta S} \quad (6.3)$$

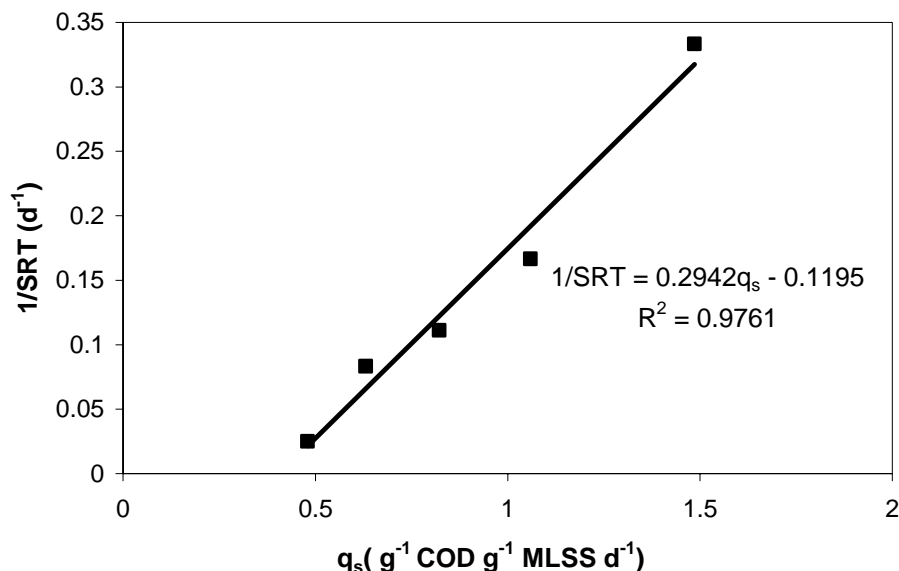
in which ΔX is increased biomass concentration, and ΔS is the substrate concentration removed. Figure 6.20 shows the relationship between the observed growth yield and the SRT. It can be seen that a longer SRT result in a lower Y_{obs} , e.g. the observed growth yield decreased from 0.23 g MLSS g⁻¹ COD at the SRT of 3 days to 0.05 g MLSS g⁻¹ COD at the SRT of 40 days.

Figure 6.20 Y_{obs} versus SRT observed in R1 to R5.

According to Figure 6.20, the true growth yield (Y_t) can be determined from the following equation:

$$\frac{1}{SRT} = Y_t \times q_s - K_d \quad (6.4)$$

in which q_s is the specific substrate utilization rate in a cycle, and K_d is the specific decay rate. The plot of $1/SRT$ versus q_s is shown Figure 6.21. It can be seen that Y_t and K_d were estimated to be 0.29 g MLSS g⁻¹ COD and 0.12 d⁻¹, respectively. Liu et al. (2005d) reported a growth yield of 0.29 MLSS g⁻¹ COD and a decay rate of 0.023 to 0.075 d⁻¹ for glucose fed aerobic granules. In activated sludge model No. 3 (Gujier et al. 1999), the decay rate for heterotrophic bacteria has been reported in the range of 0.1 and 0.2 d⁻¹ at the of 10 and 20 °C, respectively. Basically, a cycle of SBR consists of feast and famine phases (Liu and Tay 2004; McSwain et al. 2004). In this study, almost all external organics could be removed within the first half an hour of each cycle, i.e., more than 75% of each SBR cycle would be subject to famine condition, which would trigger a significant microbial decay eventually leading to the low observed growth yields.

Figure 6.21 $1/SRT$ versus q_s .

It appears from Table 6.1 that in R2 and R3 operated at the respective SRT of 6 days and 12 days, the shift pattern and distribution of microbial species isolated did not show significant difference. For instance, on day 30, 8 isolates were found in the sludges cultivated in R2 and R3, out of which 6 were the same. These seem to imply that in the present operation mode of SBRs, the selection of microbial species by the applied SRT would be weak, and such a weak selection on species may in turn, at least partially explain the fact that the properties of sludges developed in all five SBRs only showed some marginal differences as discussed earlier. As no successful aerobic granulation was observed in R2 and R3 (Figs. 6.3-6.12), it is hard to draw a solid conclusion with regard to the possible correlation between aerobic granulation and the observed changes in microbial species as shown in Table 6.1. In fact, it has been thought that aerobic granulation would not be closely related to a particular microbial species because aerobic granules grown on a very wide spectrum of organic carbons have been developed, including acetate, glucose, phenol, p-nitrophenol, nitrilotriacetic acid (NTA) and ferric-NTA complex synthetic and real wastewaters (Beun et al. 2000a; McSwain et al. 2004; Schwarzenbeck et al. 2003; Tay et al. 2001c; Nanchaiaiah et al. 2006; Yi et al. 2006).

It is apparent from Figure 6.15 that SRT in the range studied would not have a significant effect on the formation of aerobic granules in SBR. For a column SBR as illustrated in Figure 6.22, the traveling distance of bioparticles above the discharge port is L (distance between water surface and discharging port). For a designed settling time (t_s), bioparticles with a settling velocity less than L/t_s would be washed out of the reactor, while only those with a settling velocity greater than L/t_s will be retained. According to Liu et al. (2005c), a minimum settling velocity $(V_s)_{\min}$ exists in SBR, and it can be defined as follows:

$$(V_s)_{\min} = \frac{L}{t_s} \quad (6.5)$$

Equation 6.5 shows that a long L or a short settling time would result in a larger $(V_s)_{\min}$, and vice versa.

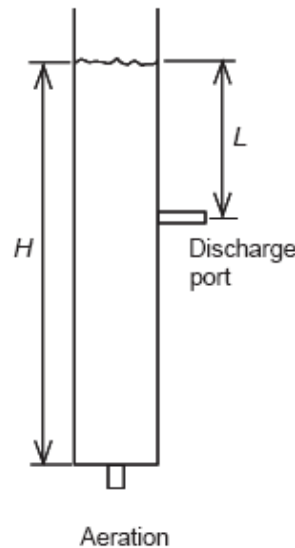


Figure 6.22 Illustration of the $(V_s)_{\min}$ concept in SBR (Liu et al. 2005c).

It has been shown that aerobic granulation in a SBR is driven by hydraulic selection pressure in terms of minimum settling velocity of bioparticles (Liu et al. 2005a). This means that to study the effect of SRT on aerobic granulation in SBR, the interference of hydraulic selection pressure needs to be avoided. In this study, in order to look into the effect of SRT on aerobic granulation without interference of

hydraulic selection pressure, the selection pressure in terms of $(V_s)_{\min}$ was minimized to an extremely low level of 0.76 to 0.78 m h⁻¹. Qin et al. (2004a, b) studied aerobic granulation at different settling times with a fixed L, while Wang et al. (2006b) investigated aerobic granulation at different L at the constant settling time. Using those data, Liu et al. (2005c) correlated $(V_s)_{\min}$ to the fraction of aerobic granules developed in SBR (Figure 6.23). For the purpose of comparison, the data obtained in this study were also plotted in the same figure.

As shown in Figure 6.23, the fraction of aerobic granules was proportionally correlated to $(V_s)_{\min}$, i.e. $(V_s)_{\min}$ can serve as an effective selection pressure to drive aerobic granulation, and highly influences the properties of stable aerobic granules. Moreover, it appears from Figure 6.23 that at a $(V_s)_{\min}$ less than 4 m h⁻¹, aerobic granulation is not favored in SBR, instead the growth of suspended sludge is greatly encouraged. It should be realized that the typical settling velocity of conventional activated sludge is generally less than 5 m h⁻¹ (Giokas et al. 2003). These imply that for a SBR operated at a $(V_s)_{\min}$ lower than the settling velocity of conventional sludge, suspended sludge could not be effectively withdrawn. As the result, suspended sludge will take over the entire reactor at low $(V_s)_{\min}$ just as observed in this study no matter how SRT was controlled. In fact, Liu and Tay (2004) reported that suspended sludge could outcompete aerobic granules, and such an outcompetition eventually led to instability and even failure of aerobic granulation. So far, evidence shows that to achieve a rapid and enhanced aerobic granulation in SBR, the minimum settling velocity $(V_s)_{\min}$ must be controlled at a level higher than the settling velocity of suspended sludge. These results seem to indicate that hydraulic selection pressure is a key towards successful aerobic granulation in SBR, while SRT would not be a primary factor that determines aerobic granulation.

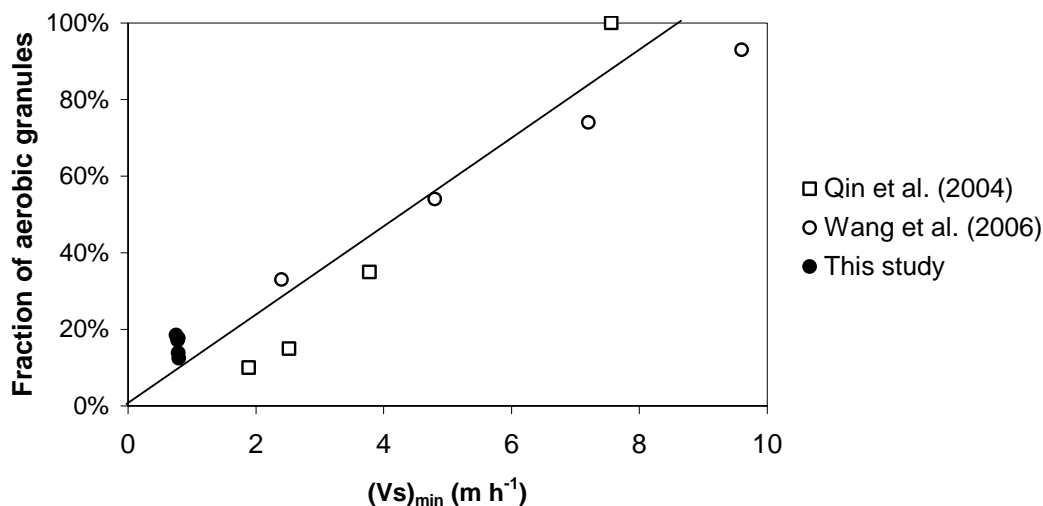


Figure 6.23 Fraction of aerobic granules versus $(V_s)_{\min}$.

The fraction of aerobic granules obtained at different SRTs were plotted in a three dimensional diagram against the corresponding $(V_s)_{\min}$ and SRT (Figure 6.24). A multiple parameter linear regression was conducted, i.e., the fraction of granules = $10.10(V_s)_{\min} + 0.26\text{SRT}$. As can be seen, the regression equation can provide a satisfactory description of the experimental data, indicated by a high correlation coefficient of 0.9885. Furthermore, Figure 6.24 reveals that the fraction of aerobic granules cultivated in SBR is largely determined by $(V_s)_{\min}$. As the coefficient before the term SRT is 39 times smaller than that before the term $(V_s)_{\min}$, the contribution of SRT to aerobic granulation would be minor compared to $(V_s)_{\min}$.

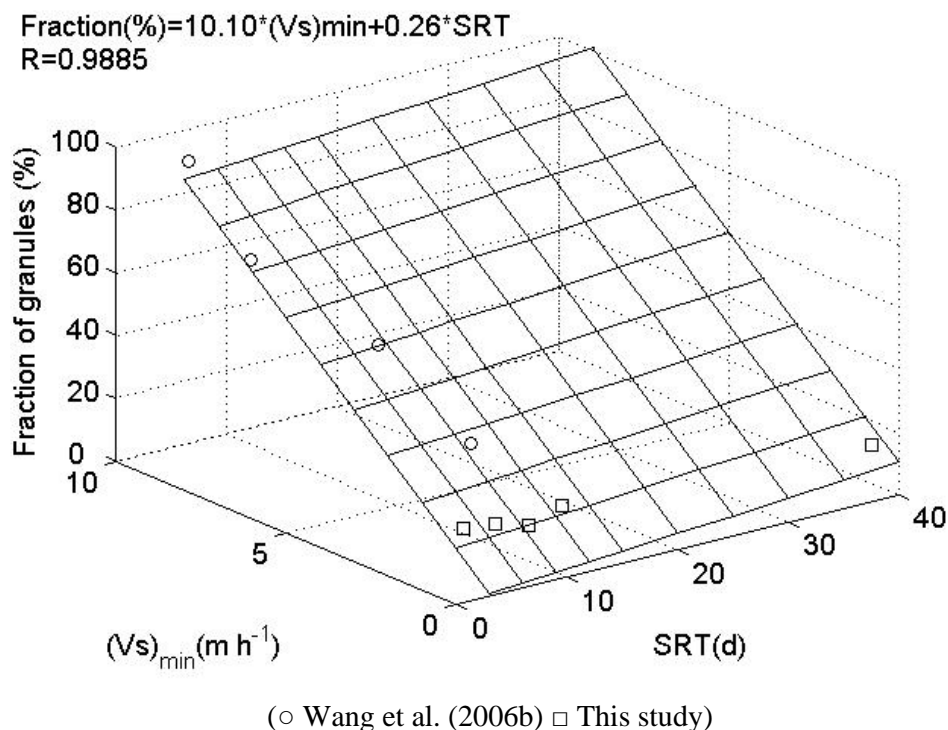
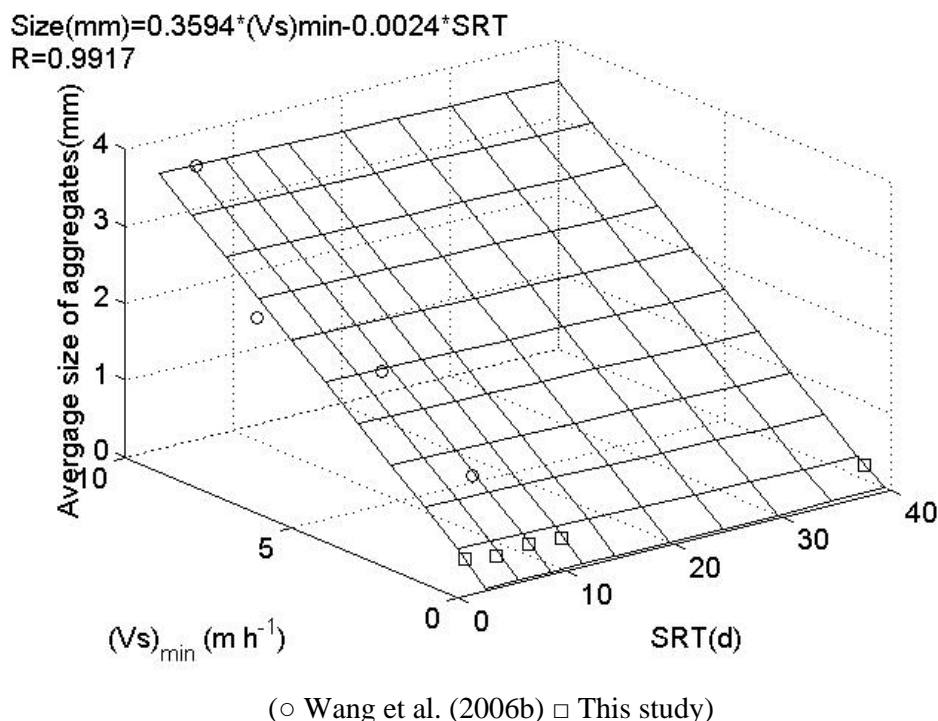


Figure 6.24 Effects of $(V_s)_{\min}$ and SRT on aerobic granulation in SBR.

The average sizes of aggregates were plotted in a three dimensional diagram against SRT and $(V_s)_{\min}$ (Figure 6.25). Large-size aggregates could form at high $(V_s)_{\min}$, but the effect of SRT on the aggregate size appears to be negligible. These observations indeed are consistent with the trend shown in Figure 6.24. Figure 6.25 further confirms that the effect of SRT on aerobic granulation would be insignificant, while the hydraulic selection pressure in terms of $(V_s)_{\min}$ is essential for aerobic granulation in SBR.

Figure 6.25 Aggregate size against $(V_s)_{\min}$ and SRT.

6.5 CONCLUSIONS

This study for the first time systematically investigated the role of SRT in aerobic granulation in SBR. For this purpose, five SBRs were operated at different SRTs in the range of 3 to 40 days, while in order to avoid the interference of hydraulic selection pressure, all the SBRs were run at extremely low $(V_s)_{\min}$ of 0.76 to 0.8 m h⁻¹. The results showed that no successful aerobic granulation was observed at all studied SRTs, i.e., bioflocs were the dominant form of biomass at the SRT studied. A comparison analysis further revealed that hydraulic selection pressure in terms of $(V_s)_{\min}$ would be much more effective than SRT for enhancing aerobic granulation in SBR. In conclusion, SRT would not be essential for successful aerobic granulation. This study offers in-depth insights into a better understanding of aerobic granulation.

CHAPTER 7

CONCLUSIONS AND RECOMMENDATIONS

7.1 CONCLUSIONS

The one-dimensional model was developed and successfully applied to simultaneously describe the diffusion profiles of organic substrate and dissolved oxygen in aerobic granules, and this model was also extended to the study of reaction kinetics in SBR. A new FDM (Finite difference method)-based numerical method was developed by which the proposed simulation models can be completely solved without any extra assumption in numerical analysis. Diffusions of substrate and dissolved oxygen were synchronously simulated by the proposed models under various conditions. It was found that diffusions of substrate and oxygen in aerobic granule would be a dynamic process, and were closely interrelated. This means that both must be considered together in future optimization of aerobic granular sludge SBR. Simulation of the overall performance of aerobic granular sludge SBR showed that dissolved oxygen would be a main limiting factor of the metabolic activity of aerobic granule; Smaller aerobic granules exhibited higher metabolic activity in terms of the substrate removal rate; For a SBR dominated by aerobic granules larger than 0.5 mm, dissolved oxygen would be the bottleneck which limits the substrate utilization rate. It is expected that the model system developed in this study can provide an effective and useful tool for predicting and optimizing the performance of aerobic granular sludge reactor.

The diffusion in aerobic granules is likely to affect the ion distribution in aerobic granules. For instance, high calcium content has been found in acetate-fed aerobic granules. It appears that the calcium accumulation needs to be analyzed together with diffusion phenomenon observed in aerobic granules. In this regard, the one-dimensional model developed was further applied to simulate the pH and carbonate profiles in aerobic granules. Calcium accumulation in acetate-fed aerobic granules was found in the form of CaCO_3 in the core of aerobic granules bigger than

0.5 mm. The model simulation revealed that its formation was related to the diffusion limitation in aerobic granules. It was found that almost all calcium accumulated in acetate-fed aerobic granules was in the form of CaCO_3 , moreover calcium carbonate was mainly situated in the central part of acetate-fed aerobic granule. It was further demonstrated that the accumulation of calcium ions was closely related to the size-dependent diffusion of dissolved oxygen inside aerobic granules.

The kinetics of aerobic granules with various sizes would depend on the size-associated diffusion resistance. However, it remains unknown that if the metabolism of aerobic granules would also be size-dependent. The respiration data showed that the metabolisms of aerobic granule can be divided into three phases: (i) a quick reduction in the external DOC concentration associated with a maximum OUR as well as a maximum CPR. In this phase, external organic carbon would likely be converted to storage materials first; (ii) after depletion of the external DOC, aerobic granules further grew on the stored materials derived from phase I. As the result, a low OUR and CPR were recorded; (iii) by the end of phase II, most stored materials were consumed, and microbial metabolism came into the endogenous respiration leading to a minimum OUR. The conversion yields of external acetate-DOC to storage material, the growth yields of biomass to storage, and growth yields of biomass on external acetate were not strongly related to the sizes of aerobic granules. The stoichiometric analyses further revealed that the metabolisms of aerobic granules would be independent of their physical sizes, while the reaction kinetics are size-dependent, i.e. smaller aerobic granules would have higher growth rates as well as higher decay rates than bigger aerobic granules.

Sludge retention time (SRT) is an important design and operation parameter of biological processes. Study of SRT in aerobic granular sludge system will offer deep insights into the mechanism of aerobic granulation as well as the kinetics and metabolism of aerobic granules. It was found that in SBRs operated at extremely low $(V_s)_{\min}$ of 0.76 to 0.8 m h^{-1} , no successful aerobic granulation was observed at the SRTs of 3 to 40 days, i.e., bioflocs were the dominant form of biomass. A comparison analysis further revealed that hydraulic selection pressure in terms of $(V_s)_{\min}$ would be much more effective than SRT for enhancing aerobic granulation in SBR. The study of SRT in aerobic granular sludge system is helpful for better understanding the

mechanism of aerobic granulation as well as the kinetics and metabolism of aerobic granules.

7.2 RECOMMENDATIONS

It is recommend to further investigate the possible operation strategy for size control in order to reduce the diffusion limitation inside aerobic granules for organic removal vrom wastewater, while for nitrogen removal, it is recommended to utilize the diffusion limitation for simultaneous nitrification and denitrification. Aerobic granule has a layered structure comprising aerobic and anaerobic zones from the surface to the center of aerobic granule. The nitrogen removal through conventional nitrification-denitrification pathway requires on alternative aerobic and anaerobic conditions.

REFERENCES

- Adav SS, Chen MY, Lee DJ, Ren NQ (2007) Degradation of phenol by *Acinetobacter* strain isolated from aerobic granules. *Chemosphere* 67: 1566-1572.
- Allsop PJ, Chisti Y, Moo-Young M, Sullivan GR (1993) Dynamics of phenol degradation by *Pseudomonas putida*. *Biotechnol Bioeng* 41: 572-580.
- Alphenaar PA, Visser A, Lettinga G (1993) The effect of liquid upflow velocity and hydraulic retention time on granulation in UASB reactors treating wastewater with a high-sulphate content. *Bioresour Technol* 43: 249-258.
- Alves M, Cavaleiro AJ, Ferreira EC, Amaral AL, Mota M, da Motta M, Vivier H, Pons MN (2000) Characterization by image analysis of anaerobic sludge under shock conditions. *Water Sci Technol* 41: 207-214.
- Alves C, Nogueira R, Brito A (2004) Poly- β -hydroxybutyrate metabolism in a biofilm reactor. *Biofilms 2004 Conference: Structure and Activity of Biofilms-Las Vegas, NV, USA*. pp 259-264.
- APHA (1998) Standard methods for the examination of water and wastewater, 20th ed., American Health Association, Washington DC, USA.
- Arcand Y, Guitot SR, Desrochers M, Chavarie C (1994) Impact of the reactor hydrodynamics and organic loading on the size and activity of anaerobic granules. *Chem Eng J Biochem Eng J* 56: 23-35.
- Avcioglu E, Orhon D, Sözen S (1998) A new method for the assessment of heterotrophic endogenous respiration rate under aerobic and anoxic conditions. *Water Sci Technol*. 38: 95-103.
- Barker, DJ. Stuckey DC (1999) A review of soluble microbial products (SMP) in wastewater treatment systems. *Water Res* 33: 3063-3082.

- Bailey JE, Ollis DF (1986) Biochemical Engineering and fundamentals. McGraw-Hill, New York, pp 210-214.
- Batstone DJ, Landelli J, Saunders A, Webb RI, Blackall LL, Keller J (2002) The influence of calcium on granular sludge in a full-scale UASB treating paper mill wastewater. *Water Sci Technol* 45: 187-193.
- Beccari M, Dionisi D, Giuliani A, Majone M, Ramadori R (2002) Effect of different carbon sources on aerobic storage by activated sludge. *Water Sci Technol* 45: 157-168.
- Beun JJ, van Loosdrecht MCM, Heijnen JJ (2002) Aerobic granulation in a sequencing batch airlift reactor. *Water Res* 36: 702-712.
- Beun JJ, Heijnen JJ, van Loosdrecht MCM (2001) N-Removal in a granular sludge sequencing batch airlift reactor. *Biotechnol Bioeng* 75: 82-92.
- Beun JJ, Paletta F, Van Loosdrecht MCM, Heijnen JJ (2000a) Stoichiometry and kinetics of poly-beta-hydroxybutyrate metabolism in aerobic, slow growing, activated sludge cultures. *Biotechnol Bioeng* 67: 379-389.
- Beun JJ, van Loosdrecht MCM, Heijnen JJ (2000b) Aerobic granulation. *Water Sci Technol* 41: 41-48.
- Beun JJ, Hendriks A, van Loosdrecht MCM, Morgenroth E, Wilderer PA, Heijnen JJ (1999) Aerobic granulation in a sequencing batch reactor. *Water Res* 33: 2283-2290.
- Beyenal H, Tanyolac A (1994) The calculation of simultaneous effective diffusion coefficients of the substrates in a fluidized bed biofilm reactor, *Water Sci. Technol.* 29 : 463–470.
- Bhunia P, Ghangrekar MM (2008) Statistical modeling and optimization of biomass granulation and COD removal in UASB reactors treating low strength wastewaters *Bioresource Technol* 99: 4229-4238.

- Bisogni JJ and Lawrence AW (1971) Relationships between biological solids retention time and settling characteristics of activated sludge. *Water Res* 5: 753-763.
- Bossier P, Verstraete W (1996) Triggers for microbial aggregation in activated sludge? *Appl Microbiol Biotechnol* 45: 1-6.
- Bright JJ, Fletcher M (1983) Amino-Acid Assimilation and Respiration by Attached and Free-Living Populations of a Marine *Pseudomonas*-Sp. *Microb Ecol* 9: 215-226.
- Bryers JD, Huang CT (1995) Recombinant Plasmid Retention and Expression in Bacterial Biofilm Cultures. *Water Sci Technol* 31: 105-115.
- Bruus JH, Nielsen PH, Keiding K (1992) On the stability of activated sludge flocs with implications to dewatering. *Water Res* 26: 1597-1604.
- Caldwell DE, Lawrence JR (1986) Growth kinetics of *Pseudomonas fluorescens* microcolonies within the hydrodynamic boundary layers of surface microenvironments. *Microb Ecol* 12: 299-312.
- Caplan SR, Westerhoff HV, Vandam K (1988) Thermodynamics and Control of Biological Free-Energy Transduction -. *Nature* 335: 507-508.
- Carucci A, Dionisi D, Majone M, Rolle E, Smurra P (2001) Aerobic storage by activated sludge on real wastewater. *Water Res* 35: 3833-3844.
- Castellanos T, Ascencio F, Bashan Y (2000) Starvation-induced changes in the cell surface of *Azospirillum*. *FEMS Microbiol Ecol* 33: 1-9.
- Chen Y, Jiang WJ, Liang DT, Tay JH (2008) Biodegradation and kinetics of aerobic granules under high organic loading rates in sequencing batch reactor. *Appl Microbiol Biotechnol* 79: 301–308.
- Chiu ZC, Chen MY, Lee DJ, Wang CH, Lai JY. (2007) Oxygen diffusion in active layer of aerobic granule with step change in surrounding oxygen levels. *Water Res* 41: 884–892.

- Chudoba J (1985) Control of activated sludge filamentous bulking. *Water Res* 19: 1017.
- Cogan NG (2003) A model of biofilm growth and structural development. PhD thesis. The University of Utah.
- Costerton JW, Irvin RT, Cheng KJ (1981) The bacterial glycocalyx in nature and disease. *Ann Rev Microbiol* 35: 299-324.
- CRC (2003) Handbook of Chemistry and Physics, 84th edn. Chemical Rubber Company, Cleveland, Ohio.
- Daffonchio D, Thavessri J, Verstraete W (1995) Contact angle measurement and cell hydrophobicity of granular sludge from upflow anaerobic sludge bed reactors. *Appl Environ Microbiol* 61: 3676-3680.
- Davies DG, Parsek MR, Pearson JP, Iglewski BH, Costerton JW, Greenberg EP. (1998) The involvement of cell-to-cell signals in the development of a bacterial biofilm. *Science* 280: 295-298.
- de Beer D, Huisman JW, Van den Heuvel JC, Ottengraf SPP (1992) Effect of pH profiles in methanogenic aggregates on the kinetics of acetate conversion. *Water Res* 26: 1329-1336.
- de Kreuk MK, van Loosdrecht MCM (2006) Formation of aerobic granules with domestic sewage. *J Environ Eng.* 132: 694-697.
- de Kreuk MK, Pronk M, van Loosdrecht MCM (2005) Formation of aerobic granules and conversion processes in an aerobic granular sludge reactor at moderate and low temperatures, *Water Res* 39: 4476-4484.
- de Taxis du Poet P, Dhulster P, Barbotin JN, Thomas D (1986) Plasmid inheritability and biomass production: comparison between free and immobilized cell cultures of *Escherichia coli* without selection pressure. *J Bacteriol* 165: 871-877.

- De Zeeuw WJ (1984) Acclimatization of anaerobic sludge for UASB reactor start-up. Ph.D. thesis, Agricultural University of Wageningen, Wageningen, the Netherlands.
- De Zeeuw WJ (1988) Granular sludge in UASB-reactors. In Granular Anaerobic Sludge: Microbiology and Technology, Lettinga G, Zehnder AJB, Grotenhuis JTC, Hulshoff Pol LW, eds, Wageningen, pp. 132-145.
- Dircks K, Beun JJ, Van Loosdrecht M, Heijnen JJ, Henze M (2001) Glycogen metabolism in aerobic mixed cultures. *Biotechnol Bioeng* 73: 85-94.
- El-Mamouni R, Leduc R, Guiot SR (1998) Influence of synthetic and natural polymers on the anaerobic granulation process. *Water Sci Technol* 38: 341-347.
- El-Mamouni R, Guiot SR, Mercier P, Safi B (1995) Liming impact on granules activity of the multiplate anaerobic reactor (MPAR) treating whey permeate. *Bioprocess Eng* 12: 47-51.
- Etterer T, Wilderer PA (2001) Generation and properties of aerobic granular sludge. *Water Sci Technol* 43: 19-26.
- Evans GM, Liu G (2003) Optimising activated sludge growth rate by intensifying hydrodynamic forces: *J Chem Technol Biotechnol* 78: 276-282.
- Fang HHP, Chui HK (1993) Maximum COD loading capacity in UASB reactors at 37°C. *J Environ Eng* 119: 103-119.
- Fang HHP, Chui HK, Li YY (1995) Effect of degradation kinetics on the microstructure of anaerobic biogranules. *Water Sci Technol* 32: 165-172.
- Fang HHP, Lau, IWC (1996) Startup of thermophilic (55 degrees °C) UASB reactors using different mesophilic seed sludges. *Water Sci Technol* 34: 445-452.
- Flora JRV, Suidan MT, Biswas P, Sayles GD (1995) A modeling study of anaerobic biofilm systems: I. Detailed biofilm modeling. *Biotechnol Bioeng* 46: 43-53.

- Fletcher M (1986) Measurement of Glucose Utilization by *Pseudomonas fluorescens* That Are Free-Living and That Are Attached to Surfaces. *Appl Environ Microbiol* 52: 672-676.
- Francese A, Cordoba P, Duran J, Sineriz F (1998) High upflow velocity and organic loading rate improve granulation in upflow anaerobic sludge blanket reactors *World J Microbiol Biotechnol* 14: 337-341.
- Gapes D, Wilen BM, Keller J (2004) Mass transfer impacts in flocculent and granular biomass from SBR systems *Water Sci Technol* 50: 203-212.
- Giokas DL, Daigger GT, Sperling M, Kim Y, Paraskevas PA (2003) Comparison and evaluation of empirical zone settling velocity parameters based on sludge volume index used a unified settling characteristics database *Water Res* 37: 3821-3836.
- Grady CPL Jr, Daigger GT, Lim HC (1999) *Biological wastewater treatment*. 2nd Edition. Marcel Dekker, Inc.
- Grady CPL Jr, Williams DR (1975) Effects of influent substrate concentration on the kinetics of natural microbial populations of continuous culture. *Water Res* 9: 171-180.
- Grotenhuis JTC, van Lier JB, Plugge CM, Stams AJM, Zehnder AJB (1991) Effect of ethylene glycol-bis(β -aminoethylether)-N,N-tetraacetic acid (EGTA) on stability and activity of methanogenic granular sludge. *Appl Microbiol Biotechnol* 36: 109-114.
- Guiot SR, Gorur SS, Bourque D, Samson R (1988) Metal effect on microbial aggregation during upflow anaerobic sludge bed-filter (UBF) reactor start-up. In *Granular Anaerobic Sludge: Microbiology and Technology*, Lettinga G, Zehnder AJB, Grotenhuis JTC, Hulshoff Pol LW, Wageningen, pp. 187-194.
- Guiot SR, Pauss A, Costerton JW (1992) A structured model of the anaerobic granules consortium. *Water Sci Technol* 25: 1-10.

- Guiot SR, Gorur SS, Bourque D, Samson R (1988) Metal effect on microbial aggregation during upflow anaerobic sludge bed-filter (UBF) reactor start-up. In: Lettinga G, Zehnder AJB, Grotenhuis JTC, Hulshoff Pol LW (eds) Granular anaerobic sludge, microbiology and technology. Wageningen. Netherland, pp 187-194.
- Gujer W, Henze M, Mino T, van Loosdrecht M (1999) Activated Sludge Model No. 3. Water Sci Technol 39: 183-193.
- Guven E (2004) Granulation in thermophilic aerobic wastewater treatment thesis. Milwaukee, WI, Marquette University.
- Henze M, Grady CPL, Jr Gujer W, Maris GVR, Matsuo T (1987) Activated sludge model No. 1. IAWPRC Scientific and Technical Report No 1, IAWPRC, London.
- Henze, M, Gujer W, Mino T, Matsuo T, Wentzel, MC, Maris GVR (1995) Activated sludge model No. 2. IAWPRC Scientific and Technical Report No 3, IAWPRC, London.
- Jang A, Yoon YH, Kim IS, Kim KS, Bishop PL (2003) Characterization and evaluation of aerobic granules in sequencing batch reactor. J Biotechnol 105: 71-82.
- Jeffrey WH, Paul JH (1986) Activity of an Attached and Free-Living *Vibrio* sp. as Measured by Thymidine Incorporation, p-Iodonitrotetrazolium Reduction, and ATP/DNA Ratios. Appl Environ Microbiol 51: 150-156.
- Jeong HS, KimYH, Yeom SH Song BK, Lee SI. (2005) Facilitated UASB granule formation using organic–inorganic hybrid polymers. Process Biochemistry 40: 89–94.
- Jiang HL, Tay JH, Liu Y, Tay STL (2003) Ca^{2+} Augmentation for enhancement of aerobically grown microbial granules in sludge blanket reactors. Biotechnol Letts 25: 95-99.

- Jiang HL, Tay JH, Tay STL (2002) Aggregation of immobilized activated sludge cells into aerobically grown microbial granules for the aerobic biodegradation of phenol. *Letts Appl Microbiol* 35: 439-445.
- Jiang HL, Tay JH, Tay STL (2004) Changes in structure, activity and metabolism of aerobic granules as a microbial response to high phenol loading. *Appl Microbiol Biotechnol* 63: 602-608.
- Kargi F, Uygur A (2002) Nutrient removal performance of a sequencing batch reactor as a function of the sludge age. *Enzyme Micro Technol* 31: 842–847.
- Kassam ZA, Yerushalmi L, Guiot SR (2003) A market study on the anaerobic wastewater treatment systems. *Water Sci Technol* 143: 179-192.
- Kemner KM, Kelly SD, Lai B, Maser J, O'Loughlin EJ, Sholto-Douglas D, Cai ZH, Schneegurt MA, Kulpa CF, Nealson KH (2004) Elemental and redox analysis of single bacterial cells by X-ray microbeam analysis. *Science* 306: 686-687.
- Kennedy KJ, Lentz EM (2000) Treatment of landfill leachate using sequencing batch and continuous upflow anaerobic sludge blanket (USAB) reactors. *Water Res* 34: 3640-3656.
- Korstgens V, Flemming HC, Wingender J, Borchard W (2001) Influence of calcium ions on the mechanical properties of a model biofilm of mucoid *Pseudomonas aeruginosa*. *Water Sci Technol* 43: 49-57.
- Kosaric N, Blaszczyk R, Orphan L, Valladares J (1990) The characteristics of granules from upflow anaerobic sludge blanket reactors. *Water Res* 24: 1473-1477.
- Kreft JU, Schink B (1993) Demethylation and Degradation of Phenylmethylethers by the Sulfide-Methylating Homoacetogenic Bacterium Strain Tmbs-4. *Arch Microbiol* 159: 308- 312.

- Kumar A, Yadav AK, Sreekrishnan TR, Satya, S, Kaushik CP (2008) Treatment of low strength industrial cluster wastewater by anaerobic hybrid reactor. *Bioresource Technology* 99: 3123-3129.
- Laspidou CS (2003) Modeling Heterogeneous biofilms including active biomass, inert biomass and extracellular polymeric substances. PhD thesis. Northwestern University. Evanston, Illinois.
- Lens P, de Beer D, Cronenberg C, Ottengraf S, Verstraete W (1995) The use of microsensors to determine distributions in UASB aggregates. *Water Sci Technol* 31: 273-280.
- Lepisto R, Rintala J (1999) Extreme thermophilic (70°C), VFA-fed UASB reactor: performance, temperature response, load potential and comparison with 35 and 55°C UASB reactors. *Water Res* 33: 3162-3170.
- Lettinga G, Rebac S, Zeeman G (2001) Challenge of psychrophilic anaerobic wastewater treatment. *Trends Biotechnol* 19: 363-370.
- Lettinga G, van Velsen AFM, Hobma SW, de Zeeuw W, Klapwijk A (1980) Use of the upflow sludge blanket (USB) reactor concept for biological waste water treatment especially for anaerobic treatment. *Biotechnol Bioeng* 22: 699-734.
- Lew B, Belavski M, Admon S, Tarre S, Green M (2003) Temperature effect on UASB reactor operation for domestic wastewater treatment in temperate climate regions. *Water Sci Technol* 48: 25-30.
- Li YQ (1998) Finite element simulation of thick biofilms at micro-scale. PhD thesis. The University of Wyoming. Laramie, Wyoming.
- Li ZH, Kuba T, Kusuda T (2006) The influence of starvation phase on the properties and the development of aerobic granules *Enzyme and Microbial Technol* 38: 670–674.

- Lin YM, Liu Y, Tay JH (2003) Development and characteristics of phosphorous-accumulating granules in sequencing batch reactor. *Appl Microbiol Biotechnol* 62: 430-435.
- Li Y, Liu Y (2005) Diffusion of substrate and oxygen in aerobic granule. *Biochem Eng J* 27: 45-52.
- Liao BQ, Droppo IG, Leppard GG., Liss SN (2006) Effect of solids retention time on structure and characteristics of sludge flocs sequencing batch reactors. *Water Res* 40: 2583-2591.
- Liss SN, Liao BQ, Droop IG, Allen DG, Leppard GG (2002) Effect of solids retention time on floc structure. *Water Sci Technol* 46: 431-438.
- Liu QS (2003) Aerobic granulation in sequencing batch reactor, Ph.D Thesis, Nanyang Technological University, Singapore, 2003, pp. 63–65.
- Liu YQ, Tay JH (2008) Influence of starvation time on formation and stability of aerobic granules in sequencing batch reactors. *Bioresource Technology* 99: 980–985.
- Liu YQ, Tay JH. (2006) Variable aeration in sequencing batch reactor with aerobic granular sludge. *J Biotechnol* 124: 38–46.
- Liu SY, Liu G, Tian YC, Chen YP, Yu HQ, Fang F. (2007) An innovative microelectrode fabricated using photolithography for measuring dissolved oxygen distributions in aerobic granules. *Environ Sci Technol* 41: 5447–52.
- Liu YQ, Liu Y, Tay JH (2005a) Relationship between size and mass transfer resistance in aerobic granules. *Lett Appl Microbiol* 40: 312-315.
- Liu Y, Liu YQ, Wang ZW, Yang SF, Tay JH (2005b) Influence of substrate surface loading on the kinetic behaviour of aerobic granules. *Appl Microbiol Biotechnol* 67: 484-488.
- Liu Y, Wang ZW, Qin L, Liu YQ, Tay JH (2005c) Selection pressure-driven aerobic granulation in a sequencing batch reactor. *Appl Microbiol Biotechnol* 67: 26-32.

- Liu LL, Wang ZP, Yao J, Sun XJ, Cai WM (2005d) Investigation on the formation and kinetics of glucose-fed aerobic granular sludge. *Enzyme Microb Technol* 36: 712-716.
- Liu Y, Tay JH (2004) State of the art of biogranulation technology for wastewater treatment. *Biotechnol adv* 22: 533-563.
- Liu Y, Yang SF, Tay JH, Liu QS, Qin L, Li Y (2004a) Cell hydrophobicity is a triggering force of biogranulation. *Enzyme Microbial Technol* 34: 371-379.
- Liu Y, Yang SF, Qin L, Tay JH (2004b) A thermodynamic interpretation of cell hydrophobicity in aerobic granulation. *Appl Microbiol Biotechnol* 64: 410-415.
- Liu Y, Yang SF, Tay JH (2004c) Improved stability of aerobic granules through selecting slow-growing nitrifying bacteria. *J Biotechnol* 108: 161-169.
- Liu QS, Tay JH, Liu Y (2003a) Substrate concentration-independent aerobic granulation in sequential aerobic sludge blanket reactor. *Environ Technol* 24: 1235-1243.
- Liu Y, Lin YM, Yang SF, Tay JH (2003b) A balanced model for biofilms developed at different growth and detachment forces. *Process Biochem* 38: 1761-1765.
- Liu Y, Xu HL, Yang SF, Tay JH (2003c) A general model for biosorption of Cd^{2+} , Cu^{2+} and Zn^{2+} by aerobic granules. *J Biotechnol* 102: 233-239.
- Liu Y, Xu HL, Yang SF, Tay JH (2003d) The mechanisms and models for anaerobic granulation in upflow anaerobic sludge blanket reactor. *Water Res* 37: 661-673.
- Liu Y, Yang SF, Liu QS, Tay JH (2003e) The Role of cell hydrophobicity in the formation of aerobic granules. *Curr Microbiol* 46: 270-274.
- Liu Y, Yang SF, Tay JH (2003e) Elemental compositions and characteristics of aerobic granules cultivated at different substrate N/C ratios. *Appl Microbiol Biotechnol* 61: 556-561.

- Liu Y, Yang SF, Xu H, Woon KH, Lin YM, Tay JH (2003f) Biosorption kinetics of cadmium (II) on aerobic granular sludge. *Process Biochem* 38: 995-999.
- Liu Y, Tay JH (2002) The essential role of hydrodynamic shear force in the formation of biofilm and granular sludge. *Water Res* 36: 1653-1665.
- Liu Y, Yang SF, Tan SF, Lin YM, Tay JH (2002) Aerobic granules: a novel zinc biosorbent. *Lett Appl Microbiol* 35: 548-551.
- Liu Y, Tay JH (2001) Metabolic response of biofilm to shear stress in fixed-film culture. *J Appl Microbiol* 90: 337-342.
- Liu Y (1995) Adhesion kinetics of nitrifying bacteria on various thermoplastic supports. *Colloids Surf B: Biointerfaces* 5: 213-219.
- Lodi A, Solisoio C, Converti A, Del Borghi M (1998) Cadmium, zinc, copper, silver and chromium(III) removal from wastewaters by *sphaerotilus natans*. *Bioprocess Eng* 19: 197-203.
- MacLeod FA, Guiot SR, Costerton JW (1990) Layered structure of bacterial aggregates produced in an upflow anaerobic sludge bed and filter reactor. *Appl Environ Microbiol* 56: 1598-1607.
- Mahoney EM, Varangu LK, Cairns WL, Kosaric N, Murray RGE (1987) Effect of Ca^{2+} on microbial aggregation during UASB reactor start-up. *Water Sci Technol* 19: 249-260.
- Majone M, Beccari M, Dionisi D, Levantesi C, Ramadori R, Tandoi V (2007) Effect of periodic feeding on substrate uptake and storage rates by a pure culture of *Thiothrix* (CT3 strain). *Water Res* 41: 177-187.
- Metcalf & Eddy I (1991) *Wastewater Engineering: treatment, disposal, and reuse.*, 3rd edn. McGraw-Hill, New York.

- McHugh S, Collins G, O'Flaherty V (2006) Long-term, high-rate anaerobic biological treatment of whey wastewaters at psychrophilic temperatures . *Bioresource Technology* 97: 1669-1678.
- McSwain BS (2005) Molecular investigation of aerobic granular sludge formation. PhD Thesis. Notre Dame, Indiana.
- Meyer RL, Saunders AM, Zeng RJ, Keller J, Blackall LL (2003) Microscale structure and function of anaerobic-aerobic granules containing glycogen accumulating organisms. *FEMS Microbiol Ecol* 45: 253-261.
- Mishima K, Nakamura M (1991) Self-immobilization of aerobic activated sludge—a pilot study of the aerobic upflow sludge blanket process in municipal sewage treatment. *Water Sci Technol* 23: 981-990.
- Mosquera-Corral A, de Kreuk MK, Heijnen JJ, van Loosdrecht MCM (2005) Effects of oxygen concentration on N-removal in an aerobic granular sludge reactor. *Water Res* 39: 2676–86.
- Moy BYP, Tay JH, Toh SK, Liu Y, Tay STL (2002) High organic loading influences the physical characteristics of aerobic sludge granules. *Letts Appl Microbiol* 34: 407-412.
- Nancharaiah YV, Schwarzenbeck, N, Mohan, TVK, Narasimhan V, Wilderer PA, Venugopalan VP (2006) Biodegradation of nitrilotriacetic acid (NTA) and ferric-NTA complex by aerobic microbial granules. *Water Res.* 40, 1539–1546.
- Ng HY (2002) Performance of a membrane reactor and a completely mixed activated sludge system at short solid retention times. PhD thesis, University of California, Berkley.
- Noyola A, Mereno G (1994) Granulation production from raw waste activated sludge. *Water Sci Technol* 30: 339-346.

- O'Flaherty V, Lens PN, de Beer D, Colleran E (1997) Effect of feed composition and upflow velocity on aggregate characteristics in anaerobic upflow reactors. *Appl Microbiol Biotechnol* 47: 102-107.
- Ohashi A, Harada H (1994). Adhesion strength of biofilm developed in an attached-growth reactor. *Water Sci Technol* 29: 10.
- Park KY, Kim DY, Chung TH (2005) Granulation in an upflow anaerobic sequencing batch reactor treating disintegrated waste activated sludge. *Water Sci Technol* 52: 105-111.
- Peng D, Bernet N, Delgenes JP, Moletta R (1999) Aerobic granular sludge—A case report. *Water Res* 33: 890-893.
- Pan S (2003) Inoculation of microbial granular sludge under aerobic conditions. PhD thesis. Nanyang Technological University. Singapore.
- Pereboom JHF, Vereijken TLFM (1994) Methanogenic granule development in full scale internal circulation reactors. *Water Sci Technol* 30: 9-21.
- Pereira MA, Roest K, Stams AJM, Mota M, Alves M, Akkermans ADL (2002) Molecular monitoring of microbial diversity in expanded granular sludge bed (EGSB) reactors treating oleic acid. *FEMS Microbiol Ecol* 41: 95-103.
- Perez J, Picioreanu C, van Loosdrecht MCM (2005) Modelling biofilm and floc diffusion processes based on analytical solution of reaction–diffusion equations, *Water Res.* 39 1311–1323.
- Pizarro GE (2001) Quantitative modeling of heterogeneous biofilm using cellular automata. PhD thesis. University of Wisconsin-madison.
- Picioreanu C, van Loosdrecht MCM, Heijnen JJ (1998) Mathematical modeling of biofilm structure with a hybrid differential-discrete cellular automata approach. *Biotechnol Bioeng* 58: 101-116.

- Pratt LA, Kolter R (1999) Genetic analysis of bacterial biofilm formation. *Curr Opin Microbiol* 2: 598-603.
- Prescott LM, Harley JP, Klein DA (1999) *Microbiology*. 4th edition, McGraw-Hill, Boston.
- Pribyl M, Tucek F, Wilderer PA, Wanner J (1997) Amount and nature of soluble refractory organics produced by activated sludge micro-organisms in sequencing batch and continuous flow reactors. *Water Sci Technol* 35: 27-34.
- Pritchett LA (2000) Analysis of a one-dimensional biofilm model. Montana State University. Montana.
- Pringle JH, Fletcher M (1983) Influence of substratum wettability on attachment of fresh bacteria to solid surface. *Appl Environ Microbiol* 45: 811-817
- Qin L, Tay JH, Liu Y (2004a) Selection pressure is a driving force of aerobic granulation in sequencing batch reactors. *Process Biochem* 39: 579-584.
- Qin L, Liu Y, Tay JH (2004b). Effect of settling time on aerobic granulation in sequencing batch reactor. *Biochem Eng J* 21: 47-52.
- Quarmby J, Forster CF (1995) An examination of the structure of UASB granules. *Water Res* 29: 2449-2454.
- Randall CW, Barnard JL, Stensel HD (1992) Design and retrofit of wastewater treatment plants for biological nutrient removal, *Water Quality Management Library*, Technomic Publishing Co. Lancaster, PA.
- Rittman BE (1987) A critical evaluation of soluble microbial formation in biological processes. *Water Sci Technol* 19: 517-528.
- Rittmann BE and McCarty PL (1981) Substrate flux into biofilms of any thickness, *J Environ Eng* 107: 831-849.

- Rittmann BE, McCartypl (1980) Evaluation of steady-state-biofilm kinetics
Biotechnology and bioengineering 22: 2359-2373.
- Rocheleau S, Greer CW, Lawrence JR, Cantin C, Laramée L, Guiot SR (1999)
Differentiation of *Methanosaeta concilii* and *Methanosarcina barkeri* in anaerobic
mesophilic granular sludge by in situ hybridization and confocal scanning laser
microscopy. Appl Environ Microbiol 65: 2222-2229.
- Rose RK (2000) The role of calcium in oral streptococcal aggregation and the
implications for biofilm formation and retention. Biochimica et Biophysica Acta
1475: 76-82.
- Rozen R, Bachrach G, Zachs B (2001) Growth rate and biofilm thickness of
Streptococcus sobrinus and *Streptococcus mutans* on hydroxapatite.
APMIS. 109:155-160.
- Rosenberg M, Gutnick D, Rosenber E (1980) Adherence of bacteria to hydrocarbons: a
simple method for measuring cell-surface hydrophobicity, FEMS Microbiol Lett 9:
29-33.
- Rouxhet PG, Mozes N (1990) Physical chemistry of the interaction between attached
microorganisms and their support. Water Sci Technol 22: 1-16.
- Santegoeds CM, Damagaad LR, Hesselink C, Zopfi J, Lens P, Muyzer G, de Beer D
(1999) Distribution of sulfate-reducing and methanogenic bacteria in anaerobic
aggregates determined by microsensor and molecular analysis. Appl Environ
Microbiol 65: 4618-4629.
- Schmidt JE, Ahring BK (1993) Effects of magnesium on thermophilic acetate-degrading
granules in upflow anaerobic sludge blanket (UASB) reactor. Enzyme Microbial
Technol 15: 304-310.
- Schmidt JE, Ahring BK (1996) Granular sludge formation in upflow anaerobic sludge
blanket (UASB) reactors. Biotechnol Bioeng 49: 229-246.

- Schmidt JE, Ahring BK (1999) Immobilization patterns and dynamics of acetate-utilizing methanogens immobilized in sterile granular sludge in upflow anaerobic sludge blanket reactors. *Appl Environ Microbiol* 65: 1050-4.
- Schroen C, Fretz CB, DeBruin V, Berendsen W, Moody HM, Roos EC, VanRoon JL, Kroon PJ, Strubel M, Janssen AEM, Tramper J (2002) Modelling of the enzymatic kinetically controlled synthesis of cephalixin - Influence of diffusion limitation. *Biotechnol Bioeng* 80: 331-340.
- Schwarzenbeck N, Erley R, Wilderer PA (2003) Growth of aerobic granular sludge in a SBR-system treating wastewater rich in particulate matter. 5th International Conference on Biofilm Systems, 14-19 September, Cape Town, South Africa.
- Sekiguchi Y, Kamagata Y, Nakamura K, Ohashi A, Harada H (1999) Fluorescence in situ hybridization using 16S rRNA-targeted oligonucleotides reveals localization of methanogenes and selected uncultured bacteria in mesophilic and thermophilic sludge granules. *Appl Environ Microbiol* 65: 1280-1288.
- Serafim LS, Lemos PC, Oliveira R, Reis MAM (2004) Optimization of polyhydroxybutyrate production by mixed cultures submitted to aerobic dynamic feeding conditions. *Biotechnol Bioeng* 87: 145-160.
- Shi H, Shiraishi M, Shimizu K (1997) Metabolic flux analysis for biosynthesis of poly-beta-hydroxybutyric acid) in *Alcaligenes eutrophus* from various carbon sources. *J Ferment Bioeng* 84: 579-587.
- Shin HS, Lim KH, Park HS (1992) Effect of shear stress on granulation in oxygen aerobic upflow sludge reactors. *Water Sci Technol* 26: 601-605.
- Sin G, Guisasola A, De Pauw DJW, Baeza JA, Carrera J, Vanrolleghem PA (2005) A new approach for modelling simultaneous storage and growth processes for activated sludge systems under aerobic conditions. *Biotechnol Bioeng* 92: 600-613.

- Show KY, Wang Y, Foong SF, Tay JH (2004) Accelerated start-up and enhanced granulation in upflow anaerobic sludge blanket reactors. *Water Res* 38: 2293–2304.
- Singh KS, Viraraghavan T (2003) Impact of temperature on performance, microbiological, and hydrodynamic aspects of UASB reactors treating municipal wastewater. *Water Sci Technol* 48: 211-217.
- Tagawa T, Syutsubo K, Sekiguchil Y, Ohashi A, Harada H (2000) Quantification of methanogen cell density in anaerobic granular sludge consortia by fluorescence in-situ hybridization. *Water Sci Technol* 42: 77-82.
- Taniguchi J, Hemmi H, Tanahashi K, Amano N, Nakayama T, Nishim T (2000) Zinc biosorption by a zinc-resistant bacterium, *Brevibacterium* sp. Strain HZM-1. *Appl Microbiol Biotechnol* 54: 581-588.
- Tay JH, Jiang HL, Tay STL (2004a) High-rate biodegradation of phenol by aerobically grown microbial granules. *J Environ Eng* 130: 1415-1423.
- Tay JH, Pan S, He YX, Tay STL (2004b) Effect of organic loading rate on aerobic granulation. I: Reactor performance. *J Environ Eng* 130: 1094-1101.
- Tay JH, Pan S, He YX, Tay STL (2004Cc) Effect of organic loading rate on aerobic granulation. Part II: Characteristics of aerobic granules. *J Environ Eng* 130, 1102-1109.
- Tay JH, Liu QS, Liu Y (2003) Shear force influences the structure of aerobic granules cultivated in sequencing batch reactor. 5th International Conference on Biofilm Systems, 14-19 September, Cape Town, South Africa.
- Tay JH, Tay STL, Ivanov V, Pan S, Liu QS (2003c) Biomass and porosity profile in microbial granules used for aerobic wastewater treatment. *Letts Appl Microbiol* 36: 297-301.

- Tay JH, Liu QS, Liu Y (2002a) Aerobic granulation in sequential sludge blanket reactor. *Water Sci Technol* 46: 13-18.
- Tay JH, Yang SF, Liu Y (2002b) Hydraulic selection pressure-induced nitrifying granulation in sequencing batch reactors. *Appl Microbiol Biotechnol* 59: 332-337.
- Tay JH, Liu QS, Liu Y (2002c) Characteristics of aerobic granules grown on glucose and acetate in sequential aerobic sludge blanket reactors. *Environ Technol* 23: 931-936.
- Tay JH, Ivanov V, Pan S, Tay STL (2002d) Specific layers in aerobically grown microbial granules. *Lett Appl Microbiol* 34: 254-257.
- Tay STL, Ivanov V, Yi S, Zhuang WQ, Tay JH (2002e) Presence of Anaerobic Bacteroides in Aerobically Grown Microbial Granules. *Microbial Ecol* 44: 278-285.
- Tay JH, Liu QS, Liu Y (2001a) Microscopic observation of aerobic granulation in sequential aerobic sludge blanket reactor. *J Appl Microbiol* 91: 168-175.
- Tay JH, Liu QS, Liu Y (2001b) The effects of shear force on the formation, structure and metabolism of aerobic granules. *Appl Microbiol Biotechnol* 57: 227-233.
- Tay JH, Liu QS, Liu Y (2001c) The role of cellular polysaccharides in the formation and stability of aerobic granules. *Letts Appl Microbiol* 33: 222-226.
- Tay JH, Xu HL, Teo KC (2000) Molecular mechanism of granulation. I: H⁺ translocation-dehydration theory. *J Environ Eng* 126, 403-410.
- Tay JH, Yan YG (1996) Influence of substrate concentration on micrional selection and granulation during start-up of upflow anaerobic sludge blanket reactors. *Water Environ Res* 68: 1140-1150.
- Thiele JH, Wu WM, Jain MK, Zeikus JG (1990) Ecoengineering high rate biomethanation system: design of improved syntrophic biomethanation catalysis. *Biotechnol Bioeng* 35: 990-999.

- Third KA, Newland M, Cord-Ruwisch R (2003) The effect of dissolved oxygen on PHB accumulation in activated sludge cultures. *Biotechnol Bioeng* 82: 238-250.
- Teo KC, Xu HL, Tay JH (2000) Molecular mechanism of granulation. II: Proton translocating activity. *J Environ Eng* 126: 411-418.
- Toh SK, Tay JH, Moy BYP, Ivanov V, Tay STL (2003) Size-effect on the physical characteristics of the aerobic granule in a SBR. *Appl Microbiol Biotechnol* 60: 687-695.
- Tsuneda S, Nagano T, Hoshino T, Ejiri Y, Noda N, Hirata A (2003) Characterization of nitrifying granules produced in an aerobic upflow fluidized bed reactor. *Water Res* 37: 4965-4973.
- Turakhia M H, W. G. Characklis (1989) Activity of *Pseudomonas aeruginosa* in biofilms: effect of Calcium. *Biotechnol Bioeng* 33: 406-414.
- Urbain V, Block JC, Manem J (1993) Bioflocculation in activated sludge: An analytical approach. *Water Res* 27: 829-838.
- Uyanik S, Sallis PJ, Anderson GK (2002) The effect of polymer addition on granulation in an anaerobic baffled reactor (ABR). Part I: process performance. *Water Res* 36: 933-942.
- Valdman E, Leite SGF (2000) Biosorption of Cd, Zn and Cu by *Saragssum* sp. waste biomass. *Bioprocess Eng* 22: 171-173.
- Van Haecht JL, Bolipombo M, Rouxhet PG (1985) Immobilization of *Saccharomyces cerevisiae* by adhesion: Treatment of the cells by Al ions. *Biotechnol Bioeng* 27: 217-224.
- Vanderhaegen B, Ysebaert E, Favere K, van Wambeke M, Peeters T, Panic V, Vandenlangenbergh V, Verstracte W (1992) Acidogenesis in relation to in-reactor granule yield. *Water Sci Technol* 25: 21-30.

- Van Langerak EPA, Gonzalez-Gil G, Van Aelst A, Van Lier JB, Hamelers HVM, Lettinga G (1998) Effects of high calcium concentrations on the development of methanogenic sludge in upflow anaerobic sludge bed (UASB) reactors. *Water Res* 32: 1255-1263.
- Visser EJ (1998) Development of evaluation of a two-dimensional microscale transport and biofilm process model. PhD thesis. Montana State University.
- Wang XH, Zhang HM , Yang FL, Wang YF, Gao MM (2008) Long-term storage and subsequent reactivation of aerobic granules. *Bioresource Technology* (In Press).
- Wang J, Yu HQ (2006) Biosynthesis of polyhydroxybutyrate (PHB) and extracellular polymeric substances (EPS) by *Ralstonia eutropha* ATCC 17699 in batch cultures *App Microbiol Biotechnol* 75: 871-878.
- Wang ZP, Liu L, Yao J, Cai W (2006a) Effects of extracellular polymeric substances on aerobic granulation in sequencing batch reactors. *Chemosphere* 63: 1728-1735.
- Wang ZW, Liu Y, Tay JH (2006b) The role of SBR mixed liquor volume exchange ratio in aerobic granulation. *Chemosphere* 62: 767-771.
- Wanner O, Gujer P (1985) A multispecies biofilm model. *Biotechnol Bioeng* 47: 172-184.
- Wentland EJ, Stewart PS, Huang CT, McFeters GA (1996) Spatial variations in growth rate within *klebsiella pneumoniae* colonies and biofilm. *Biotechnol. Prog*, 12 : 316 -321.
- Wimpenny JWT, Colasanti R (1997) A unifying hypothesis for the structure of microbial biofilms based on cellular automaton models. *FEMS Microbiol Ecol* 22: 1-16.
- Wirtz RA, Dague RR (1996) Enhancement of granulation and start-up in anaerobic sequencing batch reactor. *Water Environ Res* 68: 883-892.
- Wloka M, Rehage H, Flemming HC, Wingender J (2004) Rheological properties of viscoelastic biofilm extracellular polymeric substances and comparison to the behavior of calcium alginate gels. *Colloid Polym Sci* 282: 1067-1076.

- Wu WM (1991) Technological and microbiological aspects of anaerobic granules. Ph.D. dissertation, Michigan State University, MI, U.S.
- Wu YC., Okrutny Mark (2004) Role of phosphorus in activated sludge. *Biotechnology and Bioengineering* 24: 1813 – 1826.
- Wu WM, Hu JC, Gu XS, Gu GW (1987) Cultivation of anaerobic granular sludge in UASB reactors with aerobic activated sludge as seed. *Water Res* 21: 789-799.
- Xu HL, Tay JH (2002) Anaerobic granulation with methanol-cultured seed sludge. *J Environ Sci Health Part A* 37: 85-94.
- Yamane T (1993) Yield of poly-d(-)-3-hydroxybutyrate from various carbon-sources - a theoretical-study. *Biotechnol Bioeng* 41: 165-170.
- Yang SF, Tay JH, Liu Y (2005) Effect of substrate N/COD ratio on the formation of aerobic granules. *J Environ Eng* 131: 86-92.
- Yang SF, Liu QS, Tay JH, Liu Y (2004a) Growth kinetics of aerobic granules developed in sequencing batch reactors. *Letts Appl Microbiol* 38: 106-112.
- Yang SF, Tay JH, Liu Y (2004b) Inhibition of free ammonia to the formation of aerobic granules. *Biochem Eng J* 17: 41-48.
- Yang SF, Liu Y, Tay JH (2003) A novel granular sludge sequencing batch reactor for removal of organic and nitrogen from wastewater. *J Biotechnol* 106: 77-86.
- Yi S, Tay JH, Maszenan AM, Tay STL (2003) A culture-independent approach for studying microbial diversity in aerobic granules. *Water Sci Technol* 47: 283-290.
- Yi S, Zhuang WQ, Wu B, Tay STL, Tay JH (2006) Biodegradation of p-nitrophenol by aerobic granules in a sequencing batch reactor. *Environ Sci Technol* 40: 2396-2401.

- Yu HQ, Tay JH, Fang HHP (2001) The role of calcium in sludge granulation during UASB reactor start-up. *Water Res* 35: 1052-1060.
- Zeng P, Zhuang WQ, Tay STL, Tay JH (2007) The influence of storage on the morphology and physiology of phthalic acid-degrading aerobic granules. *Chemosphere* 69: 1751-1757.
- Zheng YM, Yu HQ, Liu SJ, Liu XZ (2006) Formation and instability of aerobic granules under high organic loading conditions. *Chemosphere* 63: 1791-1800.
- Zhou WL, Imai T, Ukita M, Li FS, Yuasa A (2007) Effect of loading rate on the granulation process and granular activity in a bench scale UASB reactor. *Bioresource Technol* 98: 1386–1392.
- Zoutberg GR, de Been P (1997) The biobed EGSB (expanded granular sludge bed) system covers shortcoming of the upflow anaerobic sludge blanket reactor in the chemical industry. *Water Sci Technol* 35: 183-188.
- Zhu J, Wilderer PA (2003) Effect of extended idle conditions on structure and activity of granular activated sludge. *Water Res* 37: 2013-2018.